Paleomagnetism of Carbonates and the Synfolding Test in the North American Cordillera

by

Samantha Reevs Nemkin

A dissertation submitted in partial fulfillment
of the requirements for the degree of
Doctor of Philosophy
(Earth and Environmental Sciences)
in The University of Michigan
2017

Doctoral Committee:

Professor Ben van der Pluijm, Co-Chair
Emeritus Professor Rob Van der Voo, Co-Chair
Assistant Professor Brian Robert Ellis
Professor Kyger C. Lohmann
Professor Larry John Ruff

Swift Dam, Pondera County, Montana

Samantha Reevs Nemkin

srnemkin@umich.edu

ORCID iD: 0000-0002-1651-7587

DEDICATION

I dedicate this thesis to my parents Karen and Oleg for supporting my interests in rocks from my childhood on, as well as my husband Sean for his continued love and support from my undergraduate through my graduate career.

ACKNOWLEDGMENTS

I would like to first thank my advisors Dr. Ben van der Pluijm and Dr. Rob Van der Voo whose hard work, patience, and guidance has provided me with many opportunities to learn and excel during my Ph.D. The measurement and analysis of the carbonate samples for my thesis posed many challenges and without the perceptive and long conversations with Ben and Rob, I would not have made it to this point. I would also like to thank; Dr. Brian Ellis, Dr. Kacey Lohmann, and Dr. Larry Ruff for serving on my committee and providing important insight and suggestions throughout my work to complete my dissertation, as well as the significant effort put in to review my thesis.

A special thank you needs to be extended to my 8th grade earth science teacher Ms. Messina for igniting my interest to teach geology and Dr. Amy Sheldon and Dr. Scott Giorgis for fostering and expanding my geologic interests during my undergraduate career. I would also like to acknowledge the Earth & Environmental Science staff, especially Bill Wilcox and Anne Hudon, for helping with everything from ordering, funding, and keeping me on track with all of my graduate requirements.

My advisors facilitated much of my funding through National Science Foundation Grants, but I would also like to acknowledge funding sources provided by the University of Michigan. Additional funding through the University of Michigan included the Scott Turner Award, the Rackham Graduate Student Research Grant, and the Rackham Graduate Travel Grant. Support for research and measurements was also provided by the Institute for Rock

Magnetism (IRM) Visiting Fellowship @ The University of Minnesota and GSA Graduate Student Research Grant. Paleomagnetic sampling is definitely a two-person job and with that, I would like to thank Dr. Josep Bedmar, Peter Cook, and Pamela Horsley for their assistance with field sampling. Also want to thank undergraduate researcher Emily Schottenfels for help with some lab measurements and a special thank you to Dr. Mike Jackson at the IRM for all of his support with measurements and numerous analysis questions.

The amount of time spent in the office analyzing samples and writing can sometimes be overwhelming, but this was made much better by great office mates, Austin and Erin, who were there for many scientific and fun conversations and lots of good laughs. My office mates also need a special recognition for putting up with my holiday decorating. My time in Ann Arbor was made even better by amazing friends who helped me step away from my work, relax, and share a drink or two or three.

My parents, sister-in-law Mary, and in-laws Helen and Tom, have all supported me throughout my pursuit to attain my Ph.D. I want to specially thank my parents, Karen and Oleg, whose love and support has propelled me to where I am today. Most of all, I'd like to thank my wonderful husband Sean who is always there for me, especially for those late night grad school pep talks.

TABLE OF CONTENTS

LIST OF FIGURES

CHAPTER 2

CHAPTER 3

CHAPTER 4

APPENDIX A

APPENDIX B

LIST OF TABLES

CHAPTER 2

CHAPTER 3

CHAPTER 4

APPENDIX A

APPENDIX B

LIST OF APPENDICES

ABSTRACT

Carbonate remagnetizations are globally widespread and typically the result of secondary magnetite growth, which, prior to the 1980's, were erroneously interpreted as primary magnetization directions. Whereas remagnetizations were eventually recognized, their timing remained mostly dated by qualitative comparison to an apparent polar wander path (APWP) after paleomagnetic field tests. This thesis demonstrates that quantitative ages can be assigned to remagnetizations by correlating synfolding remagnetization directions with ages from $^{40}Ar/^{39}Ar$ dating of individual folds.

Central to the approach in this study is sampling of local-scale carbonate folds in order to produce multiple individual fold tests, instead of one regional fold test application in a field area. Results from the North American Cordillera in Montana, Idaho/Wyoming, the Monterrey Salient in northern Mexico, and central Mexico are reported. Remagnetization ages are determined for each field area by connecting synfolding remagnetizations with fold ages, which span the Late Cretaceous to Eocene. Mississippian limestones from Montana (Chpt. 2) and the Lower Cretaceous carbonates from the Monterrey Salient (Chpt. 3) have remagnetization ages of 54 Ma and 48-52 Ma, respectively. Results from Cretaceous carbonates in central Mexico (Chpt. 4) preserve two regionally distinct remagnetization events at 77 Ma and 44 Ma. A study of folded Mississippian limestones in Idaho and Wyoming similarly indicate the presence of a remagnetization event, but results remain inconclusive for lack of suitable sampling sites (Appendix A).

Remagnetization ages coincide with periods of tectonic activity in the North American Cordillera and are interpreted as the result of chemical growth of magnetite. It is proposed that the formation mechanism of secondary remanences is from the interaction of carbonates with an iron-bearing fluid that may also have produced illitization in clay-rich interlayers. Lithology and structural characteristics influence whether or not sufficient magnetite will grow, allowing the acquisition of a permanent secondary remanence. The local-scale fold sampling scheme provides a new, detailed understanding into the development of local paleomagnetic and deformational histories across a field area.

Combining synfolding remagnetizations and fold ages provides an important method to date the timing of remagnetization acquisition in rock units, contributing significantly to the global paleopole database. Given that many carbonates worldwide are remagnetized, this coupled approach would permit broader use of the method. Moreover, the spatial distribution of syn-, pre-, and/or postfolding remanences in folds constrains local deformation events in an area and provides novel insights into the connection of remagnetization mechanism(s) and carbonate deformation.

CHAPTER 1

INTRODUCTION

A complex magnetic field is generated within Earth, resulting in a time averaged geocentric axial dipole (GAD) field that is parallel to the Earth's rotation axis at the surface (Creer, 1962; Opdyke and Henry, 1969). In the presence of this dipole field a stable magnetic direction can be preserved in rocks, commonly within the mineral phases magnetite and hematite (Cox and Doell, 1960). These directions can be recorded during formation of the unit or at a post depositional/formational time, which are called remagnetizations (Butler, 1992; McCabe and Elmore, 1989; McCabe et al., 1983; Scotese at al., 1982; Stamatakos et al., 1996).

Paleomagnetists use the preserved magnetic directions to study numerous aspects of Earth's history, with a special category being remagnetization studies. Prior to the 1980's, remagnetizations were not fully recognized and many paleomagnetic analyses were misinterpreted as primary magnetizations. Rocks were analyzed and ages were incorrectly assigned based on matching a measured direction to a portion on Earth's apparent polar wander path (APWP; Kent and Opdyke, 1979; Martin, 1975; Scott, 1979). One early example is Martin (1975), who interpreted carbonates from Ohio to have primary magnetizations carried by magnetite, even though the pole position did not match the expected position based on the formation age. The difference in the calculated pole position as compared to the expected North American APWP was attributed to incomplete stratigraphic sampling that did not allow for the averaging of secular variation (Martin, 1975). Elston and Bressler (1977) also misinterpreted a

later determined remagnetized unit in Arizona, studying the Early-Middle Cambrian Tapeats sandstone. They found that the pole diverts from the expected direction, which these authors considered a primary magnetization, and that the diversion was only a "brief excursion".

Part of this early misinterpretation was due to the fact that it was the ruling conviction that magnetite was detrital and could not grow in a rock after deposition. Many of the studied carbonates in the Appalachians are Paleozoic and have, what we now know, a late Paleozoic (Permian) remagnetization (e.g. McCabe et al., 1983). In the North American Cordillera many Paleozoic carbonates acquired Mesozoic or Cenozoic remagnetizations (e.g., Enkin et al., 2000; McWhinnie et al., 1990; Nemkin et al., 2016). However, the western remagnetizations were not recognized until the 1980's when use of the cryomagnetometer allowed for detection of the comparatively weaker western paleomagnetic intensities. Therefore, early explanations for the differences in measured versus expected poles were considered as a response to mechanical or thermal changes (Kent, 1985; Kodama, 1988; van der Pluijm, 1987).

Creer (1968) advocated for remagnetizations in lower Paleozoic rocks, as the observed shallow downward directions from these units did not match the expected directions. The remagnetizations were further supported as an occurrence based on the presence of secondary magnetic iron oxides due to soils weathering in tropical climates, but was later contradicted by McElhinny and Opdyke. (1973). McElhinny and Opdyke. (1973) did not support Creer's remagnetization hypothesis because they found similarly shallow directions in the Trenton limestone, which did not contain any soils so the unit did not require weathering at the equator. Instead the authors found positive shallow inclinations after alternating field demagnetization and proposed a proto-Atlantic ocean based on a similar pole from Colorado (McElhinny and Opdyke, 1973). Such complications arose when magnetizations were assumed to be primary and

preserved in detrital magnetite, until the early 1980's. Scotese et al. (1982) provided a pivotal change in the interpretation of magnetizations, studying Upper Silurian and Lower Devonian carbonates from the Helderberg Escarpment in NY. A fold test was applied to these samples and it was observed that the best statistical clustering of directions was at a midway point between 0-100% unfolding, instead of before or after folding. This behavior is called synfolding. The optimal (synfolding) direction fell on the Permian portion of the North American APWP; therefore, a secondary remanence (remagnetization) was assigned to these results (Scotese et al., 1982). It was determined that the carrier was magnetite and, since it was secondary, the authors concluded that authigenic growth of magnetite occurred, instead of the previously held notion of detrital magnetite carrying the remanence.

McCabe et al., (1983) further studied carbonates of the Helderberg and Bonneterre formations and this work supported later growth of magnetite, as the directions were post-depositional. Following these reinterpretations of relative timing of magnetization acquisition, the Trenton Limestone that was previously measured by McElhinny and Opdyke (1973) was re-measured. McCabe et al. (1984) thermally demagnetized the samples instead of using an alternating field as done by McElhinny and Opdyke (1973), resulting in a cleaner demagnetization with shallow negative directions instead of shallow positive. The new characteristic directions for the Trenton limestone resulted in a paleomagnetic pole that fell near the North American APWP's Permian pole. McCabe et al. (1984) concluded that the Ordovician limestones were remagnetized in the Permian.

After the pioneering work that was done in the Appalachian Mountains to unravel remagnetizations, many carbonates around the world were re-analyzed (e.g. Çinku et al., 2013; Katz et al., 1998; McCabe and Elmore, 1989; Stamatakos et al., 1996; Van der Voo and Torsvik,

2012; Weil et al., 2000; Woods et al., 2000; Zegers et al., 2003). Evidence for remagnetizations were found in Paleozoic rocks of the Appalachians, Mesozoic and Cenozoic carbonates of the North American Cordillera, Neoproterozoic-Cenozoic rocks in South America, as well as many units in Europe (e.g., Enkin et al., 2000; Font et al., 2012; Gillet and Karlin, 2004; McCabe et al., 1984; McWhinnie et al., 1990; Weil et al., 2012; Xu et al., 1998; Zwing et al., 2009).

The timing of a remagnetization is not determined by dating the sampled rock, but is qualitatively dated by comparison to an APWP for a region or assigned age range if a paleomagnetic field test is applied (Ballard et al., 1986; Stearns and Van der Voo, 1987). Thus, there was a need to assign a more quantitative date as magnetite can not be directly dated. A solution is offered by combining radiometric $^{40}Ar/^{39}Ar$ fold dating in areas with synfolding remagnetizations. Illitization from smectite or illite precursors is common in naturally deformed rocks (e.g., Vrolijk and van der Pluijm, 1999), allowing radiometric dating of deformation, including folding (Fitz-Díaz and van der Pluijm et al., 2013). A paleomagnetic fold test is completed by measuring samples from each limb of a fold and progressively unfolding the respective directions based on bedding dips (Tauxe and Watson, 1994; Watson and Enkin, 1993). If the tightest clustering (represented by the k parameter) of the measured directions from both limbs is between 10-90% unfolding, then it is considered a synfolding remagnetization (Fisher, 1953; Watson and Enkin, 1993). Within 10% or beyond 90% is statistically inconclusive. Linking the radiometric folding date to synfolding remagnetization is possible because the $^{40}Ar/^{39}Ar$ method dates illitization that occurs during folding (Fitz-Díaz and van der Pluijm, 2013; Fitz-Díaz et al., 2014 & 2016) as well as remagnetization that also occur during folding (Nemkin et al, 2016).

The synfolding analysis of deformed carbonates is the focus of this thesis and specifically applied to carbonates in the North American Cordillera from Canada to Mexico. Fold dating in the frontal Canadian and Montana Rockies have resulted in Eocene remagnetization ages, based on comparison with paleomagnetic synfolding results (Chpt. 2) (Enkin et al., 2000; Nemkin et al., 2016; Pana and van der Pluijm, 2015). To the south, remagnetizations were dated in the Monterrey Salient and central portion of the Mexico fold-thrust belt (Chpts. 3 & 4). In the Monterrey Salient a similar Eocene age is found for synfolding remagnetizations (Chpt. 3). Farther to the south, in central Mexico, a second, Cretaceous synfolding remagnetization is also preserved (Chpt. 4).

Along with quantitatively dating remagnetizations, an attempt was also made to determine the primary or secondary nature of orogenic rotation in the Monterrey Salient (Chpt. 3). The paleomagnetic data hints at a rotation, as explained in chapter 3, so calcite twinning was attempted to test this interpretation. However, after studying numerous thin sections it became evident that these muddy carbonates do not show any calcite twins, so complementary calcite-twinning analysis that was successful elsewhere (e.g., Kollmeier et al., 2000; Hnat et al., 2008) was not pursued further.

The key aspect of the approach is that magnetite needs to grow during folding in order to preserve a synfolding remagnetization. Instead of less well-constrained regional analyses, local folds are the target of the studies in this dissertation, in order to determine the age and pre- syn- or postfolding nature of the remagnetization for each fold. Targeting local folds does limit the wide-scale sampling of a region, but provides a much higher resolution study of the deformational and remagnetization history for an area.

Three studies are described in this dissertation, examining aspects of remagnetization and regional applications, from north to south along the Cordillera. Appendix A includes an incomplete study in the western US that can be used toward future analysis. Data from published chapters is and will be publically available in the paleomagnetic MagIC database.

Chapter 2 was published in Lithosphere (Nemkin et al., 2016) and examines samples from local scale folds within the Mississippian Madison Group of the frontal Montana Rockies. Directions have ~70° inclinations, which suggest a remagnetization because Mississippian directions should result in very shallow 0-10° inclinations. Individual and local fold tests produced pre- and synfolding directions, the synfolding directions further support a remagnetization of the sampled carbonates. Synfolding results are more inboard and the prefolding results are a part of the more frontal folds of the belt. This remagnetization is a product of a chemical growth of magnetite in the samples that formed superparamagnetic (SPM) and single-domain (SD) grains. Magnetite likely grew as a result of interaction with fluids and based on magnetic intensity results in the study area, it is suggested that the fluids were more dominant inboard and diminished towards the east. We surmise that low fluid activity in the foreland (most eastern sample) did not allow sufficient magnetite to grow and record a stable direction. By utilizing synfolding results and previously determined deformation ages for the Rocky Mountains, an Eocene age of the remagnetization can be assigned. Based on the relative timing of remagnetization, two folding events are determined, folding commenced (i.e. synfolding magnetization) during a remagnetization event while the most frontal portion was still undeformed (i.e. prefolding magnetization) and this frontal portion was folded after the remagnetization event.

Chapter 3 is under review for publication in Tectonophysics and examines the Lower Cretaceous La Peña-Cupido and La Peña-Tamaulipas Inferior formations from the Monterrey Salient. The salient is part of the Mexican Fold-Thrust Belt in Northeast Mexico. Sampling of local carbonate folds resulted in eight synfolding remagnetizations (set A), one prefolding site (set B), and three complex results (set B). The complexity surrounding three of the folds is that the tests reveals k-versus-unfolding percentage diagrams with maximum unfolding peaks at 100 to 130 percent. These high percentages are likely the result of two deformation phases, an earlier horizontal folding phase and a later vertical rotation. The counterclockwise vertical rotation is further verified by a declination-strike test of set A and site means that show a departure from expected directions. A chemical remanent magnetization (CRM) carried by magnetite is postulated as the remanence carrier. Magnetite is present in the samples in a range of superparamagnetic (SPM) to single domain (SD) grains. In order to ascertain a remagnetization age, synfolding results are paired with published $^{40}Ar/^{39}Ar$ illite ages of folding, resulting in an age of 48-52 Ma. Note that results in the central Sierra Madre Oriental to the south of the Monterrey Salient (see Chpt. 4) also show an Eocene folding and remagnetization age.

Chapter 4, published in Geosphere (Nemkin et al. 2015), examines carbonates of the Tamaulipas Formation from the central Mexican Fold-Thrust Belt, Mexico. All of the samples are remagnetized and the remanence is carried by single domain magnetite. This chemical growth of magnetite is likely the result of rock interactions with an infiltrating Fe-bearing fluid. Ten individual folds tests throughout the study area produced six synfolding and four postfolding magnetizations. By combining previously determined $^{40}Ar/^{39}Ar$ folding ages with synfolding results, two distinct remagnetization events are recognized, at ~77 Ma and ~44 Ma. The older folding and remagnetization occurred in the Zimapán Basin and the younger event (44 Ma) in the

Tampico-Misantla Basin to the west, indicating that deformation traversed from west to east in the region.

Appendix A is a study of folded carbonate rocks in the ID-WY segment of the Cordillera that provided limited results. As compared to the expected shallow directions for Mississippian rocks, the results from Idaho show a clear remagnetization with steeper 60-70° inclinations. After site selection criteria, one fold in the Idaho portion of the study region provides a postfolding result. With the exception of two clearly present day field directions from two Wyoming sites, the remaining directions from Wyoming were considerably more scattered, leaving only two interpretable sites. The directions from these two sites are of normal polarity with steep inclinations. However, a more easterly declination (~80°) from one site does not fit with the expected direction for Wyoming. Given the limited availability of local folds, regional sampling in the area and comparison with synfolding results to the north (Montana, Chpt. 2) and south (Mexico, Chpts. 3 & 4) may better constrain the preservation and relative timing of ancient directions.

Appendix B explores the possibility of remagnetizations in Morocco and, instead, found primary Permian directions that contribute to our understanding of the Pangea A vs. Pangea B controversy. This controversy involves the Carboniferous-Early Permian configuration of Pangea ever since paleomagnetists postulated an overlap of the continents when trying to fit together the APWP's of Gondwana and Laurussia. Obtaining ages from the continent of Gondwana itself is very important because using proxies may have different ages. For example, comparing ~295 Ma rocks from Baltica and ~275 Ma results from Morocco ignores a ~20 myr mismatch. This may result in an error of up to 8 degrees, given Pangea's drift of 0.4 degrees per myr during the Early Permian. The results of this study support previously published directions based on more

precise age determinations (average U/Pb 284.7±6 Ma), which places rock units in the Early Permian (at the base of the Artinskian Stage). Most of the sites contain hematite as the remanence carrier and two sites resulted in magnetite carrying the recorded direction. Six sites have SE declinations and near-zero inclinations. From this study, two conclusions are drawn involving the inclination and age of the directions. The near-zero inclinations (as well as the average declination of about 135 degrees from Morocco) are expected from a conventional Pangea-A fit and the ages place the rocks in the Early Permian.

CHAPTER 2

REMAGNETIZATION AND FOLDING IN THE FRONTAL MONTANA ROCKY MOUNTAINS[1]

ABSTRACT

Local-scale folds within the Mississippian Madison Group of the frontal Montana Rockies preserve pre- and synfolding remagnetization data. Paleomagnetic results display inclinations of ~70°, in contrast to the expected shallower directions for North American Mississippian rocks. The magnetization is chemical in origin, preserved in superparamagnetic to single-domain magnetite grains from fluid activity. Magnetic intensity results in the study area suggest that mineralization was more prevalent in the interior of the fold-and-thrust belt and diminished toward the east, resulting in lower intensities from less magnetite growth in the very frontal portions of the belt into the foreland. Fold test results of individual folds show syn- and prefolding remagnetizations as a function of location across the belt, with synfolding results in more westerly locations and prefolding results in the most frontal folds of the belt. By comparing our synfolding results with previously determined deformation ages for the Rocky Mountains, an Eocene (53.6 Ma) age for the remagnetization can be assigned. Based on the relative timing of remagnetization, a spatial pattern of folding in the study area is revealed. Major folding commenced (i.e., synfolding magnetization) during an Eocene remagnetization event, while the most frontal portion remained undeformed (i.e., prefolding magnetization) and was subsequently folded after regional remagnetization.

[1] Nemkin, S.R., Lageson, D., van der Pluijm, B., and Van der Voo, R., 2016, Remagnetization and folding in the frontal Montana Rocky Mountains: Lithosphere, v. 8, p. 716-728, doi: 10.1130/L579.1.

2.1 INTRODUCTION

Remagnetization of carbonates is globally extensive (McCabe and Elmore, 1989; Jackson and Swanson-Hysell, 2012; Van der Voo and Torsvik, 2012). It is generally inferred that carbonate remagnetizations are of chemical origin, given that alternative mechanisms (thermal or viscous) can be rejected based on predicted burial temperatures (Elmore et al., 2012; McCabe and Elmore, 1989; Font et al., 2012; Zegers et al., 2003). Chemical carbonate remagnetization can be the result of the growth of magnetite to a stable single-domain state, preserving a paleomagnetic remanence. Several mechanisms have been proposed as the catalyst for this pervasive chemical remagnetization in carbonates, including organic matter maturation, illitization, orogenic fluid movement, and hydrocarbon migration (Katz et al., 1998). Of these mechanisms, two ideas for the facilitation of chemical remagnetization seem to dominate the literature, orogenic fluid movement and illitization. In these cases, magnetite authigenesis occurs during the interaction with orogenic brine, when iron (Fe) is released during the process of converting smectite to illite, or as a combination of both (Elmore et al., 2012; Evans et al., 2000; Lewchuk et al., 2003).

Evans et al. (2012) used isotope data as support for a connection between chemically remagnetized rocks and orogenic fluid movement. Where the rocks were remagnetized, the isotope data revealed $^{87}Sr/^{86}Sr$ values that were more radiogenic than coeval seawater, suggesting that the area had experienced diagenetic fluid movement. Where the rocks were not remagnetized, the $^{87}Sr/^{86}Sr$ fell within the range of coeval seawater values, which would suggest the rocks were unaltered by outside fluids.

Alternatively, during illitization, smectite will transform to illite as temperatures increase with burial (Altaner and Ylagan, 1997). During illitization, iron is released, and this iron can

enable magnetite growth (Hirt et al., 1993). Woods et al. (2002) and Gill et al. (2002) supported illitization-induced remagnetization through a presence-absence test. Both studies looked at sedimentary rocks in which the occurrence of illite, from clay diagenesis (illitization), was associated with chemically remagnetized rocks, whereas the presence of smectite was associated with primary and/or weaker secondary magnetizations (Gill et al., 2002).

The timing of remagnetization in Mississippian carbonates from NW Montana is examined in this study in order to constrain the paleomagnetic history in the study area and its relation with deformation. Prior studies in the region have mostly focused on regional sampling to examine the mechanism and relative timing of magnetization (Eldredge and Van der Voo, 1988; Gill et al., 2002; Elliott et al., 2006; O'Brien et al., 2006, 2007). This study targeted individual folds to test for synfolding remagnetization and spatial variation of magnetic intensities in the deformation belt in terms of the relative timing of acquisition.

2.2 GEOLOGIC SETTING

The North American Cordillera extends from Canada to southern Mexico and was formed by Sevier and Laramide orogen-style deformation from the mid-Mesozoic to Eocene (Burch el et al., 1992; Dickinson, 2004). The portion of the Sevier orogen in NW Montana crops out from Glacier-Waterton National Park on the Canadian border to the Helena Salient in west-central Montana. This study focused on the very frontal segment of the Rocky Mountains in NW Montana. The frontal Rockies in the study region trend roughly N-S and were previously delineated into four subbelts with thrusts and associated folds in each section (Mudge, 1970, 1982). K-Ar dates from bentonites and structural evidence in the Montana Rockies indicate that deformation occurred ~72–54 m.y. ago (Elliott et al., 2006; Hoffman et al., 1976; McMannis, 1965).

Samples were collected from the frontal portion of the Montana Rockies, where N-S trending, eastward-verging folds and associated imbricate thrust faults sole into a regional décollement (Mudge, 1982). The regional décollement in the area dips to the west and progresses up section from Mesoproterozoic rocks in the west to Cretaceous rocks in the east (Sears, 2001). In the north, deformation began with emplacement of the Mesoproterozoic Belt-Purcell Supergroup over Cretaceous sedimentary rocks by the Lewis thrust fault (Willis, 1902; Sears et al., 2005). Within the frontal segment of the belt, deformation resulted in ~20 large imbricate thrusts that merge into a décollement in Cambrian shale (Mudge, 1982), including the Allan, Palmer, Beaver, Norwegian, French, Home, and Diversion thrusts (Lageson, 1987). These thrusts and folds verge to the east and place Mississippian carbonates over younger Cretaceous sandstones and shales (Mudge, 1970). Later modification of the Rockies in this area included Basin and Range extension with reactivation of thrust ramps as normal faults (Fuentes et al., 2011).

Mesoproterozoic rocks dominate the Montana Rockies except on the very eastern edge, where Paleozoic and Mesozoic rocks crop out (McMannis, 1965). The paleomagnetic target unit of this study was the Madison Group, consisting of limestone and dolomite that are typically thrusted on Cretaceous shales throughout the eastern (frontal) edge of the frontal Rockies. The Madison Group was deposited on a shallow platform during the Mississippian (359–323 Ma; Smith et al., 2004). It is estimated that the Madison unit is ~500 m thick in the frontal Rockies and thins to the east, toward the foreland (Deiss, 1943; Mudge, 1970).

The Madison Group is an unconformity-bounded carbonate unit with two internal composite sequences (Smith et al., 2004). It is subdivided into the Allan Mountain and Castle Reef Limestones in the frontal Rockies, which are equivalent to the Lodgepole and Mission

Canyon Limestones in the foreland (Mudge et al., 1962). The Madison Group has been thrusted on top of the Cretaceous Kootenai Formation, and both the Sun River and Teton Canyon transversely cut across the range, allowing for sampling of the folded Madison Group (Lageson, 1987).

2.3 METHODS

Sampling

The Mississippian Madison Group was the target of this study because access to local-scale folds is possible (Fig. 2.1). Two sites were also collected from the Cretaceous Colorado Group (HS1 and HS2), but these resulted in spurious demagnetization patterns and will not be discussed further. From the Madison Group, 17 sites were sampled: 13 from five local-scale folds (including three fold hinges) and four individual sites. One of the individual sites, SR1, was collected from a small exposure of the Madison Group in the foreland, also called the Sweetgrass Arch.

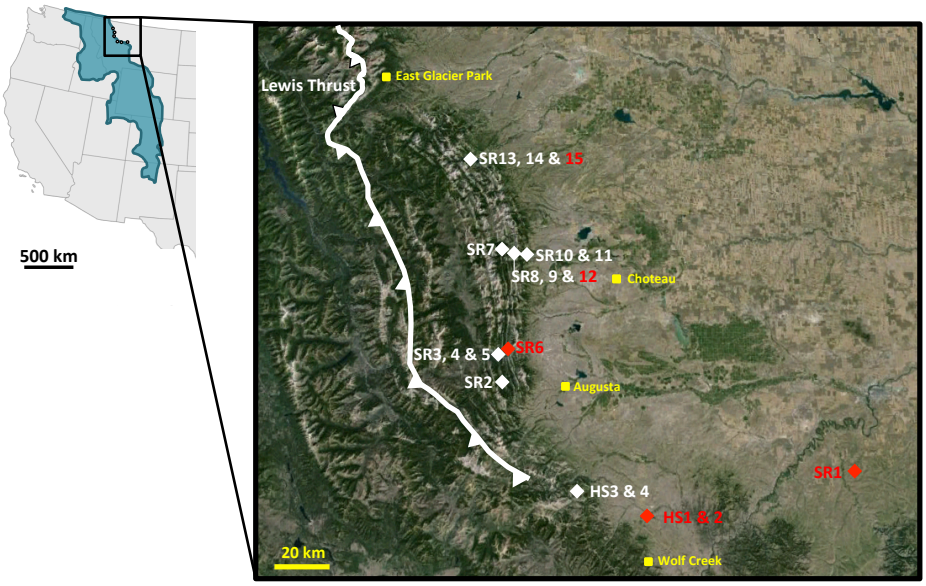

Figure 2.1: General outline of the Rocky Mountain region with corresponding field area in the frontal Montana Rockies (modified from http://geomaps.wr.usgs.gov/parks /province/rockymtn.html). Each marker corresponds to a sampled fold or individual site. Every fold includes two sites, with some adding a third site in the hinge. Red marker/text indicates a fold/site that was not interpretable due to spurious magnetic behavior during laboratory demagnetization.

The Sweetgrass Arch lies to the east of the Rockies in a relatively flat-lying, broadly uplifted area. Six to 10 cores were collected per site using a portable Pomeroy EZ Core Drill. A Brunton compass and inclinometer were used to determine the orientation of the beds, and the azimuth and plunge of the cores.

Laboratory

Cores were brought back to the University of Michigan and cut with a dual-bladed saw to 2.2 cm specimen lengths. Alumina cement was used to glue broken specimens back together. All specimens were labeled using Velvet Underglaze nonmagnetic temperature-resistant paint.

A three-axis 2G superconducting magnetometer was used to measure remanent magnetizations in a magnetically shielded room with a rest field of <200 nT. A trial run with both alternating field (AF) and thermal demagnetization showed similar magnetic directions (Fig. 2.2). However, the results with AF demagnetization revealed much smoother decay of the magnetization for all of the SR sites, which resulted in lower maximum angular deviations for

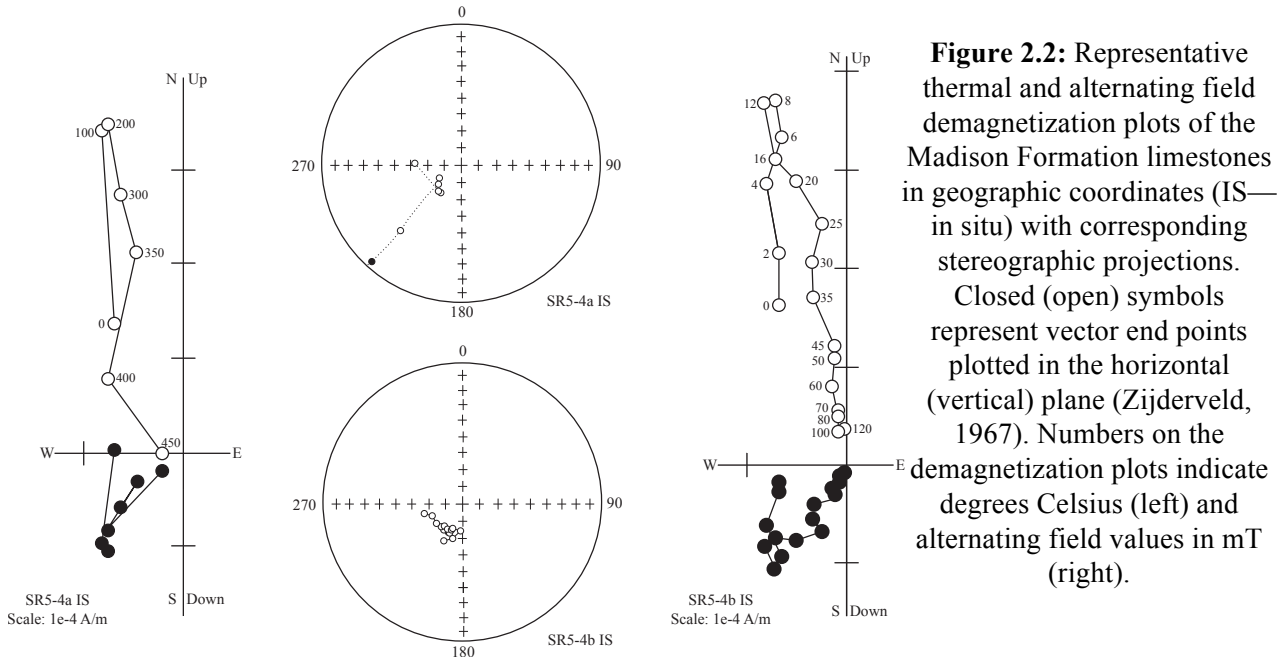

Figure 2.2: Representative thermal and alternating field demagnetization plots of the Madison Formation limestones in geographic coordinates (IS—in situ) with corresponding stereographic projections. Closed (open) symbols represent vector end points plotted in the horizontal (vertical) plane (Zijderveld, 1967). Numbers on the demagnetization plots indicate degrees Celsius (left) and alternating field values in mT (right).

AF-treated samples as compared to thermally demagnetized samples. Therefore, after the trial run, AF demagnetization was used to demagnetize the rest of the SR samples, with the exception of HS3 and HS4, which were thermally demagnetized. In order to reduce the acquisition of a viscous magnetization, specimens were measured directly after each demagnetization step.

A Lowrie test was performed using an ASC Scientific Impulse Magnetizer to impart a magnetization on a sample that was then thermally demagnetized. Magnetization was also applied and then demagnetized with AFs for a partial anhysteretic remanence experiment in order to examine the magnetic domain state. Magnetic hysteresis loops were acquired using a Princeton Measurements vibrating sample magnetometer at the Institute for Rock Magnetism in order to determine the distribution of magnetic coercivities. An AGICO MFK1-FA Susceptibility Bridge with CS4 furnace was utilized to determine the Curie point of the remanence- carrying magnetic mineral. Low-temperature measurements were also conducted at Institute for Rock Magnetism using a Quantum Design Magnetic Properties Measurement System to identify magnetic mineralogy by observing magnetic transitions and susceptibility dependence over a temperature range of 20–300 K.

Paleomac software by Cogné (2003) was used to analyze final demagnetization results with principal component analysis (Kirschvink, 1980). Site means were calculated by averaging the sample set directions (Fisher, 1953). In or0der to determine the relative timing of magnetization acquisition (pre-, syn-, or postfolding), the fold test proportionally untilts the fold limbs from measured bedding dips to horizontal (Tauxe and Watson, 1994; Watson and Enkin, 1993).

2.4 PALEOMAGNETIC RESULTS

This study presents the results of 13 out of 17 sites collected from the Madison Group;

the remaining four sites could not be analyzed due to spurious decay. Samples were not considered for further site analysis if the maximum angular deviation angle was greater than 20°. The magnetic characteristic directions of sites from the Mississippian Madison Group (HS3–HS4 and SR1–SR15) are shown in Table 2.1.

AF demagnetization of the SR sites revealed two vectors, a likely viscous present-day field component and the characteristic remanent magnetization (ChRM). The present-day field component was eliminated by 8–15 mT, and the characteristic remanent magnetization in the samples was nearly completely eliminated by 90–130 mT (Fig. 2.3). In the few trial samples that were thermally demagnetized, the ChRM was unblocked by 400–420 °C. The samples displayed laboratory heating-induced growth of a new mineral (suggested by a spike in the magnetic intensity) after heating the samples past 420 °C (Fig. 2.4B). For HS3 and HS4, thermal demagnetization was used to acquire the ChRM, which, in contrast to the SR sites, had normal polarity. In order to determine the characteristic direction, a steeper northward and normal-polarity component was first removed, as seen in Figure 2.3, for the HS and SR sites.

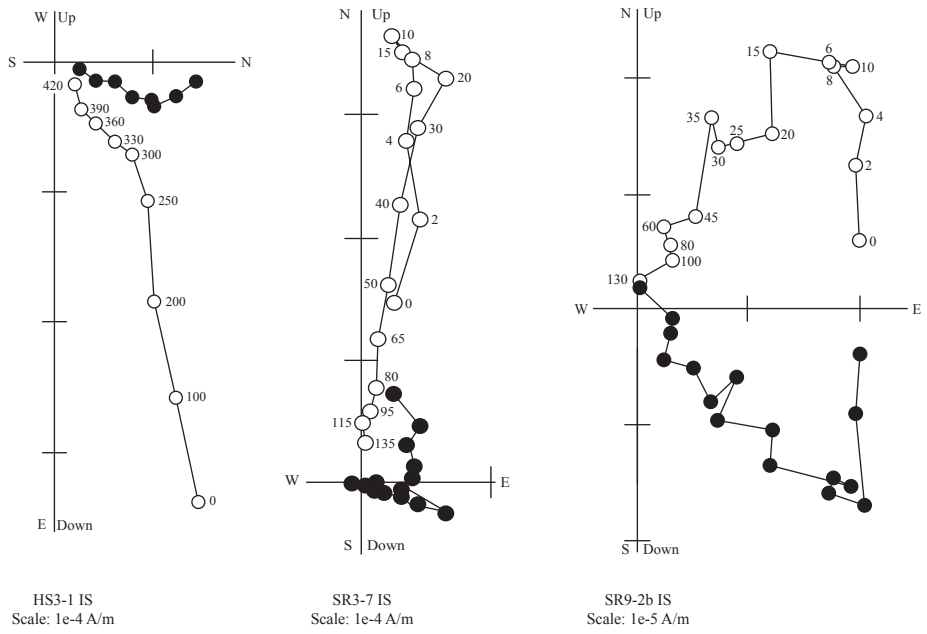

Figure 2.3: Representative thermal and alternating field demagnetization plots of the Madison Group limestones in geographic coordinates (IS—in situ; Zijderveld, 1967). Closed (open) symbols represent vector end points plotted in the horizontal (vertical) plane. Numbers on the demagnetization plots indicate degrees Celsius (HS3-1) and alternating field values in mT (SR3-7 and SR9-2b).

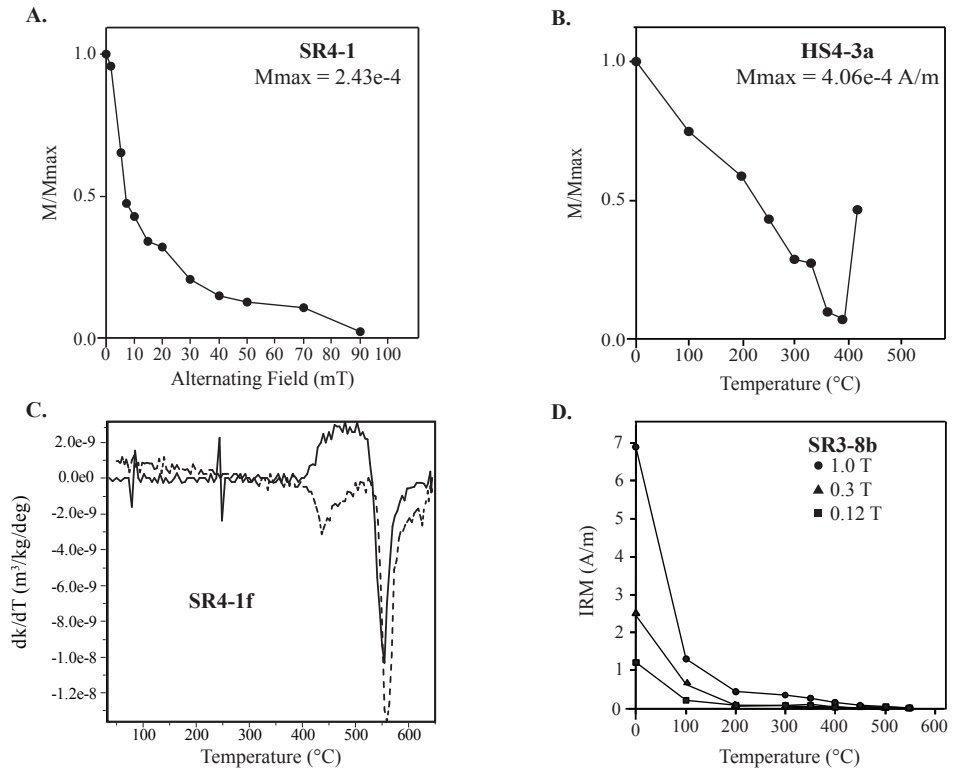

Figure 2.4: (A) Normalized alternating field demagnetization intensity plot for SR4-1 showing near-complete elimination of the remanence at 90 mT. Mmax—maxi- mum magnetization; M/Max—measured magnetization divided by the maximum magnetization. (B) Intensity plot showing normalized magnetic intensity vs. temperature in degrees Celsius. HS4-3a is representative of samples that show a characteristic spike in magnetization after ~400 °C. (C) Derivative plot of susceptibility vs. temperature with solid/ dashed line representing heating/cooling curve. Plot depicts a Curie temperature of ~565 °C. (D) Thermal demagnetization of a three-dimensional isothermal remanent magnetization (IRM) acquired in an orthogonal system with the applied fields of 1.0 T, 0.3 T, and 0.12 T (Lowrie, 1990).

A three-dimensional isothermal remanent magnetization was applied using an ASC Scientific Impulse Magnetizer and then demagnetized, revealing goethite by the occurrence of a highly coercive component and corresponding low unblocking temperature (~120–150 °C). Continued decay of the other size fractions to ~550 °C supported the presence of magnetite (Fig. 2.4D; Lowrie, 1990). Low-temperature experiments indicated goethite at low temperatures but not at room temperature, leaving magnetite as the main remanence carrier. Partial anhysteretic remanent magnetization of a few samples as well as wasp-waisted hysteresis loops revealed a

larger contribution of superparamagnetic grains as compared to solely single- or multidomain grains (Fig. 2.5; Tauxe et al., 1996). The following hysteresis parameters indicated a combination of superparamagnetic and single-domain grains: quality factor (Qf), remanent magnetization (Mr), saturation magnetization (Ms), coercive remanent magnetization (Brh), and coercive force (Bc; Fig. 2.6; Table 2.2; Day et al., 1977; Dunlop, 2002a, 2002b; Jackson and Solheid, 2000). Brh provides an estimate for Bcr (remanent coercive force).

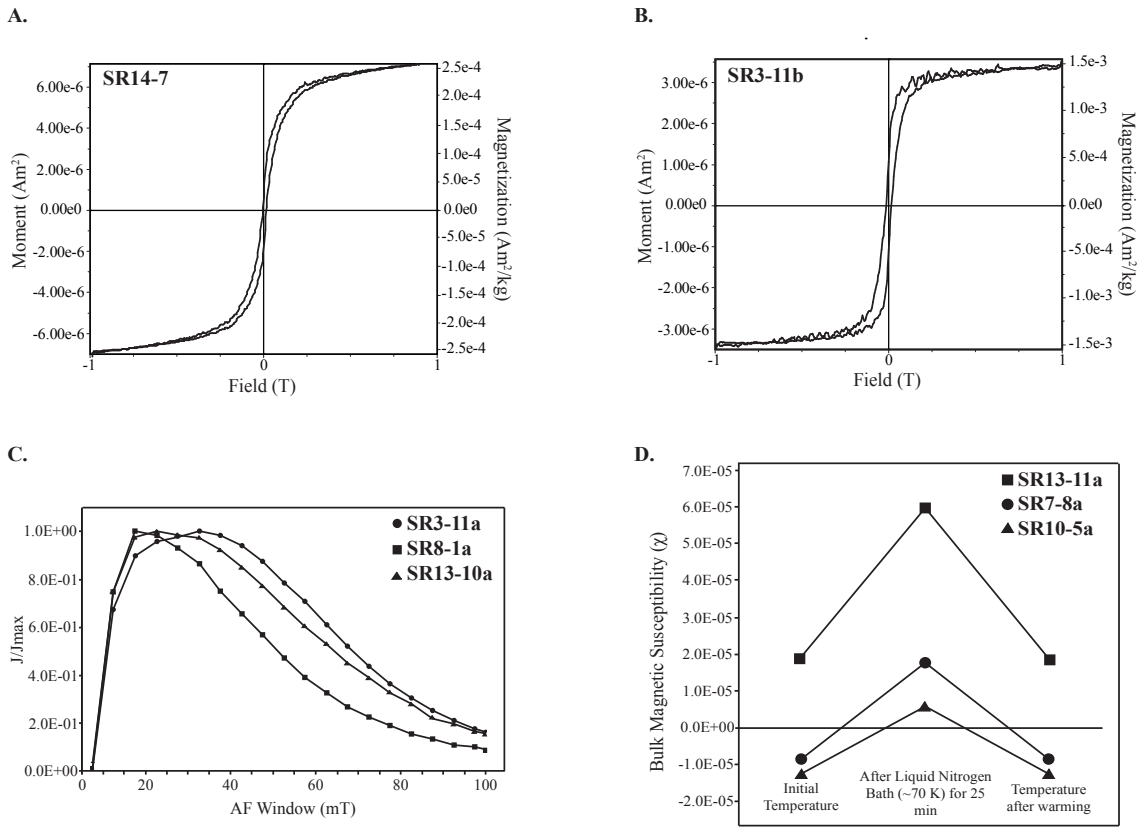

Figure 2.5: (A) Hysteresis loop corrected for diamagnetic and paramagnetic background. (B) Hysteresis loop corrected for diamagnetic and paramagnetic background. (C) Partial anhysteretic magnetization of three specimens from the study area. The *y-axis* is normalized to the highest magnetization measured (Jmax). AF—alternating field. (D) Plot showing the bulk magnetic susceptibility of representative samples before being placed in liquid nitrogen, after being place in liquid nitrogen and cooling to ~70 K, and after warming for 1 h.

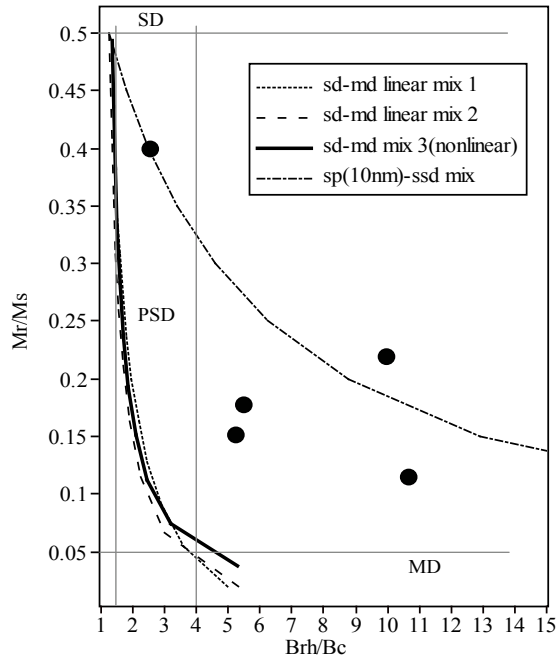

Figure 2.6: Hysteresis parameters with Dunlop mixing lines for Madison Group limestone samples from Montana (Day et al., 1977; Dunlop, 2002a, 2002b). Mr—remanent magnetization; Ms—saturation magnetization; Brh—median field of the Mrh remanent magnetization; and Bc—coercive force. Brh provides an estimate for Bcr (remanent coercive force). SD—single domain; PSD—pseudo– single domain; MD—multidomain. Hysteresis parameters are also depicted in table 2.2. Samples were chosen for the Day plot with a Qf (quality factor) of 1.2 or higher (Jackson and Solheid, 2000).

Sites SR2–SR14 (excluding SR6 and SR12 for spurious behavior) have upward and steep reversed polarity directions (~–70°), with SW to SE declinations. The two sites from the Madison Group in the Helena Salient (sites HS3 and HS4) preserve directions to the NW with normal polarities and steep directions (~+75°). The sampled sites include five local-scale folds. Three folds (A, D, and E) resulted in synfolding remagnetization directions using the Watson and Enkin fold test to proportionally untilt the beds, while the other two (folds B and C) preserve prefolding remagnetizations (Fig. 2.7).

2.5 DISCUSSION

The frontal Rocky Mountains of NW Montana expose folded Mississippian Madison Group carbonates that allow for paleomagnetic analysis of local-scale folds. As determined with three-dimensional demagnetization and high-temperature susceptibility experiments of representative samples, magnetite is the magnetic carrier (Fig. 2.4). The derivative of susceptibility versus degrees Celsius shows a Curie temperature of ~565 °C (Fig. 2.4C).

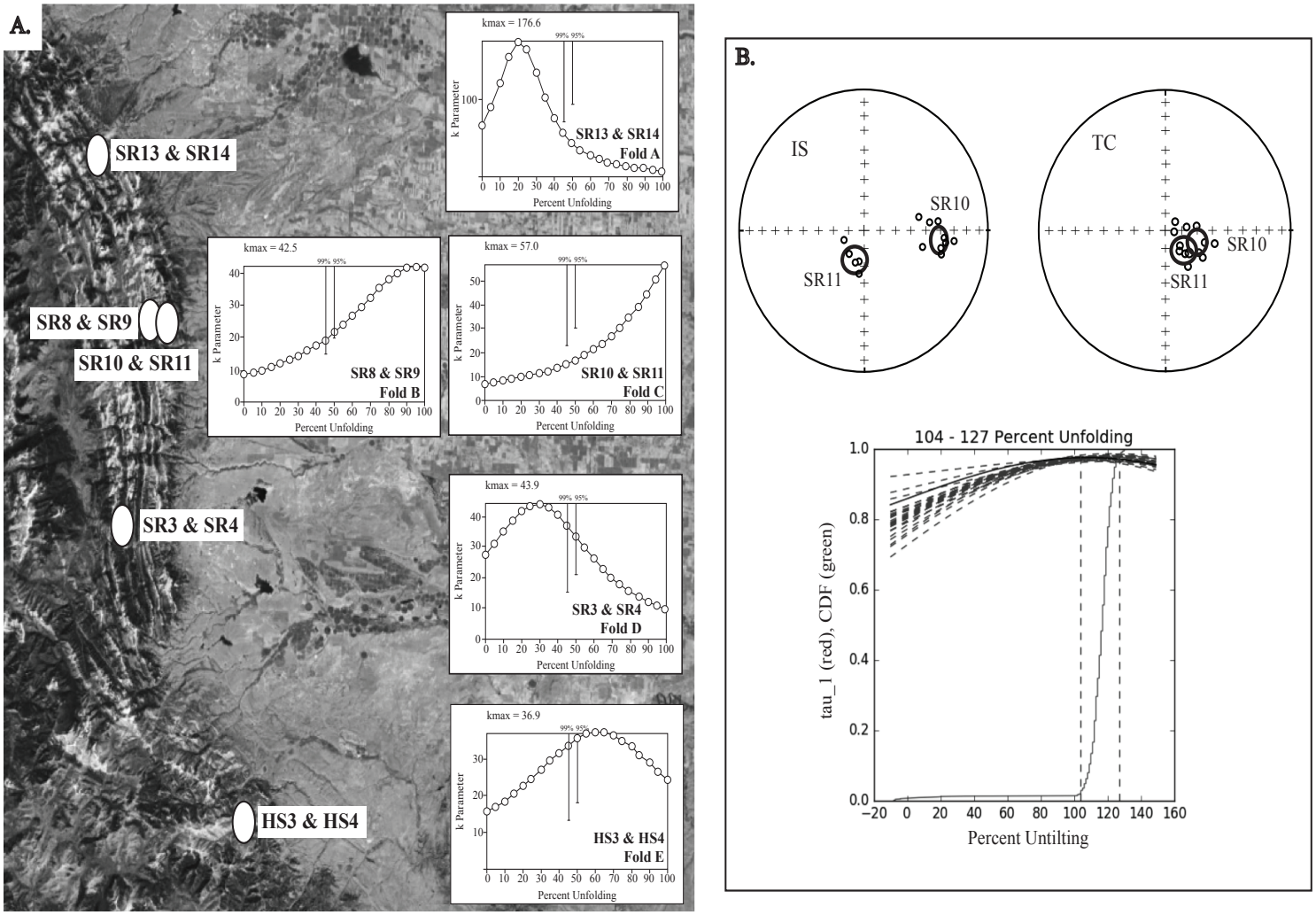

Figure 2.7: (A) Field area with corresponding fold test for each local fold. On each fold test plot, the 99% and 95% bars indicate the level of significance of the *k* ratio with respect to k_{max} (precision parameter that is a proxy for kappa [measure of the dispersion of a population that describes maximum clustering]; Fisher, 1953). (B) In situ (IS) and tilt-corrected (TC) stereographic projections of the site means of SR10 and SR 11 with a corresponding fold test (CDF—cumulative distribution function; Tauxe and Watson, 1994).

The initial field cooling and ferrimagnetic signal after warming during field-cooled–zero- field-cooled (FC-ZFC) experiments did not show a clear Verwey transition (Fig. 2.8). The initial field cooling also depicted a hyperbolic positive increase in the magnetization upon cooling to 20 K due to the overwhelming contribution of the paramagnetic behavior within the samples (Fig. 2.8A). Therefore, the ferrimagnetic component (Verwey transition) was masked by the more prevalent diamagnetic/paramagnetic signal of the samples during initial field cooling and suppressed during subsequent warming and cooling curves.

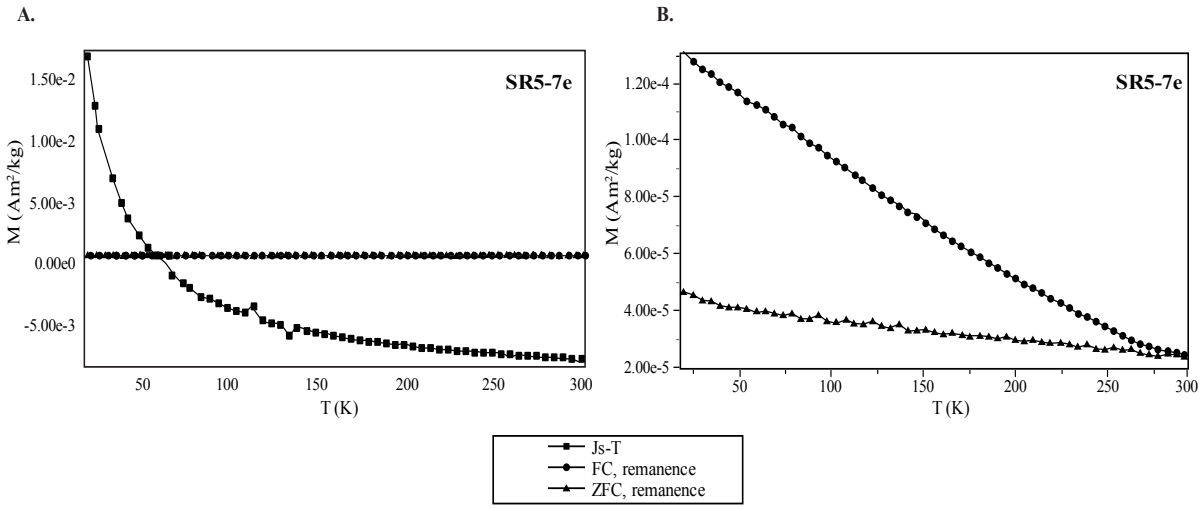

Figure 2.8: (A) Squares (Js-T) represent the acquired remanence of the sample in a 2.5 T applied field upon cooling from 300 K to 20 K. (B) Thermal demagnetization of low-temperature remanence for sample SR5-7e. Field-cooled (FC) remanence was imprinted by cooling in a 2.5 T field from 300 K to 20 K; zero-field-cooled (ZFC) remanence was imparted isothermally at 20 K by application and removal of a 2.5 T field (after zero field cooling from 300 K). Both remanences were measured while warming in a zero field.

Goethite was also present in the samples, as indicated by the Lowrie test and FC-ZFC curves. The Lowrie test displayed a highly coercive component that decayed by ~120–150 °C (Fig. 2.4D; Strangway et al., 1968). The FC-ZFC curves revealed a high magnetization of the FC curve at 20 K as compared to the lower magnetization of the ZFC curve at 20 K after a room-temperature magnetic saturation, which is indicative of goethite (Fig. 2.8; Guyodo et al., 2003).

Magnetite occurred as single-domain grains accompanied by a large superparamagnetic component in the samples from this study. Partial anhysteretic magnetization of a few samples indicated a magnetic carrier size dependence in the plot that could represent either a multidomain or super- paramagnetic/single-domain component. Size dependence was revealed by a peak in the normalized magnetization of each sample in the AF window 0–50 mT (Fig. 2.5C). Solely stable single-domain magnetic carriers will have a normalized peak at a higher AF window (~50–100 mT; Jackson et al., 1988). The peak in normalized magnetization that suggests a superparamagnetic/single-domain or multidomain magnetic carrier demonstrates similar behavior to what is observed in partial anhysteretic plots from the remagnetized Trenton Limestone in the eastern United States (McCabe et al., 1985).

Wasp-waisted hysteresis plots and results displayed in a Day diagram suggested a large superparamagnetic component in the samples (Fig. 2.6). A strong frequency dependence from 20 to 300 K also indicated a broad distribution of nanoparticle sizes (Fig. 2.9; Jackson and Swanson-Hysell, 2012; Worm, 1998). A robust paramagnetic contribution was seen in the hyperbolic rise of the susceptibility from ~50 to 20 K (Fig. 2.9A) and was removed to observe the large distribution of nanosizes (Fig. 2.9B). A Curie- Weiss model paramagnetic susceptibility ($k\,[T] = c/[T - è]$) was constructed interactively and subtracted from the measured susceptibilities. Bulk susceptibility revealed a large paramagnetic contribution of the samples after being placed in liquid nitrogen for ~25 min (Fig. 2.5D). This spike in susceptibility of the samples after being cooled to ~70 K is interpreted to be due to the paramagnetic nature of the samples responding to the presence of an ambient magnetic field when their thermal barrier was weakened (Tauxe, 2010).

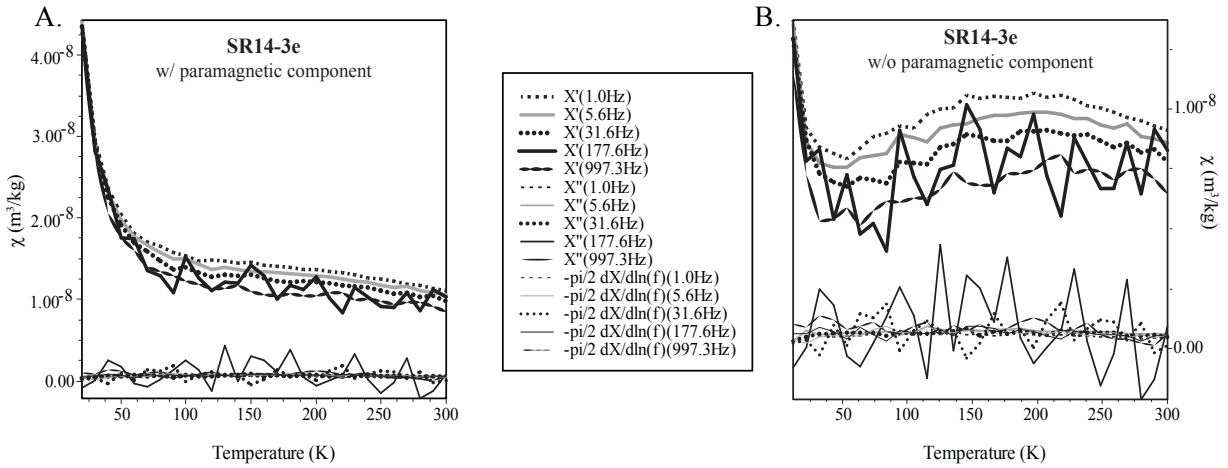

Figure 2.9: (A) In- and out-of-phase susceptibility at five frequencies for SR14-3e. Susceptibility as a result of the application of different frequencies was measured from 20 K to 300 K. (B) Correction for paramagnetic component that reveals a frequency dependence over the temperature range of 20–300 K, indicating a broad size distribution of nanoparticles (Jackson and Swanson-Hysell, 2012).

The ChRM observed after removal of the present-day field component is secondary, given its steeply upward remanence (~70°–75°) as compared to an expected shallower, North American Mississippian direction (Besse and Courtillot, 2002; Torsvik et al., 2012). Directions from the Madison Group sampled by O'Brien et al. (2007) also showed steep and upward directions (~70°) that ranged from southeasterly to south-southwesterly (Fig. 2.10). An imprecise age range of Late Cretaceous to Eocene can be assigned to the remagnetization event based on comparison to expected paleomagnetic directions for North America. However, this age can be further refined by correlating published deformation ages with our reported synfolding magnetization results. The refined age of the remagnetization is Eocene (53.6 Ma) based on deformation ages in the Montana Rockies (Elliott et al., 2006; Hoffman et al., 1976; McMannis, 1965), nearby southern Alberta Rockies (Pană and van der Pluijm, 2015), and northern Wyoming Rockies (Solum and van der Pluijm, 2007).

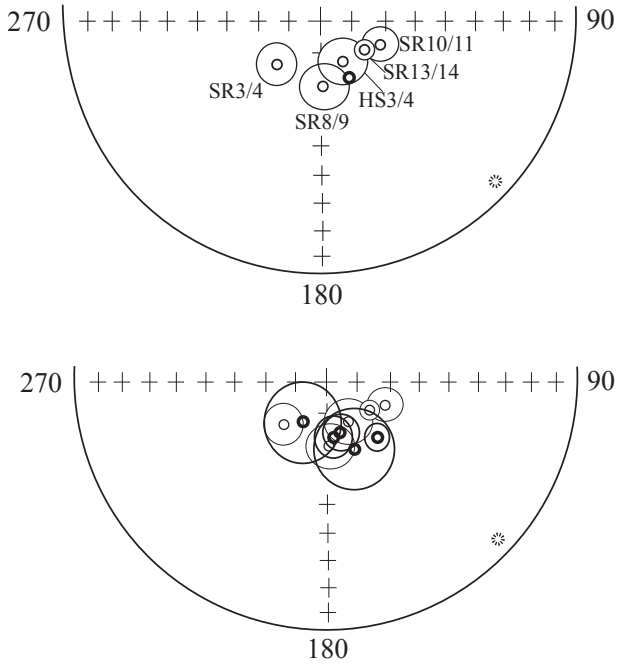

Site	kmax	% Unfolding	Declination	Inclination
SR3/4	43.9	30	225.4	-70.3
SR8/9	42.5	100	177.0	-69.5
SR10/11	57.0	100	112.5	-70.2
SR13/14	176.6	20	122.9	-73.8
HS3/4*	36.9	60	151.1	-75.2
O'Brien 1	**31.7**	**75.5**	**171.2**	**-70.7**
O'Brien 2	**50.8**	**93.6**	**167.6**	**-71.4**
O'Brien 3	**62.7**	**97.3**	**138.9**	**-64.6**
O'Brien 4	**15.1**	**60.9**	**208.4**	**-74.0**
O'Brien 5	**29.6**	**43.9**	**157.7**	**-65.9**

Figure 2.10: Stereonet with expected directions and results from this study. The dashed circle represents the expected Mississippian direction for Montana (determined from Besse and Courtillot, 2002;Torsvik et al., 2012); solid thick circle represents the expected reversed Late Cretaceous to Eocene direction in the top plot. The plotted site means represent optimal clustering for each fold (values listed in table) for this study (black) and that of O'Brien et al. (2007; thicker black lines shown in bottom plot). *HS3/4 is represented by the inverse of the optimal direction (declination, inclination: 331.1, 75.2).

In the study area, the remagnetization spans a reversal, as seen by down and steep directions from HS3 and HS4 and up and steep directions from the remaining sites. Samples to the east of the Rockies deformation front (site SR1) are represented by a clear present-day field magnetic component and then spurious decay of the remaining magnetization. A similar result was observed in foreland Cretaceous rocks studied by Gill et al. (2002). Thus, there was not sufficient magnetite growth to preserve Cretaceous–Eocene remagnetization away from the orogenic front in the foreland or Sweetgrass Arch.

Both syn- and prefolding remagnetizations were found in the study area by proportionally unfolding the fold limbs with the Watson and Enkin fold test method (Watson and Enkin, 1993; Fig. 2.7). When untilting was carried out in an asymmetric fashion, the results stayed synfolding

in character. All of the fold tests were from outcrop-scale folds, which best allow an incremental fold test to determine the relative timing of the remagnetization. Folds A, D, and E (tighter folds) showed synfolding remagnetizations, whereas folds B and C (comparatively more open folds) preserved prefolding remagnetizations. With incremental unfolding in fold SR10/SR11, the k_{max} (maximum clustering) surpassed 100% unfolding due to a slightly more scattered site average for SR10. As seen in the stereographic projections for in situ and tilt-corrected data, the directions from each limb approach each other upon tilt correction, but they do not fully overlap (Fig. 2.7B). Therefore, an eigenvalue and bootstrapping fold test method (Tauxe and Watson, 1994) was employed, showing that the optimal clustering occurred shortly after 100% unfolding, at ~104%-127% unfolding.

O'Brien et al. (2006, 2007) sampled the same Mississippian carbonates and found pre- and synfolding and tilting magnetizations in the frontal Montana Rockies. Those authors conducted a fold test when they were able to sample a fold, and where they could not sample a fold; they conducted tilt tests for samples taken from local thrusts. Similar to this study, a synfolding remagnetization was found near fold A (O'Brien et al., 2007). Within the Teton Canyon (North and South Forks of the Teton River) in the vicinity of folds B and C, O'Brien et al. (2007) found both pre- and synfolding/tilting magnetizations. A prefolding magnetization was found in the Teton anticline, i.e., the very frontal portion of the deformation belt, and a pretilting magnetization was observed in the Teton River thrusts, all comparable to the prefolding results in the same area from this study. A synfolding magnetization was also found in the Teton Canyon area, in contrast to the prefolding results from their work and this study (O'Brien et al., 2006, 2007). Tilt tests for thrusts in the Sun River Canyon (around fold D) revealed syntilting (O'Brien et al., 2006) and then pretilting magnetizations (O'Brien et al., 2007). This change was

likely due to an increased number of sites that were measured and analyzed in the later paper. The pretilting result from the Sun River Canyon is in contrast to the synfolding result from fold D, likely due to the regional thrust sampling versus local fold sampling of this study.

Other studies in the area used regional tilt tests for Cretaceous-aged thrusts, as opposed to local-scale folds sampled in the Mississippian Madison Group limestone for this study. Elliott et al. (2006) found a pretilting chemical remagnetization in Cretaceous carbonate concretions from three sampled sites in the frontal Rockies near fold D from this study. However, this pretilt result may not be reliable due to the very few samples used for the tilt test and its regional application. Gill et al. (2002) also sampled Cretaceous rocks in the frontal Rockies near fold D and found pretilting or, possibly, early synfolding magnetization in a single regional fold test.

Fold test results in the study area show that folding coincided with remagnetization, whereas in the very frontal portion of the belt, it post- dated remagnetization. Notably, the difference between these behaviors correlates with fold style and location in the fold-and-thrust belt. Where folding postdates remagnetization, folds are open and located in the most frontal part of the belt, whereas folds formed during remagnetization are well developed, tight, and to the west of the frontal most portion of the deformation belt. This pattern indicates progressively younger and less- intense folding from the west to the east, a common observation in foreland fold-and-thrust belts.

Our interpretation is also supported by higher to lower ChRM magnetic intensity results from more interior locations to the most frontal locations of the sampled folds. The intensity values were determined after removal of the present-day field component to reflect the ChRM within the samples. Folds A and D are more westerly, followed by fold E, and, lastly, by folds B and C. Measured ChRM intensities are systematically lower toward the east (Fig. 2.11).

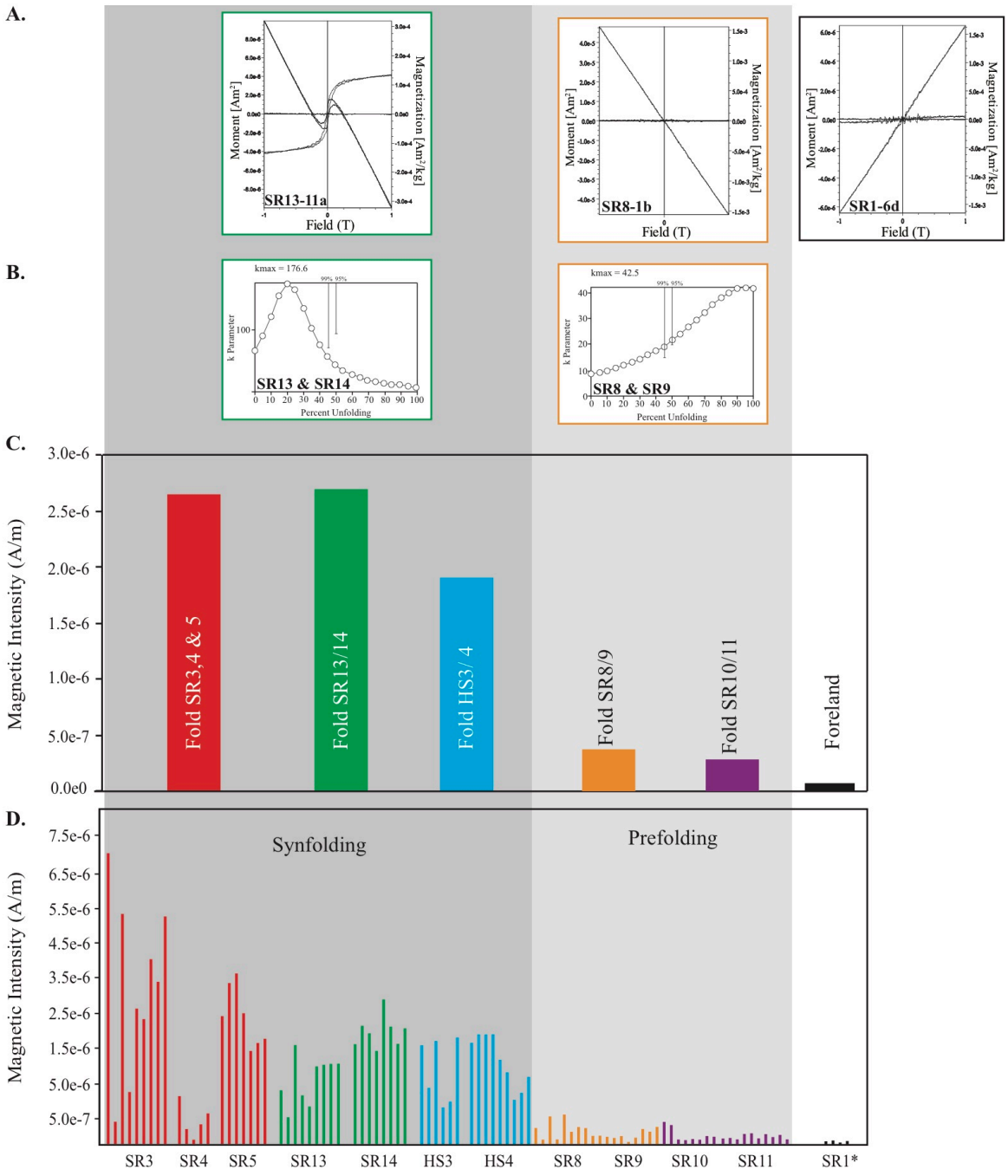

Figure 2.11: (A) Representative hysteresis plots from a sample with synfolding remagnetization, prefolding remagnetization, and the foreland. (B) Representative fold tests from samples with synfolding remagnetization and prefolding remagnetization. The *x*-axis and y-axis of the fold test plots are % unfolding and *k* (proxy for kappa), respectively (Fisher, 1953). (C) Average characteristic remanent magnetization (ChRM) magnetic intensities from each fold. (D) Magnetic intensity of samples in the study area from each fold after subtraction of the present-day field component, the k_{max}. SR1* is an individual site in the foreland.

Folds A, D, and E show higher intensities, while folds B and C have comparatively lower intensities. Site SR1, away from the deformation front, has intensities too low for an ancient magnetization to be observed, extending the pattern of lower/negligible intensities to the east in the foreland. The ChRM intensity values from site SR4 are lower than the other synfolding sites, and there is no obvious explanation as to why this occurs. However, the average ChRM intensity of folds SR3, SR4, and SR5 has a relatively high average compared with the other synfolding sites. In addition, a stronger ferrimagnetic component is depicted in hysteresis loops from folds A, D, and E as compared to samples from folds B and C, where the diamagnetic signal within the samples is more prevalent (Fig. 2.11).

According to a study by Hoffman and Hower (1979), maximum burial temperatures in the area were roughly 100–200 °C. Therefore, a thermoviscous remagnetization is not considered as the remagnetization mechanism based on the time-temperature relationship of magnetite (Pullaiah et al., 1975). Instead, the mechanism is interpreted as a chemical remagnetization due to growth of magnetite. Other paleomagnetic studies in the Montana Rockies have proposed illitization and fluid flow (± hydrocarbon migration) for the origin of the remagnetization in the area. In the study by Gill et al. (2002), illitization of smectite was proposed as the mechanism of remagnetization, based on the correlation of remagnetization in Cretaceous rocks in the frontal Rockies with higher percentages of illite, and in contrast, a lack of remagnetization in the foreland (Sweetgrass Arch), which is associated with higher ratios of smectite to illite. Elliott et al. (2006) also favored illitization as the mechanism for remagnetization in the area, but they were unable to constrain the paleomagnetic pole age well enough to conclude whether the characteristic magnetization was acquired prior to or during illitization. O'Brien et al. (2006, 2007) proposed remagnetization by fluids (including hydrocarbon migration) in the

Mississippian Madison Group, supported by higher $^{87}Sr/^{86}Sr$ values of remagnetized carbonates and the presence of hydrocarbons in vugs of the Madison Group limestone. We conclude that rock- fluid interaction and/or an illitization-induced chemical reaction each or both may have been responsible for the observed remagnetization, with neither mechanism uniquely constrained by our study and prior work (Gill et al., 2002; O'Brien et al., 2007).

Whereas a single mechanism for the chemical remagnetization experienced by Mississippian Madison Group limestone may not be discernible, there is clearly an association with deformation-associated fluid activity. Remagnetizations are a global occurrence; with individual remagnetization events typically correlated in time with local deformation events (e.g., McCabe et al., 1989; Stamatakos and Hirt, 1994; Weil et al., 2000; Van der Voo and Torsvik, 2012). In central Mexico, the Cretaceous Tamaulipas Formation displayed two distinct remagnetization events (ca. 77 Ma and ca. 44 Ma; Fitz-Díaz et al., 2014) that are correlated with a progression of deformation and fluid activity from the west to the east in the Sierra Madre Oriental (Nemkin et al., 2015). Elsewhere in the North American Cordillera, including Wyoming and Canada, remagnetization events are also Cretaceous to Eocene in age, and associated with deformation in the area (McWhinnie et al., 1990; Enkin et al., 2000; Cioppa et al., 2004).

In our study area, there is strong evidence that remagnetization progressed from west to east, weakening toward the foreland. This is recorded by magnetic intensity measurements and their diminishing values from more westerly folds in the study area to a broadly uplifted Madison carbonate sequence in the foreland. Folds A, D, and E show higher intensities (more magnetite growth), while folds B and C are comparatively lower (less magnetite growth). Site SR1, away from the deformation front, has intensities too low for ancient magnetization to be preserved, reflecting little to no observed magnetite growth (Fig. 2.11).

Progression of magnetite growth was likely due to orogenic fluid activity in the Montana Rockies. In northern Spain's Cantabrian arc, Weil and Van der Voo (2002) found evidence to support a tectonically related, fluid-mediated growth of magnetite, which led to pervasive chemical remagnetizations. Another example of fluid-mediated magnetite growth is the remagnetization detected in the Devonian Swan Hills Formation of Alberta, Canada (Gillen et al., 1999). Fluid activity/presence within the North American Cordillera is supported by strontium isotope data ($^{87}Sr/^{86}Sr$), fluid inclusion analysis, and the presence of calcite veins (Lerman, 1994; O'Brien et al., 2007). We conclude that fluid-mediated growth of magnetite occurred during the Eocene, based on the correlation of synfolding remagnetization and previously determined deformation ages in the frontal region of the North American Rockies. The trend of higher to lower magnetic intensities (i.e., more to less magnetite growth) from the westerly folds to the foreland suggests that fluid activity was spatially limited, in contrast to widespread foreland activity in the Appalachians of eastern North America (Stamatakos et al., 1996; Cederquist et al., 2006; Hnat et al., 2009). Remagnetized rocks are observed in the Montana Rockies fold-and-thrust belt, but no remagnetization was detected in the foreland, reflecting the limited extent of fluid activity, mineralization, and chemical remagnetization of the Madison Group limestone.

2.6 CONCLUSIONS

In the study area, a pervasive Eocene remagnetization is preserved in the deformed Mississippian Madison Group limestone that constrains the structural and magnetization history of the Montana Rocky Mountains. Remagnetization records both syn- and prefolding acquisition, and a pattern of progressively less growth of magnetite toward the foreland. Prefolding magnetizations indicate a late phase of folding in the most easterly portion of the Montana

Rockies, as compared to synfolding remagnetizations to the west or more interior of the fold-thrust belt.

As shown, magnetite growth resulted in a combination of superparamagnetic and single-domain grains, with a stronger diamagnetic/paramagnetic signal masking the ferrimagnetic signal in the prefolding sites as compared to synfolding sites. Given the low metamorphic conditions and likely chemical remagnetization, a local fluid origin is favored over a thermal or mechanical origin for this event. This fluid acted in a relatively narrow region, as seen by decreasing magnetic intensities toward the frontal portion of the belt and almost negligible intensities in the foreland. Therefore, we conclude that the Eocene remagnetization observed in the Montana Rockies was the result of chemically induced magnetite growth from fluids that were active during major deformation in the orogenic front, with a trend of decreasing magnetite growth toward the foreland.

TABLES

Table 2.1: Paleomagnetic data for samples collected from the Mississippian Madison Group in the frontal Montana Rockies.

					Bedding		IS Mean Magnetization		TC Mean Magnetization		Statistics	
	Site	**Latitude** (°N)	**Longitude** (°W)	**n/N**	**Strike**	**Dip**	**Dec.**	**Inc.**	**Dec.**	**Inc.**	**a95** IS&TC	**k** IS&TC
Helena Salient	1	47°5’36”	112°3’34.7”	spurious decay did not allow for analysis of site								
	2	47°5’36”	112°3’34.7”	spurious decay did not allow for analysis of site								
	3	47°9’33.5”	112° 19’ 2.5”	4/6	100.7	58.7	14.3	36.5	161.7	84.0	13.6	46.8
	4	47°9’35.4”	112° 19’ 10”	8/8	163.8	26.3	4.6	75.1	288.6	65.1	5.1	117.1
Montana Rockies	1	47°12’56”	111°11’27”	spurious decay did not allow for analysis of site								
	2	47°31’55.3”	112°45’29.1”	3/5	158.3	33.0	220.6	-45.6	180.1	-69.5	7.4	277.4
	3	47°36’37”	112°44’18.8”	7/9	354.0	32.7	220.3	-83.0	256.2	-52.0	7.3	69.2
	4	47°36’36.2”	112°44’17.9”	5/7	190.0	35.0	225.4	-57.5	162.3	-60.4	6.5	141
	5	47°36’37”	112°44’18.5”	7/8	238.7	34.7	207.4	-71.7	170.2	-43.5	4.4	189.1
	6	47°37’1.2”	112°43’51.3”	spurious decay did not allow for analysis of site								
	7	47°53’17.2”	112°43’13.5”	9/11	172.5	46.8	234	-40.8	169.3	-68.8	3.9	178.5
	8	47°53’11.2”	112°42’42.3”	5/8	146.5	25	216.1	-55.3	180.8	-76.1	4.4	301.6
	9	47°53’10.4”	112°42’31.7”	4/9	348.0	33.3	128.7	-56.0	188.1	-63.5	10.9	71.9
	10	47°53’16.1”	112°39’24.3”	8/10	359.0	31.8	97.4	-36.1	106.7	-67.2	6.8	68.3
	11	47°53’3.5”	112°40’0.1”	4/9	159.0	19.3	202.4	-72.3	130.8	-75.5	10.7	74.5
	12	47°53’11.1”	112°42’36.8”	spurious decay did not allow for analysis of site								
	13	48°9’56.8”	112°52’21.5”	8/11	321.0	64.5	92.0	-66.3	210.2	-41.9	4.1	181.9
	14	48°9’50.1”	112°52’23.3”	7/9	204.7	18.3	126.9	-77.6	119.8	-59.5	5.0	148.3
	15	48°9’51.9”	112°52’24.2”	spurious decay did not allow for analysis of site								

Note: n/N—number of samples accepted/measured; IS—in situ; TC—tilt-corrected; a95—radius of 95% cone of confidence in degrees; k—precision parameter (Fisher, 1953). Tilt correction is 100% untilting. Strike and dip were measured in degrees using the left-hand rule (LHR). HS1 and HS2 are from the Cretaceous Colorado Group and resulted in spurious decay. HS3–HS4 and SR1–SR15 are sites collected from the Madison Group limestone**.**

Table 2.2: Hysteresis data of representative samples from the Mississippian Madison Group limestone.

Sample	Qf	M_r ($Am^2 kg^{-1}$)	M_s ($Am^2 kg^{-1}$)	Brh* (mT)	Bc (mT)	M_r/M_s	Brh/Bc
HS4-1a	1.27	2.07 e-5	9.46 e-5	140.46	14.06	0.22	9.99
SR5-1c	1.48	2.51 e-5	6.28 e-5	37.59	14.75	0.40	2.55
SR6-6b	1.67	1.37 e-5	1.19 e-4	107.06	10.05	0.12	10.65
SR13-11a	1.90	2.39 e-5	1.35 e-4	57.26	10.46	0.18	5.47
SR14-7	2.18	4.15 e-5	2.73 e-4	53.10	10.14	0.15	5.24

Note: Qf—quality factor; Mr—remanent magnetization; Ms—saturation magnetization; Brh— provides an estimate for Bcr (coercivity of remanence); Bc—coercive force.

CHAPTER 3

CONCURRENCE OF FOLDING AND REMAGNETIZATION EVENTS IN THE MONTERREY SALIENT (NE MEXICO) ENLARGING THE PALEOPOLE DATABASE[2]

ABSTRACT

Carbonate formations from many locales reveal magnetizations that are secondary. Attaching a numerical age to these magnetizations would provide information on orogenic processes as well as enhance the paleopole database. To contribute to the effort of remagnetization dating, Lower Cretaceous formations from the Monterrey Salient in northeast Mexico, a part of the Mexican Fold-Thrust Belt, were sampled. Individual fold tests reveal eight site-pair synfolding remagnetizations (set A) of Eocene age. The remanence is a chemical remanent magnetization (CRM) carried by magnetite. The magnetization of set B is possibly due to an early carbonate alteration that produced a remanence significantly older than folding. A complexity of set B is that the site pairs reveal k-versus-unfolding percentage diagrams with maximum unfolding peaks at 100 to 130 percent. An explanation of multiple deformation phases with an earlier horizontal folding phase and a later vertical axis rotation is proffered for the past 100% peaks of the B sites. The later deformation, rotations about vertical axes, are revealed by a declination-strike test in set A sites and site means of the full collection that deviate counterclockwise from the reference declination. By combining synfolding results with published $^{40}Ar/^{39}Ar$ illite ages of folding, remagnetization ages in set A sites of 48-52 Ma are

[2] Nemkin, S.R., Chávez-Cabello, G., Fitz-Diaz, E., van der Pluijm, B., and Van der Voo. *in review* Tectonophysics.

obtained. The magnetization in set B sites is likely older, though not well constrained. Interestingly, prior results from the central Sierra Madre Oriental, to the south, show two remagnetization events, Late Cretaceous and Early Eocene in age, in a succession from W to E. The age of folding and remagnetization acquisition in set A sites along the Monterrey Salient are concurrent with the frontal, remagnetized folds in the central Sierra Madre Oriental. Thus, the timing of major remagnetization in the Monterrey Salient occurred in the Eocene adding a well-dated event to the paleomagnetic database.

3.1 INTRODUCTION

Remagnetization of carbonates has become recognized as a widespread global occurrence, with many acquired during folding (Elmore et al., 2012; McCabe et al., 1983; McCabe and Elmore, 1989; Miller and Kent, 1988 Scotese et al., 1982; Stamatakos et al., 1996; Van der Voo and Torsvik, 2012). Prior attempts to date remagnetization events were qualitatively done by comparison to an apparent polar wander path (APWP) or an estimated age range based on conventional fold tests (e.g. Gillett and Karlin, 2004; Scotese et al., 1982). With recent developments of the $^{40}Ar/^{39}Ar$ fold dating technique (Fitz-Díaz and van der Pluijm, 2013; van der Pluijm et al., 2001), remagnetizations can be quantitatively dated when it occurred during folding; i.e., synfolding remagnetization. Key to the application of this approach is to target individual folds in local study areas, instead of a regional application of a fold test. This technique has been successfully applied to carbonates in the North American Cordillera from Canada to Mexico (e.g. Enkin et al., 2000; Nemkin et al., 2015; Nemkin et al., 2016; Pana and van der Pluijm, 2014). For example, in the Sierra Madre Oriental of central Mexico, fold ages from west (77 Ma) to east (44 Ma) are associated with synfolding remagnetizations (Nemkin et

al., 2015) and there are likely more carbonate remagnetizations around the world that can be dated through associated folding.

Well-exposed, folded carbonates are found in the Monterrey Salient of the Mexican Fold-Thrust belt in northeast Mexico. In this region limited paleomagnetic work has been reported, with work prior to the 1990's not recognizing a possible role of secondary magnetizations. In one of the earliest studies, Nairn (1976) argued for a primary magnetization in Upper Cretaceous, Lower Jurassic and Upper Triassic rocks. However, the study lacked stratigraphic controls that might have hinted at remagnetization. Gose et al. (1982) sampled Mesozoic red beds as well as some limestones and concluded that the magnetizations are primary, based on evidence of positive fold tests and mixed polarities. The authors note that their results deviate greatly from the expected North American directions, but attribute this difference to local rotations, which instead could include remagnetization. Kleist et al. (1984) sampled the Lower Cretaceous Cupido limestone in NE Mexico and concluded that the magnetization was primary and reflected a rotation of the Monterrey Salient.

Clement et al. (2000) studied mid-Cretaceous limestones and argued for primary magnetizations based on comparison to expected inclinations. The declinations vary greatly, which the authors used as evidence for rotations. Samples from two different canyons in the south of our studied area (La Boca and Santa Rosa) revealed normal and reversed polarities (Clement et al., 2000). This result hints that the samples may contain a remagnetization, given that the formations have been deposited during the long Cretaceous normal polarity chron, meaning a primary magnetization would not show dual polarities. Publications after 1990 began to recognize remagnetizations in the Monterrey Salient. Nowicki et al. (1993) reported synfolding magnetizations to the southwest of our study area.

The Monterrey Salient was chosen for this study of remagnetizations and folding because previous paleomagnetic work suggested that the carbonates preserve a magnetization of possibly secondary origin. In addition, the area provides excellent access to many mesoscale folds, presenting opportunities to study multiple, individual fold and their fold tests. In support of this study, folding in the Salient was recently dated by the $^{39}Ar/^{40}Ar$ method as Eocene (48-52 Ma; Fitz-Díaz et al., 2016), allowing for the quantitative correlation with remagnetization timing.

3.2 GEOLOGY

Tectonic activity along the western margin of North America resulted in Farallon plate subduction and continuous accretion during the late Mesozoic – early Cenozoic, leading to Laramide and Sevier style deformation in the North American Cordillera (Armstrong, 1974; DeCelles, 2004; Dickinson, 2004; Gray and Lawton, 2011). The North American Cordillera outcrops from Canada to southern Mexico, where its external tectonic manifestation is the Mexican Fold-Thrust Belt (MFTB; Fig. 3.1). The Sierra Madre Oriental is a local topographic manifestation of the Mexican Fold-Thrust Belt, which is dominantly an ENE verging thin-skinned fold-thrust belt (Campa-Uranga, 1983, Guzman and Cserna, 1963). The MFTB is primarily composed of folded Mesozoic sedimentary units, including Late Jurassic-Early Cretaceous carbonates, detached from basement units along Middle Jurassic evaporates and black shale (Guzman and Cserna, 1963; Eguiluz de Antuñano et al., 2000; Fitz-Díaz et al., 2011; Lawton et al., 2009; Suter, 1987). Regions within the MFTB show varying amounts of deposition with lateral facies variations, which were controlled by the distribution of Cretaceous paleogeographical elements. Paleographical features were inherited from the distribution of horsts and grabens formed during the rifting stage of the Gulf of Mexico in the Middle Jurassic (Goldhammer, 1999). The succession of rocks deformed in the Monterrey Salient is relatively

thick, and was deposited mostly in the Central Mexico Basin (Tardy et al., 1975), which was located between the Coahuila paleo-island and the Valles-San Luis Potosi platform, to the north and south, respectively. Middle Jurassic evaporites are thicker at the Monterrey Salient area and die out to the platforms, where the carbonates vary to shallower water platformal facies (Goldhammer, 1999).

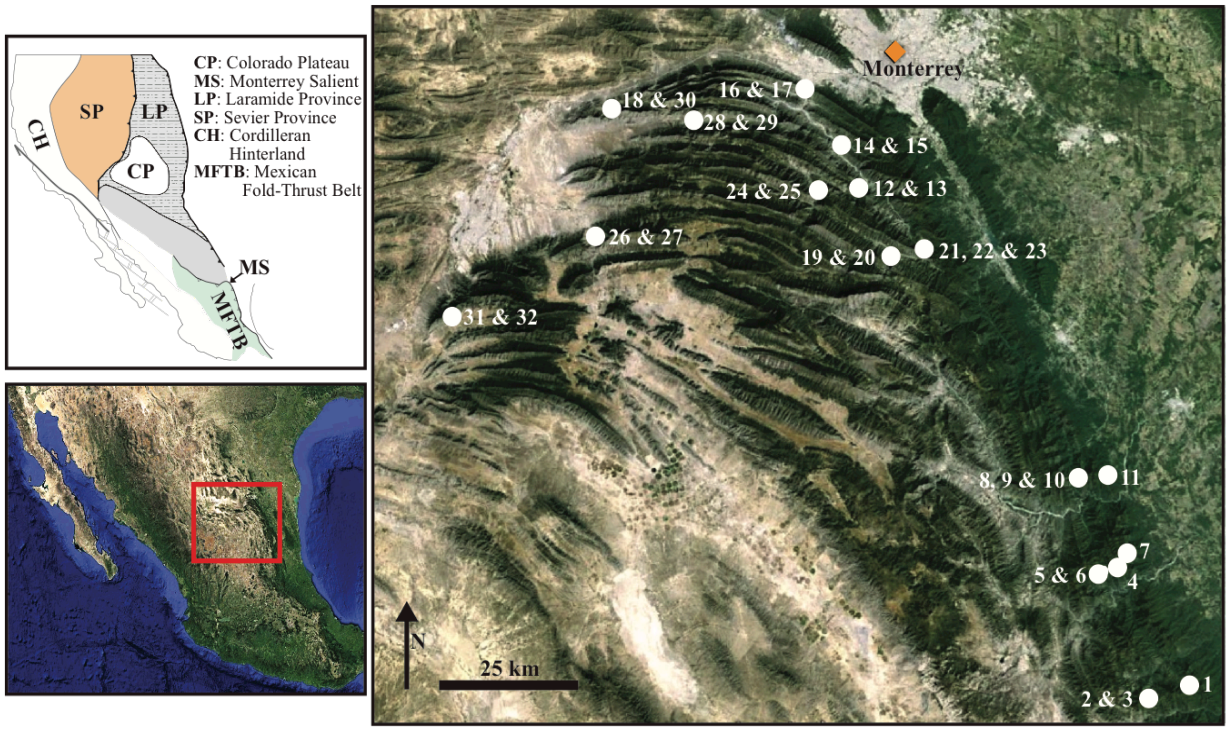

Figure 3.1: General tectonic map for the North American Cordillera (modified from Armstrong,1974; Fitz-Diaz et al., 2011). Google Earth image with each marker corresponding to a sampled fold or individual site in the Monterrey Salient of northeastern Mexico. Every fold includes two sites.

The Monterrey Salient shows abrupt trend changes in the northeastern portion of the Mexican Fold-Thrust Belt, possibly due to variant stratigraphy and paleogeography (Padilla y Sánchez, 1982; Prost, 1996, Fig. 3.1). At the salient, the trend of the belt changes northward from N-S to E-W (Campa-Uranga, 1983). Structural styles also vary based on the lithology, position around the curvature, and structural setting. In the Monterrey Salient a thick evaporite

detachment produces large upright, isoclinal folds in the middle of the curvature (Prost 1996; Camerlo, 1998). Folds become asymmetrical and show vergence to the north on the western side of the salient (Higuera-Díaz et al., 2005). Similarly, to the south, folds verge to the east and are associated with frontal thrusts (Chávez-Cabello et al., 2011).

The Lower Cretaceous La Peña-Cupido and La Peña-Tamaulipas Formation limestones are prevalent folded units throughout the Salient. The Cupido Formation is a shallow water carbonate unit that is interbedded with bentonitic shales (Goldhammer, 1999; Fitz-Díaz et al., 2016). Deepening of the Cupido followed by widespread platform drowning resulted in the deposition of the La Peña Formation (Lehmann et al. 1998, 1999). These thick shallow-water Cretaceous carbonates are later covered by Upper Cretaceous terrigenous units (Goldhammer, 1999). However, in the southern part of the Monterrey Salient, the Cupido Formation shows facies variations to deeper water sedimentary conditions. In the Santa Rosa and la Boca canyons and the Rayones section, the equivalent basinal carbonates (dark gray thinly bedded mudstone) to the Cupido are locally known as the Tamaulipas Formation (Goldhammer, 1999). In this area, sample collection was located in the transition between the Tamaulipas Inferior and the La Peña Formation.

3.3 METHODS

Sampling

A total of thirty-two sites were collected, twelve sites from km-scale folds in the La Peña-Cupido Formations in the northern portion of the Monterrey Salient, and twenty in the La Peña-Tamaulipas Formations in the southernmost localities (Santa Rosa and La Boca canyons and road to Rayones) (Fig. 3.1). Samples were collected with a portable Pomeroy EZ Core Drill and oriented with an inclinometer and Brunton compass. The strike and dip of the sampled beds were

measured with a Brunton compass using the left hand rule (LHR) convention (fingers point in strike direction and thumb points down dip). For beds that are overturned, the bedding information in Table 3.1 reflects the conventions that comply with the Paleomac program by Cogné (2003).

Laboratory Work

Samples were cut to 2.5 cm length with a dual bladed saw at the University of Michigan paleomagnetic laboratory. Velvet Underglaze non-magnetic temperature resistant paint was used to label all of the samples and alumina cement was used when necessary to glue samples back together. Typically weak remanent magnetizations were measured using a three-axis 2G superconducting magnetometer. An ASC TD-48 demagnetizer was used to thermally demagnetize the samples to ~500°C. All specimens were measured and demagnetized in a magnetically shielded room, with a rest field of 200 nT, to prevent accumulation of any unwanted viscous magnetization.

Demagnetization data were analyzed with the PaleoMac software by Cogné (2003) and graphed in orthogonal or stereographic projections (Zijderveld, 1967). Sites were not included for further analysis if the site k value (Fisher, 1953) is less than 10. Principal component analysis (PCA) was used to examine the data and the fold test was applied in order to determine whether the magnetizations were acquired pre-, syn-, or postdeformation (Kirschvink, 1980). The fold test proportionally untilts the fold limbs from the current configuration to horizontal (0-100% unfolding) using the field-measured bedding dips (Tauxe and Watson, 1994; Watson and Enkin, 1993). In order to perform a fold test past 100% unfolding a similar method as the one that is described by Watson and Enkin (1993) is used in Stereonet 9 (Cardozo and Allmendinger, 2013) to progressively unfold each limb and calculate the k parameter (amount of clustering) after each

step. Synfolding magnetizations were unambiguously diagnosed for any fold test where the peak k parameter fell between 10-90% unfolding; these samples are grouped as set A. The convention for prefolding magnetization is to have a peak k value at ~100% unfolding, whereas post-folding is around 0 unfolding. For the situation in our study where fold test results reach a maximum k value outside the window of 0-100% unfolding, these samples are grouped in set B. Both sample sets have distinct areal distribution in the region and a discussion of possible explanations for this pattern will be presented in a separate section below.

Three orthogonal magnetizations (120mT, 300mT and 1000mT) were imparted on selected samples with an ASC Scientific Impulse Magnetizer and then thermally demagnetized in order to perform a Lowrie test. The remanence carrying magnetic mineral was also determined by utilizing an AGICO MFK1-FA Susceptibility Bridge with CS4 furnace to determine the Curie point of the measured samples. Magnetic hysteresis loops were acquired using a Princeton Measurements vibrating sample magnetometer at the Institute for Rock Magnetism (IRM). Low temperature measurements were also conducted at the IRM using a Quantum Design Magnetic Properties Measurement System (MPMS) to measure susceptibility dependence over a temperature range of 20-300K (Jackson et al., 1993).

3.4 RESULTS

The magnetic directions from 32 sampled sites of the La Peña-Cupido and La Peña-Tamaulipas limestones are listed in Table 3.1. Four sites (2, 8, 9, & 15) could not be analyzed due to spurious decay of the magnetization and an additional four sites (18, 19, 21 & 23) were not included in individual fold test analyses due to site-average k values being below the threshold minimum of 10. Thermal heating to ~500°C was employed to reveal the characteristic magnetic components, after which typically a spike in magnetization was observed, likely due to

laboratory-induced growth of magnetic minerals. Most samples display two magnetic components, the present day field and a characteristic component (Fig. 3.2).

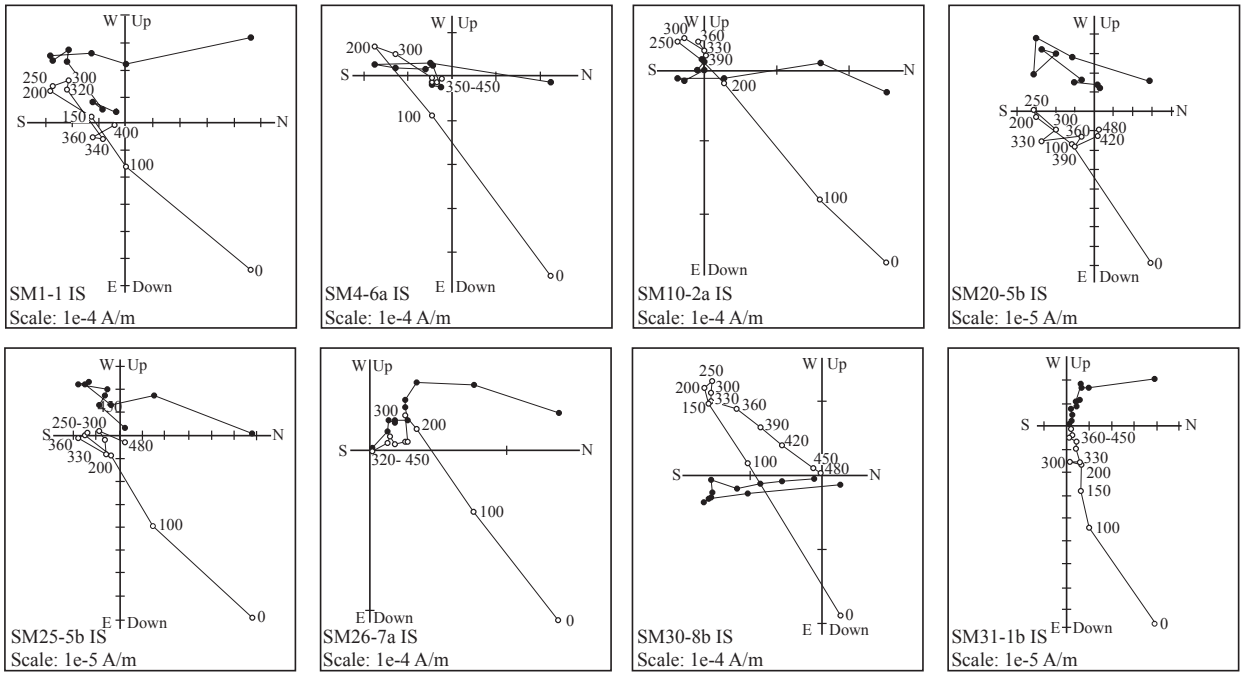

Figure 3.2: Representative thermal demagnetization plots of the Lower Cretaceous La Peña-Cupido and La Peña-Tamaulipas Inferior formation limestones in geographic coordinates (IS, in situ) (Zijderveld, 1967). Closed (open) symbols represent vector endpoints plotted in the horizontal (vertical) plane. Numbers on the demagnetization plots indicate degrees Celsius.

The characteristic component is carried by magnetite as indicated by a Curie temp of ~580°C during high temperature susceptibility experiments and a Lowrie test (Fig. 3.3). A sharp decline of the high coercivity component around 100°C indicates the presence of goethite in some samples and the continued decay to ~500°C is representative of magnetite. Magnetite in the samples occurs as superparamagnetic (SPM) and single domain (SD) grains with hysteresis parameters of Qf: quality factor, Mr: remanent magnetization, Mrs: saturation magnetization, Brh: median field of the Mrh remanent magnetization, and Bc: coercive force. (Fig. 3.4; Table 3.2) (Day et al., 1977; Jackson and Solheid, 2000; Dunlop, 2002a, 2002b). Brh provides an

estimate for Bcr. Alternating current (AC) susceptibility tests in synfolding samples from the NS trending portion of the Monterrey Salient show a strong susceptibility dependence from 20-300K, indicating a very sizeable superparamagnetic component (Fig. 3.5a). In the EW trending portion of the belt, in the B direction sites, a strong paramagnetic contribution is seen in the AC susceptibility test (Fig. 3.5).

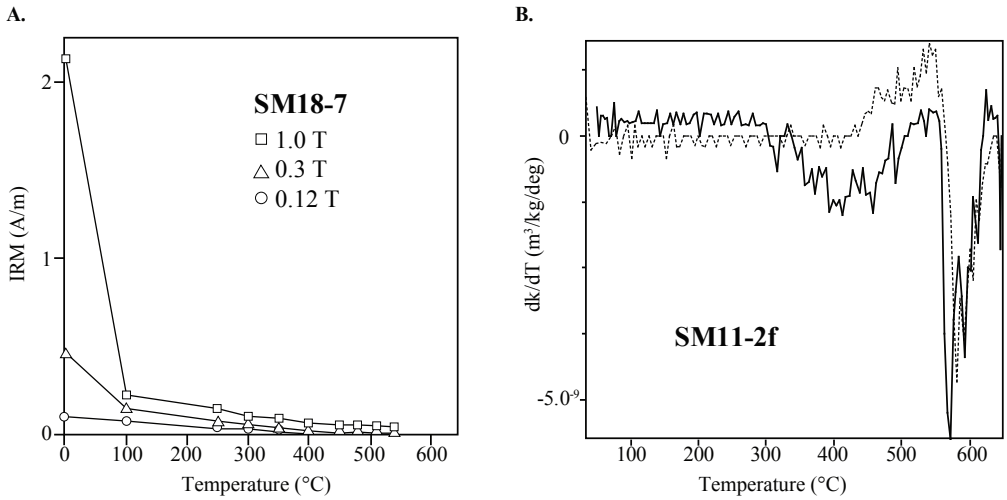

Figure 3.3: (A) Thermal demagnetization of a three-dimensional isothermal remanent magnetization (IRM) acquired in an orthogonal system with the applied fields of 1.0 T, 0.3 T, and 0.12 T (Lowrie, 1990). (B) Derivative plot of susceptibility versus temperature with dashed/solid line representing heating/cooling curve. Depicts a curie temperature of ~575°C.

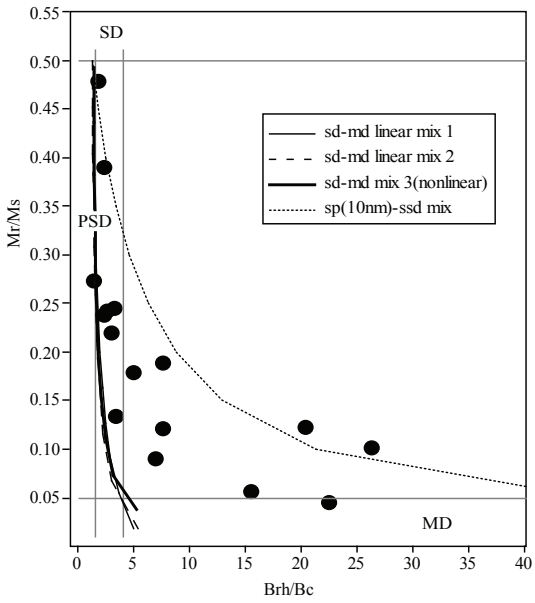

Figure 3.4: Hysteresis parameters with Dunlop mixing lines for limestone sameples from the Monterrey Salient (Day et al., 1977; Dunlop, 2002a,b). Qf: quality factor, Mr: remanent magnetization, Ms: saturation magnetization, Brh:median field of the Mrh remanent magnetization, and Bc: coercive force. Brh provides an estimate for Bcr. Hysteresis parameters are also depicted in table 3.2. Samples were chosen for the Day plot with a Qf (quality factor) of 1.2 or higher (Jackson and Solheid, 2000).

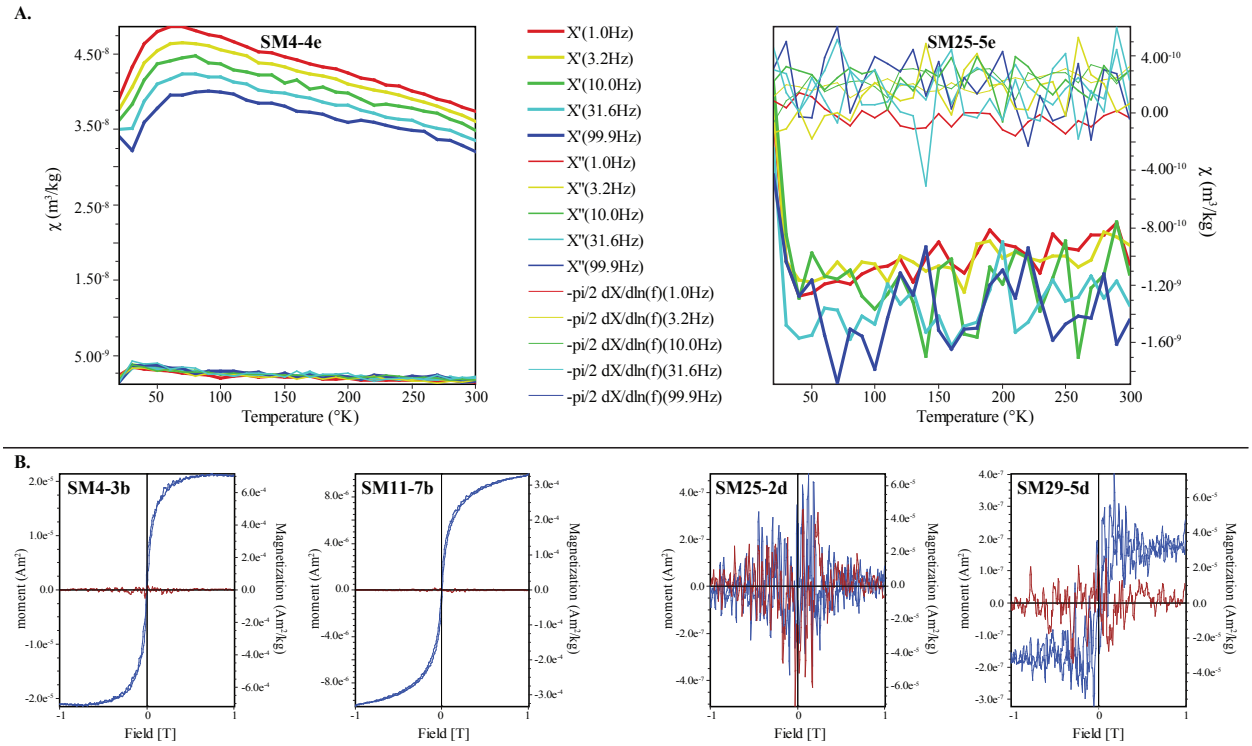

Figure 3.5: (A) In- and out of-phase susceptibility at five frequencies for two samples from the Monterrey Salient. Susceptibility as a result of the application of different frequencies was measured from 20 to 300 K. Each plot depicts the correction for paramagnetic component that reveals a frequency dependence over the temperature range of 20-300K. SM4-4e has a broad size distribution of ferrimagnetic nanoparticles and SM25-5e has a stronger paramagnetic as compared to the ferrimagnetic component (Jackson et al., 1993). (B) Hysteresis loops of representative samples in study area corrected for diamagnetic and paramagnetic background with blue/red representing the ferrimagnetic component/error respectively.

Fold test results across the area produce synfolding or complex results, grouped as set A and B, respectively, including two regional tests for SM19-23 and SM29/SM30 (Fig. 3.6d). Optimal directions for the area are upward and moderate to the S-SE or steep to moderate downward to the N-WNW (Fig. 3.6a). The set A magnetizations span a reversal as seen in upward directions to the S-SE and downward directions to the N-WNW. All of set B directions are downward to the N-WNW. We consider the possibility that the anomalous B results may represent an ancient or remagnetized direction.

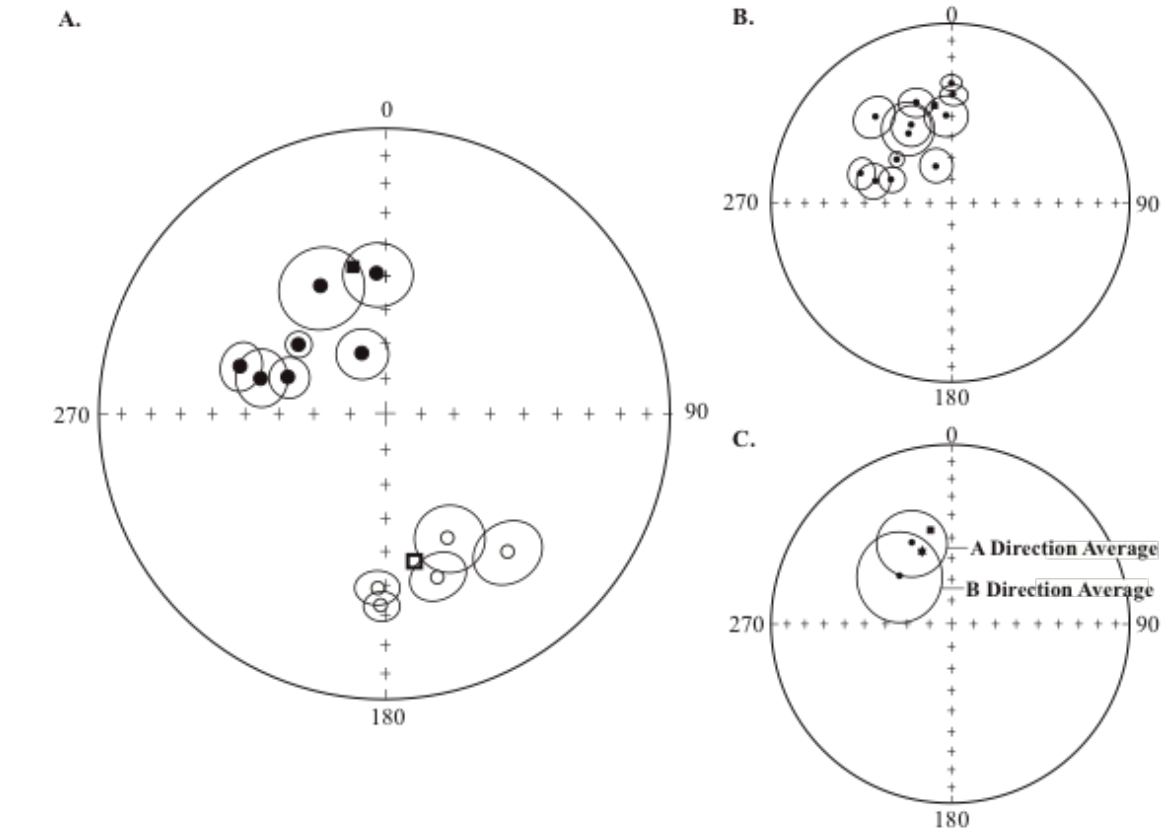

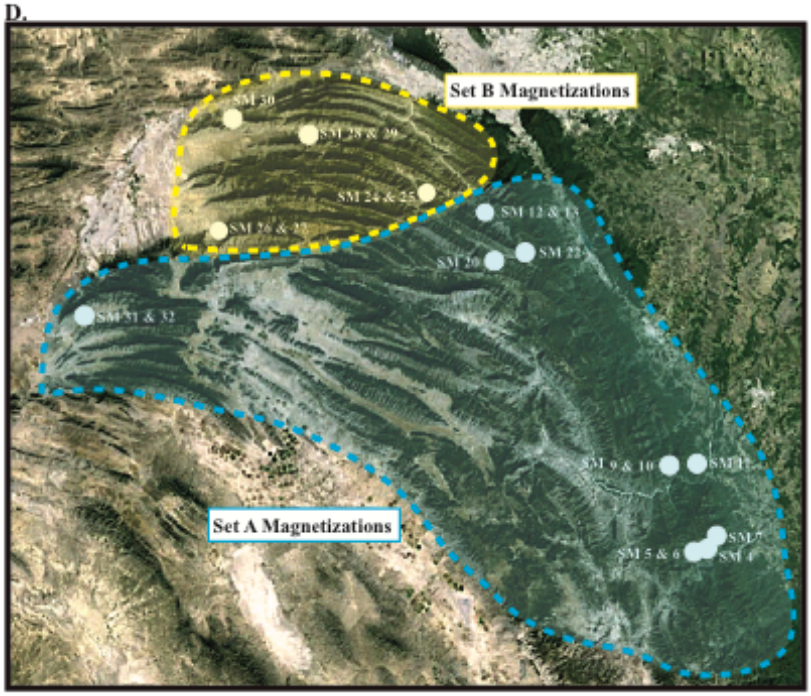

Figure 3.6: (A) Stereonet with optimal directions (circles) from individual fold tests for this study with the expected normal and reversed Eocene direction (closed square and open respectively) for northern Mexico. (B) All optimal directions in normal polarity with expected Eocene (square) (determined from Besse and Courtillot, 2002 and Torsvik et al., 2012). (C) Average of set A directions and set B directions compared to expected Eocene (square) and Early Cretaceous (star) directions for Mexico. (D) Field area with interpretable sites. Blue/yellow shaded regions represent the set A/B magnetizations clusters respectively.

3.5 INTERPRETATION

Rock Magnetism

The La Peña-Cupido and La Peña-Tamaulipas Inferior Formation limestones in the Monterrey Salient of the Mexican Fold-Thrust Belt contain a magnetization that is carried by magnetite as determined by three-dimensional demagnetization of an IRM (Fig. 3.3a). Magnetite is also shown with a derivative of susceptibility versus degrees Celsius experiment that reveals a Curie temperature of ~580° (Fig. 3.3b; Lowrie, 1990). A Day plot depicts a mix of this magnetite in superparamagnetic (SPM) and single domain (SD) grains (Table 3.2; Fig. 3.4).

A strong frequency dependence, as seen in Fig 3.5a, also supports a broad distribution of SPM-SD particle sizes (Jackson and Swanson-Hysell, 2012; Worm, 1998). There is a large paramagnetic component, but it is removed interactively with a Curie-Weiss model paramagnetic susceptibility ($k(T)=c/(T-\theta)$). Therefore, a large SPM contribution is seen when samples are significantly influenced by frequency changes for the in-phase susceptibilities after removal of the paramagnetic factor. Figure 3.5b does show a very minor frequency dependence, but here the paramagnetic signal is still very strong even after using the Curie-Weiss Model based on the in-phase susceptibility falling below the out of phase susceptibility (Worm, 1998). The mix of superparamagnetic to single domain grain sizes is an expected occurrence for remagnetized carbonates from the growth of magnetite (Jackson and Swanson-Hysell, 2012; Suk and Halgedahl, 1996; Xu et al., 1998). There is another pattern observed in the magnetization between the NS trending and EW trending portion of the belt. The magnetizations in the northern folds (set B) of the Monterrey Salient show overall weaker signals in ferrimagnetic strength from hysteresis plots as compared to the synfolding sites of set A (Fig. 3.5b).

Directional Analysis

Two consistent vectors are seen throughout analysis of samples, a present-day field component to the north and down, and a characteristic component. Characteristic directions are to the WNW-N with downward polarities and S-SE with upward polarities (Fig. 3.6a). The present-day field vector is strong as seen in a viscous remanent magnetization experiment by Schottenfels (2015). In that study, the shielded room provided a relatively field free environment, where after a few weeks and a measurement once a week, there was no longer any change in the magnetic intensity. The samples are then kept outside of the shielded room in the presence of a geomagnetic field over a span of a few weeks and measured once a week, which resulted in a clear increase in the intensity. Subsequently, the samples are placed back in the shielded room where the earlier intensity gain was then decaying.

Fold Test Analysis

Multiple synfolding magnetizations are documented in the Monterrey Salient by stepwise untilting both limbs of the limestone folds with the Watson and Enkin fold test method in the PaleoMac program (Cogné, 2003; Watson and Enkin, 1993). For the site-pairs that anomalously reach a peak of percent unfolding outside the zero to one hundred window, the Stereonet 9 program was used to incrementally unfold the limbs past 100% unfolding (Cardozo and Allmendinger, 2013).

Most of the fold tests are from large outcrop scale folds where limbs and fold axial planes are clearly identified, but two tests consist of a regional application where a local fold test could not be performed. Synfolding magnetizations were found in eight well-behaved folds (seven local and one regional) and arrive at synfolding results that have a parameter peak between 10-90% unfolding (Fig. 3.7). The SM19-23* fold test is kept in this synfolding A-group because the

optimal clustering peak is outside the range of 90-100% unfolding.

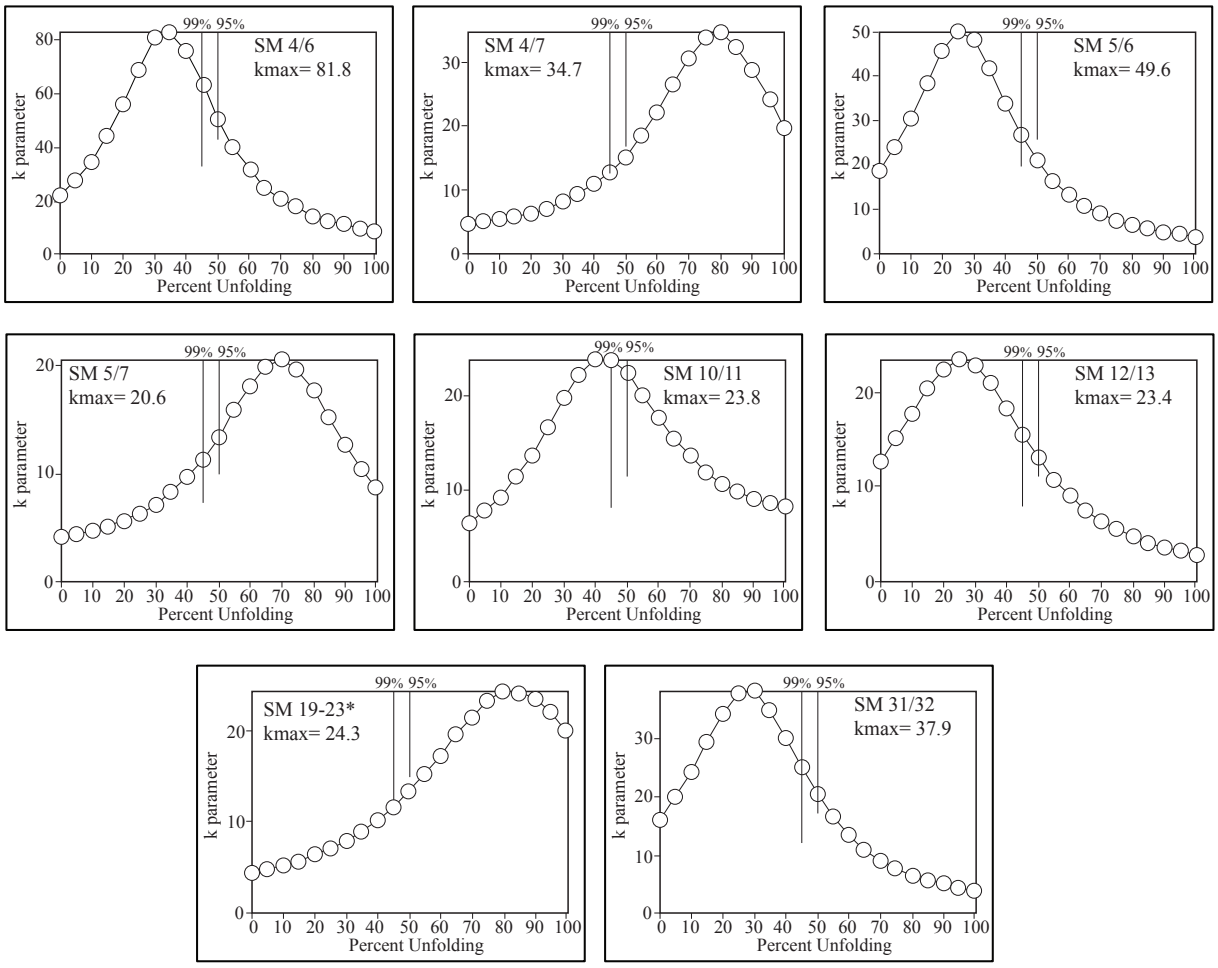

Figure 3.7: Set A fold tests from the Monterrey Salient. On each fold test plot, the 99% and 95% bars indicate the level of significance of the k ratio with respect to the kmax (precision parameter that is a proxy for kappa, a measure of the dispersion of a population that describes maximum clustering) (Fisher, 1953). * Indicates a regional application of the paleomagnetic fold test.

Low site k values from SM18, SM19, SM21, and SM23 did not allow for the completion of local, individual fold tests. However, with oppositely dipping limbs in the area, two regional fold tests were completed. A fold test was conducted for SM30 with a nearby oppositely dipping limb (SM29). For SM19-23, the low k-value sites (19, 21, and 23) were all dipping the same way and a fold test could only be completed by combining the few samples from each low k-value

site together to use for a regional test with SM20 and 22.

From fold test results, two different characteristic directions are observed, slightly steeper directions from the set B sites and comparatively shallower directions for set A sites. The average direction for set-A synfolding sites falls near the expected Eocene direction for this location, which constrains a remagnetization age for these samples. The expected directions for the Cretaceous are very similar, but synfolding results prove that this magnetization is a remagnetization in these Lower Cretaceous carbonates. A trend is also observed in the intensity of the ferrimagnetic signal between the set B and set A sites. The B set of magnetizations shows overall weaker signals in the ferrimagnetic strength from hysteresis plots as compared to the remagnetized synfolding A sites (Fig. 3.5b). In hysteresis plots from the B sites, the paramagnetic contribution from the sample dominates the measured signal, resulting in large errors that overwhelm the very weak ferrimagnetic signal.

The anomalously behaved k-versus-unfolding sites

As mentioned earlier, four site pairs (3 local and 1 regional) (Fig. 3.8) do not behave according to expectations. We consider these set B pairs uncharacteristic. The atypical results reach a maximum peak of k past 100%. Because such anomalous results require some searching for plausible explanations, we devote here a brief session to this intriguing aspect.

When k-versus-unfolding percentage peaks are outside the conventional 0-100% window, the diagrams must be extended beyond 100%, labeling them anomalous. In fact, because the k-versus-% unfolding diagrams look like prefolding diagrams, it is tempting to attribute the higher maximum percentages to statistical complexities or the field setting. However, peaks at 100 to 130 percent in three site-pairs may remain unexplained that way. Instead we offer an alternative interpretation involving interacting deformation phases, an earlier folding phase and a later

rotation, which affected the simplistic unfolding in a fold test. Evidence for this secondary rotation is discussed below.

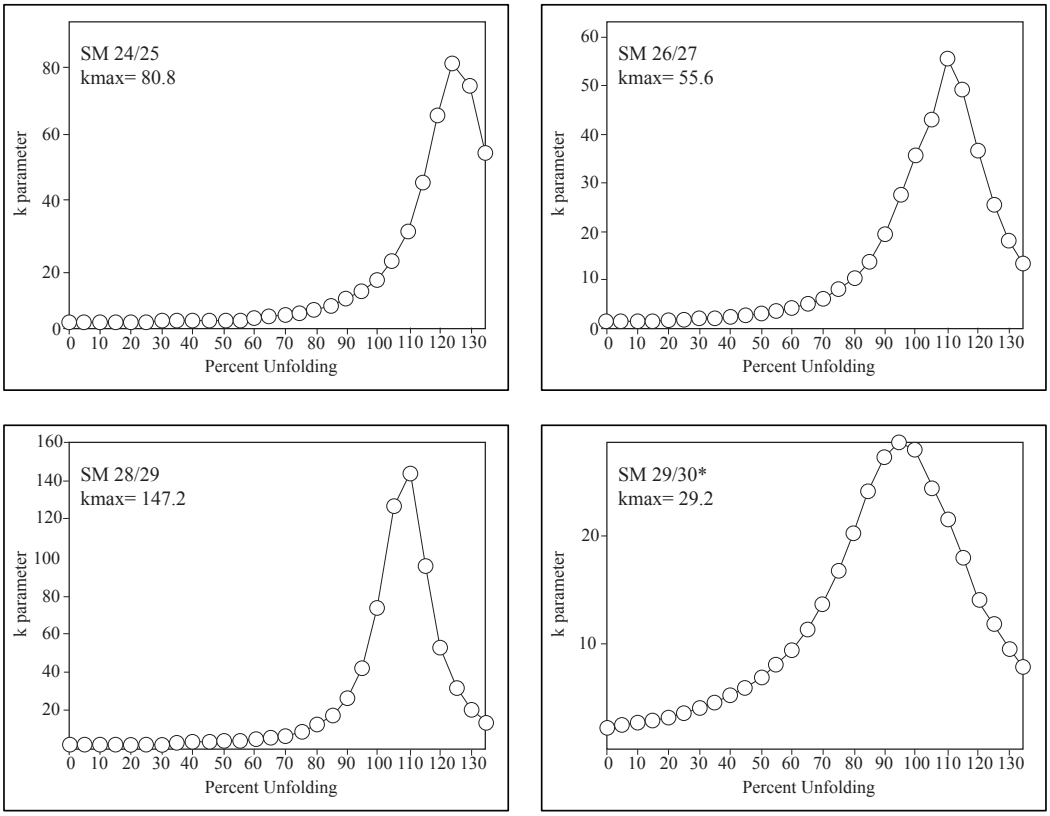

Figure 3.8: Set B fold tests from the Monterrey Salient. One fold test (SM29/30*) is done in the Paleomac program that proportionally unfolds the limbs of the fold from 0-100% (Cogné, 2003; Watson and Enkin, 1993). Fold tests are completed for the other three folds by using the Stereonet program to unfold the limbs past 100% (Cardozo and Allmendinger, 2013; Watson and Enkin, 1993). * Indicates a regional application of the paleomagnetic fold test.

Monterrey Salient Rotation

Prior studies in the salient have mentioned counterclockwise (CCW) rotations of the belt, some as large as 130° (Gose et al., 1982; Nowicki et al., 1993; Urrutia-Fucugauchi, 1981). To test the nature of curvature of the Monterrey Salient, synfolding directions of set A are plotted versus regional strike (Eldredge et al., 1985). A trendline is used to evaluate secondary curvature with a linear best-fit line through the data. A slope of 1 represents full oroclinal bending (also

called secondary curvature) and a slope of 0 indicates primary curvature. Intermediate values signify varying degree of secondary curvature.

The declinations used are the averages of synfolding set A directions from the NS segment of the study area (SM 4-11), the average of the transition zone (SM 12-13 & 19-23), and the direction from the EW portion (SM 31-32). Only the synfolding result is utilized from the EW segment of the study area. The slope of the best-fit line is .67, representing significant secondary rotation (Fig. 3.9). Optimal directions in stereographic projection show similar large CCW rotation for the B directions from the Eocene declination for Mexico (Fig. 3.6). Therefore, secondary rotations are preserved in the data, both for set A and set B samples, with a large CCW rotation of the today's EW trending portion of the salient. It can be concluded that rotation of a portion of the salient is significant, implying that some deformation must have occurred in response to the rotation.

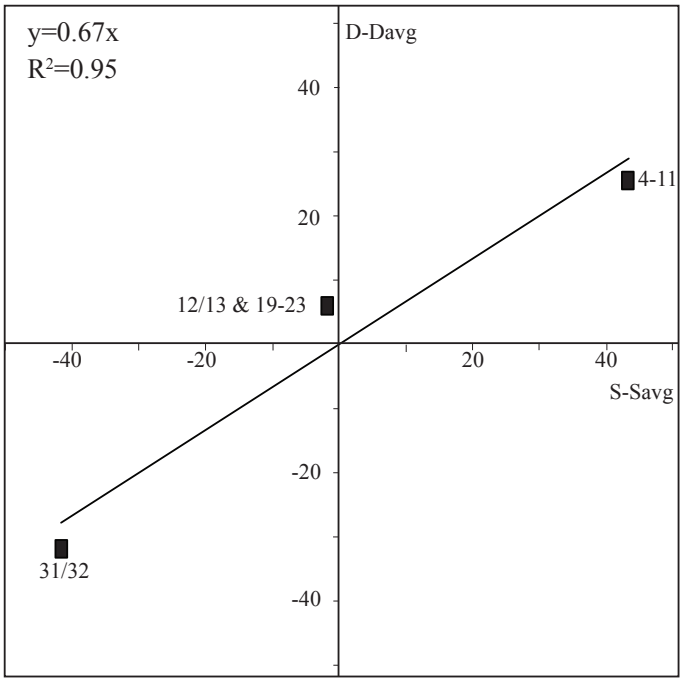

Figure 3.9: Optimal declination vs. regional strike plot for synfolding A directions from the Monterrey Salient limestones with a slope of 0.67 representing a secondary oroclinal rotation. Declination deviations from a mean reference direction (D_{avg} 137.9°) of site means plotted against strike deviatons from a reference strike (S_{avg} 121.7).

Remagnetization Age

Only an imprecise age can be assigned to the remagnetization event observed in the southern folds in the study area based on a comparison to expected directions, calculated from the lengthy and rather feature less reference APWP. This, in turn, yields an imprecise age estimate as young as Eocene for these Lower Cretaceous limestones (Besse and Courtillot, 2002**).** However, from ages obtained using $^{40}Ar/^{39}Ar$ fold dating on sampled folds in the Monterrey Salient, a quantitative age of 48-52 Ma can be assigned to synfolding remagnetization, placing it in the Eocene. Linking the measured deformation date to remagnetization is possible because the $^{40}Ar/^{39}Ar$ method is dating illitization that occurred during folding (Fitz-Díaz and van der Pluijm, 2013; Fitz-Díaz et al., 2014 & 2016). If magnetization acquisition happened during folding, then remagnetization and illitization occurred simultaneously during folding. Set A sites with synfolding directions have upward S-SE and downward WNW-to-N directions indicating that the remagnetization spanned a reversal in the Early Eocene. Fold dating in the northern folds of the study area produced an age of ~52 Ma, of which the magnetization of B sites much be older (Fitz-Díaz et al., 2016).

Eocene remagnetization observed in the southeastern Monterrey Salient was also seen in central Mexico, east of Mexico City, in the Sierra Madre Oriental (SMO). Similar deformation ages were obtained from fold dating in the Monterrey Salient and frontal, eastern folds of the SMO in central Mexico (Fitz-Díaz et al., 2016). Also, two remagnetization events were found in the SMO of central Mexico (Late Cretaceous and Early Eocene); comparable to the set-A remagnetization of this study area within a similar range of frontal deformation ages in central Mexico.

Based on the presence of SPM-SD magnetite and predicted burial temperatures, the remagnetization is interpreted to represent fluid-mediated chemical authigenic growth of magnetite. Elsewhere in the frontal North American Cordillera, in Montana and Canada, remagnetizations of Eocene age are also observed to be associated with deformation-mediated fluid presence (Enkin et al., 2000; Cioppa et al, 2004; Nemkin et al., 2016) as well as many global examples (e.g., Evans et al., 2000; Evans et al., 2012; Zechmeister et al., 2012; Zegers et al., 2003; Zwing et al., 2009). Maximum burial temperatures in the study area were roughly 150-200° C, implying that a thermoviscous remagnetization in the area is not likely, given the time-temperature relationship of magnetite (Gray et al., 2001; Guzzy-Arredondo et al., 2007, Pullaiah et al., 1975).

3.6 CONCLUSIONS

Synfolding results (set A samples) are found in the La Peña -Cupido and La Peña-Tamaulipas limestones from the Monterrey Salient, with directions representing a remagnetization in the Eocene. The remagnetization age in synfolding sites is constrained by previously published fold ages of 48-52 Ma in these Early Cretaceous limestones (Fitz-Díaz et al., 2016). Four fold test results (set B) in the northernmost area are complex and may represent an earlier magnetization than the set A remanence. Of these sites, optimal directions acquired after 100% unfolding may reflect the effects of a late rotation after magnetization acquisition. This later deformation event is well preserved in set A samples as vertical-axis rotation of the belt, and is also observed in set B samples as a CCW rotation in the northern segment of the study area.

The remagnetization mechanism in the area is likely fluid-mediated growth of magnetite that resulted in superparamagnetic to single domain magnetite grains. The timing of the last

remagnetization in the Monterrey Salient of northern Mexico (48-52 Ma) falls within the range of that for the frontal portion of the Sierra Madre Oriental in central Mexico (~44 Ma; Nemkin et al., 2015). Subsequent to Eocene synfolding remagnetization, the northern area underwent counterclockwise rotation that produced the characteristic oroclinal structure of the Monterrey Salient.

TABLES

Table 3.1: Paleomagnetic data for Lower Cretaceous La Peña-Cupido and La Peña-Tamaulipas Inferior formation samples collected from the Monterrey Salient in NE Mexico.

				Bedding		IS Mean Magnetization		TC Mean Magnetization		Statistics	
Site	**Latitude (°N)**	**Longitude (°W)**	**n/N**	**Strike**	**Dip**	**Dec. (°)**	**Inc. (°)**	**Dec. (°)**	**Inc. (°)**	**$a95_{IS\&TC}$**	**$k_{IS\&TC}$**
1	24°44’52.7”	99°47’38.2”	8/8	136.0	52.0	223.4	-22.9	216.8	-74.8	3.0	349.4
2	24°43’53.8”	99°51’44.3”	Chaotic decay did not allow for site analysis								
3*	24°43’40.5”	99°53’17.3”	6/8	340	124.7	304.9	-15.5	346.9	37.5	5.6	146.7
4	24°54’34.8”	99°56’17.9”	7/8	153.5	56.5	188.7	-22.5	151.5	-41.0	6.4	89.5
5	24°54’35.9”	99°55’27.0”	7/8	140.8	72.4	194.2	-26.4	119.8	-55.1	9.7	40.1
6	24°54’35.9”	99°55’27.0”	7/8	323.2	65.7	166.0	-45.4	192.8	-2.6	7.4	67.6
7*	24°55’48.8”	99°54’6.9”	5/8	341.5	115.4	121.7	0.3	180.9	-35.5	19.7	16.1
8	25°2’33.9”	99°59’8.2”	Chaotic decay did not allow for site analysis								
9	25°2’33.9”	99°59’8.2”	Chaotic decay did not allow for site analysis								
10	25°2’33.9”	99°59’8.2”	5/7	168.7	74.2	172.0	-52.3	117.7	-14.4	16.7	21.9
11*	25°2’31.9”	99°56’15.0”	6/8	315.8	138.6	113.7	-18.4	164.2	0.0	10.7	39.9
12	25°29’11.9”	100°21’48.0”	5/8	110.6	74.5	177.9	-29.9	72.1	-64.7	11.1	48.8
13	25°29’11.9”	100°21’48.0”	6/8	320.0	58.4	164.3	-59.6	201.3	-16.0	17.4	15.8
14	25°33’14.3”	100°23’37.7”	8/8	121.6	51.0	201.7	-38.3	123.8	-82.3	7.6	54.0
15	25°33’14.3”	100°23’37.7”	Chaotic decay did not allow for site analysis								
16	25°34’59.0”	103°37’21.1”	5/9	116.6	78.5	185.6	-36.0	60.9	-59.0	16.8	21.6
17	25°34’59.0”	103°37’21.1”	4/8	296.7	87.3	182.8	-36.5	179.3	44.9	16.6	31.6
18	25°36’43.9”	100°48’50.3”	5/6	250.3	79.4	185.6	9.6	250.4	65.0	34.0	6.0
19	25°22’16.9”	100°18’44.1”	3/8	128.8	63.8	357.4	43.1	271.3	52.4	45.9	8.3
20	25°23’13.2”	100°18’11.1”	9/9	297.2	54.0	256.3	37.5	314.5	51.1	8.3	39.0
21	25°23’14.9”	100°14’60.0”	4/8	121.6	65.6	13.6	-12.6	4.2	49.0	42.2	5.7
22	25°24’15.9”	100°15’5.3”	11/12	301.1	69.5	241.0	19.5	304.3	61.9	9.9	22.3
23	25°23’14.9”	100°14’60.0”	7/8	118.1	55.8	285.0	-68.7	2.0	-36.3	38.0	4.1
24	25°27’56.6”	100°26’18.6”	5/8	111.4	75.1	352.7	-30.6	339.2	52.0	12.5	59.3
25	25°28’46.6”	100°25’24.8”	5/8	309.3	79.3	252.2	8.6	336.6	52.7	11.4	71.0
26	25°23’8.4”	100°47’47.5”	7/7	80.1	69.0	314.7	-10.4	293.2	47.2	6.2	80.8
27*	25°25’1.8”	100°48’20.7”	6/8	233.0	109.9	172.7	9.1	282.1	41.7	9.1	45.7
28	25°33’13.0”	100°38’44.8”	5/8	86.1	67.4	331.1	-7.6	307.7	55.9	5.5	155.1
29	25°32’49.4”	100°38’44.4”	6/9	269.3	87.6	201.9	17.4	316.3	57.4	5.3	133.6
30	25°34’58.6”	100°47’18.4”	8/8	60.2	37.9	168.2	-38.2	199.4	-71.3	3.4	273.0
31	25°13’37.7”	101°1’41.9”	7/8	53.9	50.9	299.9	42.5	215.4	71.6	7.8	60.6
32	25°13’50.4”	101°1’59.1”	3/9	238.8	78.8	247.8	55.5	294.7	4.2	24.6	26.1

Note: n/N, number of samples accepted/measured; IS Dec., In situ declination; IS Inc., In situ inclination; TC Dec., Tilt-corrected declination; TC Inc., Tilt-corrected inclination; a95, radius of confidence circle in degrees; k, precision parameter (Fisher,1953). Tilt-correction is the full correction (past 100%) for 24-30 and 100% un-tilting for the remaining sites. Strike and dip are measured in degrees using the left hand rule (LHR). * indicates overturned bed and strikes are rotated 180 degrees to comply with Paleomac conventions (Cogne, 2003). Gray shading indicates a site that was not used in further analysis because the site k value is less than 10.

Table 3.2: Hysteresis data of representative samples from the Lower Cretaceous La Peña-Cupido and La Peña-Tamaulipas Inferior formations collected from the Monterrey Salient in NE Mexico.

Sample	Qf	M_r (Am^2 kg^{-1})	M_s (Am^2 kg^{-1})	Brh (mT)	Bc (mT)	M_r/M_s	Brh/Bc
SM1-1	2.38	1.35e-03	3.47e-03	153.24	65.98	0.3888	2.3225
SM1-4d	1.37	1.18e-04	5.39e-04	30.57	10.12	0.2189	3.0208
SM4-3b	1.91	6.40e-5	7.068e-4	30.91	4.47	0.0905	6.9150
SM4-4d	1.40	2.47e-05	4.41e-04	54.65	3.51	0.0560	15.5698
SM5-7a	2.23	8.35e-05	4.68e-04	121.05	24.48	0.1784	4.9449
SM6-4	2.47	8.18e-04	3.44e-03	59.81	26.25	0.2381	2.2785
SM9-6a	2.40	1.78e-5	3.948e-4	64.54	2.87	0.0451	22.4878
SM10-4a	1.86	7.01e-05	5.82e-04	72.97	9.66	0.1205	7.5538
SM11-7b	1.57	3.61e-5	2.69e-4	20.93	6.13	0.1342	3.4144
SM13-3b	1.84	6.39e-05	1.34e-04	364.76	203.10	0.4787	1.7960
SM22-6b	1.38	6.80e-6	5.564e-5	164.99	8.07	0.1222	20.4449
SM24-2a	1.66	1.40e-05	7.47e-05	62.83	8.26	0.1875	7.6065
SM26-3a	1.45	9.34e-6	9.264e-5	275.01	10.48	0.1008	26.2414
SM29-2a	1.98	4.28e-05	1.78e-04	70.18	21.34	0.2404	3.2887
SM31-4b	2.18	7.63e-05	2.79e-04	44.42	31.49	0.2736	1.4106

Note: Qf—quality factor; Mr—remanent magnetization; Ms—saturation magnetization; Brh— provides an estimate for Bcr (coercivity of remanence); Bc—coercive force.

Table 3.3: Values that represent the kmax, percent unfolding, and optimal directions obtained after the paleomagnetic fold test for samples from the Monterrey Salient.

Fold	kmax	% Unfolding	Declination (°)	Inclination (°)
4/6	81.8	35	181.0	-33.0
4/7	34.7	80	161.9	-40.2
5/6	49.6	25	182.4	-38.8
5/7	20.6	70	153.1	-49.6
10/11	23.8	40	138.9	-35.6
12/13	23.4	25	356.9	49.3
19-23*	24.3	80	291.5	60.7
24/25	80.8	125	337.9	52.4
26/27	55.6	110	287.9	44.8
28/29	147.2	110	312.3	56.8
29/30*	29.2	95	339.6	71.8
31/32	37.9	30	286.3	53.3

Note: *Represents a regional application of the fold test.

CHAPTER 4

DATING SYNFOLDING REMAGNETIZATION: APPROACH AND FIELD APPLICATON (CENTRAL SIERRA MADRE ORIENTAL, MEXICO)[3]

ABSTRACT

Growth of magnetite has been variably linked to fluid-bearing events or clay diagenesis, and the development of a chemical remagnetization as a result of such events. In this study we examine remagnetized carbonate rocks from the central Sierra Madre Oriental (the Mexican fold-thrust belt) in order to develop a method for dating synfolding remagnetizations. By combining $^{40}Ar/^{39}Ar$ deformation ages with new paleomagnetic results, we present a quantitative method for absolute dating of synfolding remagnetization. We find that the history of the central Sierra Madre Oriental involved two separate remagnetization events in our study area; synfolding remanence acquisition ca. 77 Ma (Late Cretaceous) in the Zimapán Basin and a younger synfolding remagnetization event ca. 44 Ma (mid-Eocene) in the Tampico-Misantla Basin. The growth of magnetite leading to chemical remagnetization detected in these limestones is interpreted as the result of rock interactions with an Fe-bearing fluid.

4.1 INTRODUCTION

Carbonates that contain interlayered shales with radiometrically datable authigenic illite present an opportunity to directly determine the age of syn-folding paleomagnetic remagnetizations. By combining radiometric Ar/Ar dating of illitization in folds and thrusts with

[3] Nemkin, S.R., Fitz-Diaz, E., van der Pluijm, B., and Van der Voo, R., 2015, Dating synfolding remagnetization: Approach and field application (central Sierra Madre Oriental, Mexico): Geosphere, v. 11, p 1-12, doi: 10.1130/GES01187.1.

synfolding remagnetization, an absolute age for synfolding remagnetizations can be determined. Prior to this study, the common way to date a remagnetization event was qualitatively, through comparison of a determined magnetic direction to the apparent polar wander path of the region. In deformed areas, the age range of the remagnetization episode can be estimated relative to folding, through application of the paleomagnetic fold test (Facer, 1983).

Tohver et al. (2008) dated remagnetization events in the Cantabrian- Asturian Arc (northwestern Spain) by applying Ar/Ar dating to clays collected from the area. The clays were associated with limestone layers that had undergone three remagnetization events (Weil et al., 2000). Tohver et al. (2008) obtained three different ages with this technique; however, one age was out of sequence with the predetermined order of remagnetization events.

Remagnetization in carbonates typically occurs by the growth of superparamagnetic to stable single-domain magnetite from the release of iron (Fe) during mineral reactions or from the introduction of an Fe-bearing fluid (Elmore et al., 2012; Evans et al., 2000; Lewchuk et al., 2003). For example, during illitization, smectite transforms to illite, releasing Fe as temperatures increase with burial (Altaner and Ylagan, 1997). The growth of magnetite into a stable single-domain structure allows a remanent magnetization to be acquired, resulting in a chemically remagnetized unit (Hirt et al., 1993; McCabe et al., 1989).

Katz et al. (1998) presented evidence of a strong or detectable chemical remagnetization in the limestone-marl sequences of their study area, the Vocontian Trough (southeastern France). This remagnetization is only present where there is also evidence of clay diagenesis. This hypothesis was further supported by Katz et al. (2000), Gill et al. (2002), and Woods et al. (2002). The occurrence of illite is associated with chemically remagnetized rocks in these studies, and the presence of smectite is associated with primary magnetizations or comparatively

weaker chemical remagnetizations. Elmore et al. (2001), Evans et al. (2000), and Zegers et al. (2003) also presented evidence for the link between Fe-bearing fluid (Mississippi Valley–type and orogenic) movement and the growth of magnetite; they used fluid inclusions and stable isotope data to correlate the presence of remagnetized rocks with evidence of fluid migration. Thus, while the growth of magnetite has been well studied, dating of remagnetization events remains a challenge; the latter provided the motivation for this study.

Illitization from smectite or illite precursors is common in naturally de- formed rocks (e.g., Vrolijk and van der Pluijm, 1999), offering the potential for radiometric dating of deformation (van der Pluijm et al., 2001). Illitization associated with flexural folding of carbonate-shale successions in the study area (central Sierra Madre Oriental, Mexico) was examined (Fitz-Díaz and van der Pluijm, 2013; Fitz-Díaz et al., (2014). Scanning electron microscopy, X-ray diffraction, stable isotope, and geochronological analyses of samples from several folds showed that illite grew along shear-related horizons during folding. The studied clay samples in central Mexico were collected along the same Aptian–Albian shale horizon and in all cases these samples provided well- defined Ar-Ar illite ages that were younger than deposition. This is in good agreement with textural observation showing only one generation of authigenic illite in these rocks (Fitz-Díaz et al., 2014).

By combining newly determined ages of illitization in folds with new paleomagnetic results in Mexico's central Sierra Madre Oriental, this study demonstrates the ability to associate a radiometric age with synfolding remagnetizations. Extensive work has shown that many carbonates around the world have been remagnetized (Jackson and Swanson-Hysell, 2012; McCabe and Elmore, 1989; Van der Voo and Torsvik, 2012), highlighting the potentially wide-scale application of this approach.

4.2 GEOLOGIC SETTING

The specimens analyzed for this study are carbonate successions from the Tamaulipas Formation in the Sierra Madre Oriental (central Mexico). From the structural point of view, the Sierra Madre Oriental is an east-northeast– verging thin-skinned fold-thrust belt, also known as the Mexican fold-thrust belt. It is ~100–250 km wide, thinning to the southeast and dominated by Cretaceous carbonates (Fitz-Díaz et al., 2011a; Guzmán and de Cserna, 1963). The study area spans four Cretaceous paleogeographical areas: the Zimapán and Tampico-Misantla Basins and the Valles–San Luis Potosi and El Doctor Plat- forms. The El Doctor Platform is thrusted by the Tolimán Sequences on the western side of the study area (Fig. 4.1).

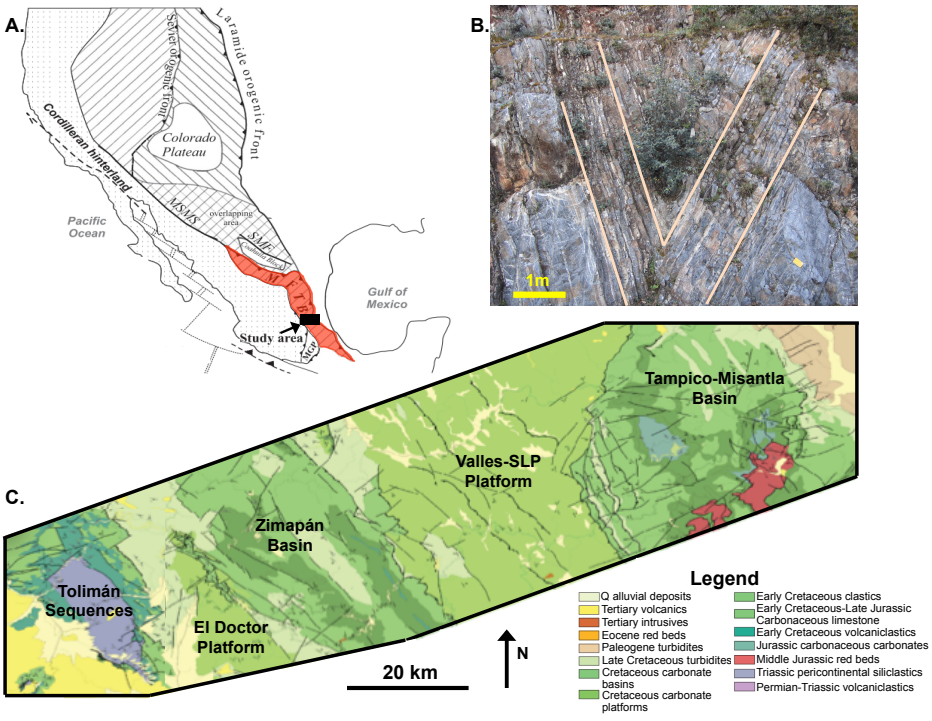

Figure 4.1: (A) General tectonic map for western North America with location of study area. MGP—Morelos-Guerrero Platform; SMF—San Marcos fault; MFTB—Mexican fold-thrust belt (red shaded area); MSMS—Mojave-Sonora megashear (modified from Armstrong, 1974; Fitz-Díaz et al., 2011a). (B) Field photograph showing example of a studied fold (sites 24 and 25). (C) Geologic map of study area with basins and platforms labeled (modified from Fitz-Díaz et al., 2012). Valles-SLP—Valles–San Luis Potosi Platform.

The highs and lows related to the carbonate basins and platforms were created in the Jurassic with the opening of the Gulf of Mexico, resulting in basin- and-range–type extension (Carrillo-Martinez et al., 2001; Gray et al., 2001). The carbonates were deposited in the Barremian–Cenomanian and the basinal deposits are characterized by deep-water muddy carbonates, whereas the platform rocks are fossiliferous shallow bank deposits (Imlay, 1944; Suter, 1987). Deformation of the area occurred during the Late Cretaceous to Paleogene, with the basins dominated by folding and intense water-rock interaction (see Fitz-Díaz et al., 2011b, for details); while the platforms were thrust dominated and showed much less fluid-rock interaction (Aranda-Gómez et al., 2000; Fitz-Díaz et al., 2012).

Deformation in the central Sierra Madre Oriental was dated (Fitz-Díaz et al., 2014) using the Ar/Ar illite dating technique; that study targeted fold and thrust dating in the region. The absolute age of folds was determined by clay grain-size separation, illite polytype characterization, and 40Ar/39Ar dating of multiple size fractions (Fitz-Díaz and van der Pluijm, 2013; Haines and van der Pluijm, 2008). Ages of thrusting were determined for the Tolimán Sequences (83.5 ± 1.5 Ma) on the western edge of the study area, the western and eastern Zimapán Basin (82 ± 0.5 Ma and 76.5 ± 1.0 Ma, respectively), and the western and eastern Tampico-Misantla Basin (64 ± 2.0 Ma and 43.5 ± 0.5 Ma, respectively); see Figure 4.2 for details (Fitz-Díaz et al., 2014). The ability to successfully date mesoscopic folds made this an ideal area to test the feasibility of absolute dating of synfolding remagnetizations.

4.3 METHODS

Sampling

Twenty-eight sites from the Barremian–Cenomanian Tamaulipas Formation were sampled in the central Sierra Madre Oriental (Mexican fold-thrust belt) (Fig. 4.2). The

Tamaulipas Formation is the focus of this study because of the accessibility and large-scale areal extent of this unit. Local-scale folds were targeted and 6–10 samples were collected per site using a portable Pomeroy EZ Core Drill. A Brunton compass and inclinometer were used to determine the azimuth and plunge of the core samples and the orientation of the beds.

Laboratory

Cored samples were cut to 2.2 cm length with a dual bladed saw at the University of Michigan. Broken samples were glued back together with alumina cement and all specimens were labeled with Velvet underglaze nonmagnetic temperature-resistant paint.

All specimens were measured and demagnetized in a magnetically shielded room, with a rest field of <200 nT, to minimize accumulation of any viscous magnetization. Remanent magnetizations were measured using a three-axis 2G superconducting magnetometer. Specimens were thermally demagnetized using an ASC TD-48 demagnetizer after trials revealed that a separate magnetic vector did not always become apparent when using the alternating field demagnetization technique. Thermal treatment revealed two magnetic components, whereas alternating field demagnetization revealed only one. The specimens were heated to ~420 °C, after which we typically observed a spike in magnetization intensity, due to growth of a new mineral. Results from the demagnetization process were analyzed with the Paleomac software by Cogné (2003) and graphed in orthogonal or stereographic projections (Zijderveld, 1967). Principal component analysis was used to analyze the demagnetization data and the fold test was applied in order to determine the relative timing of magnetizations; i.e., prefolding, synfolding, or postfolding (Kirschvink, 1980; Tauxe and Watson, 1994; Watson and Enkin, 1993). The fold test proportionally untilts the fold limbs with different dips, utilizing the fold axis to anchor the rotation

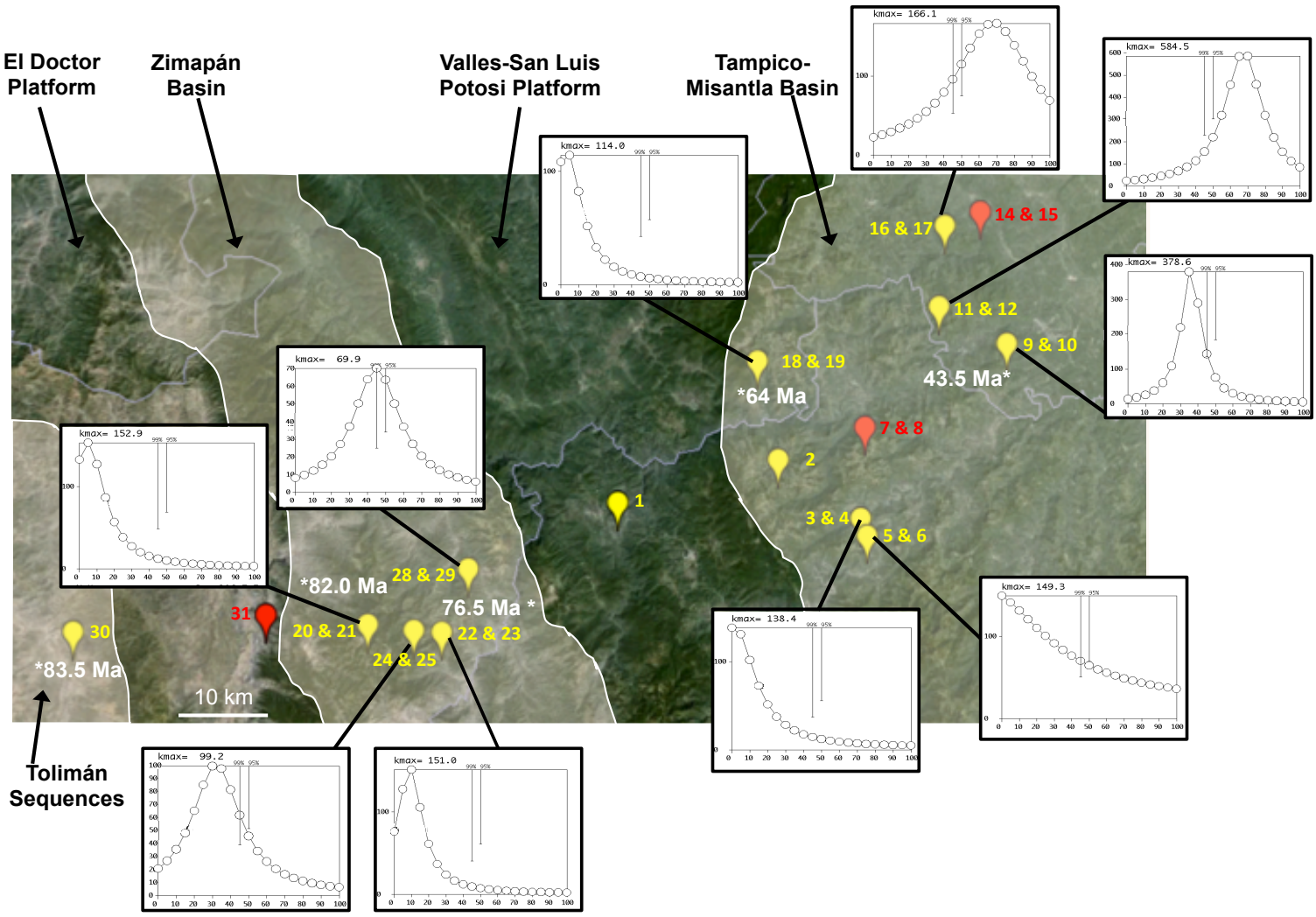

Figure 4.2: Each marker corresponds to a fold (two sites) in the study area with the corresponding fold test. Four unpaired sites are also shown (1, 2, 30, and 31). The x-axis and y-axis of the fold test plots are percent unfolding and k (proxy for kappa), respectively (Fisher, 1953). On each fold test plot, the 99% and 95% bars indicate the level of significance of the k ratio with respect to the kmax (precision parameter that is a proxy for kappa [measure of the dispersion of a population] that describes maximum clustering). Red markers indicate a fold or site that was not interpretable due to chaotic behavior during demagnetization. Five Ar/Ar ages of folding or deformation are shown with a white star (from Fitz-Díaz et al., 2014).

4.4 PALEOMAGNETIC RESULTS

Magnetic directions from 28 sites in the mid-Cretaceous section of the Tamaulipas Formation in the central Sierra Madre (CSM) are summarized in Table 4.1. Thermal demagnetization revealed a characteristic component below ~420 °C, after which samples show a spike in magnetization (Fig. 4.3A). Magnetite is the principal carrier of the magnetization as determined by three-dimensional (3D) isothermal remanent magnetizations (IRMs), performed with an ASC Scientific Impulse Magnetizer followed by thermal demagnetization of the samples (Fig. 4.4A; Lowrie, 1990). Due to chaotic decay of the magnetization during demagnetization, 5 sites could not be interpreted; the remaining 23 sites show the removal of a present-day field component from 0 to ~200 °C and a characteristic magnetization direction from 200 to ~420 °C (Fig. 4.3B).

Throughout the study area, 23 sites generated interpretable results including 10 fold tests applied to paired sites, as labeled in Figure 4.2. Sites from the Valles–San Luis Potosi Platform, Tolimán Sequences, and El Doctor Platform were analyzed for comparison and did not provide a fold test option. Paleomagnetic directions in the Tolimán Sequences and Zimapán Basin are down- ward and northwesterly, which we interpret to be of normal polarity. Directions in the Tampico-Misantla Basin are reversed and cluster in the southeastern quadrant (Fig. 4.5). The characteristic direction in fold 5-6 is anomalous due to the very shallow directions of site 6.

Figure 4.2 shows the fold test results for two paired sites from each of the sampled folds in the study area. Eight site pairs yielded a synfolding or late synfolding remagnetization and two site pairs produced postfolding remagnetizations (Fig. 4.2). The Zimapán Basin yielded four folds with a synfolding magnetization (one being very late synfolding). Three folds in the eastern side of the Tampico-Misantla Basin produced synfolding results; one fold in the western side of

the Tampico-Misantla Basin is very late synfolding and the other two produced postfolding magnetizations.

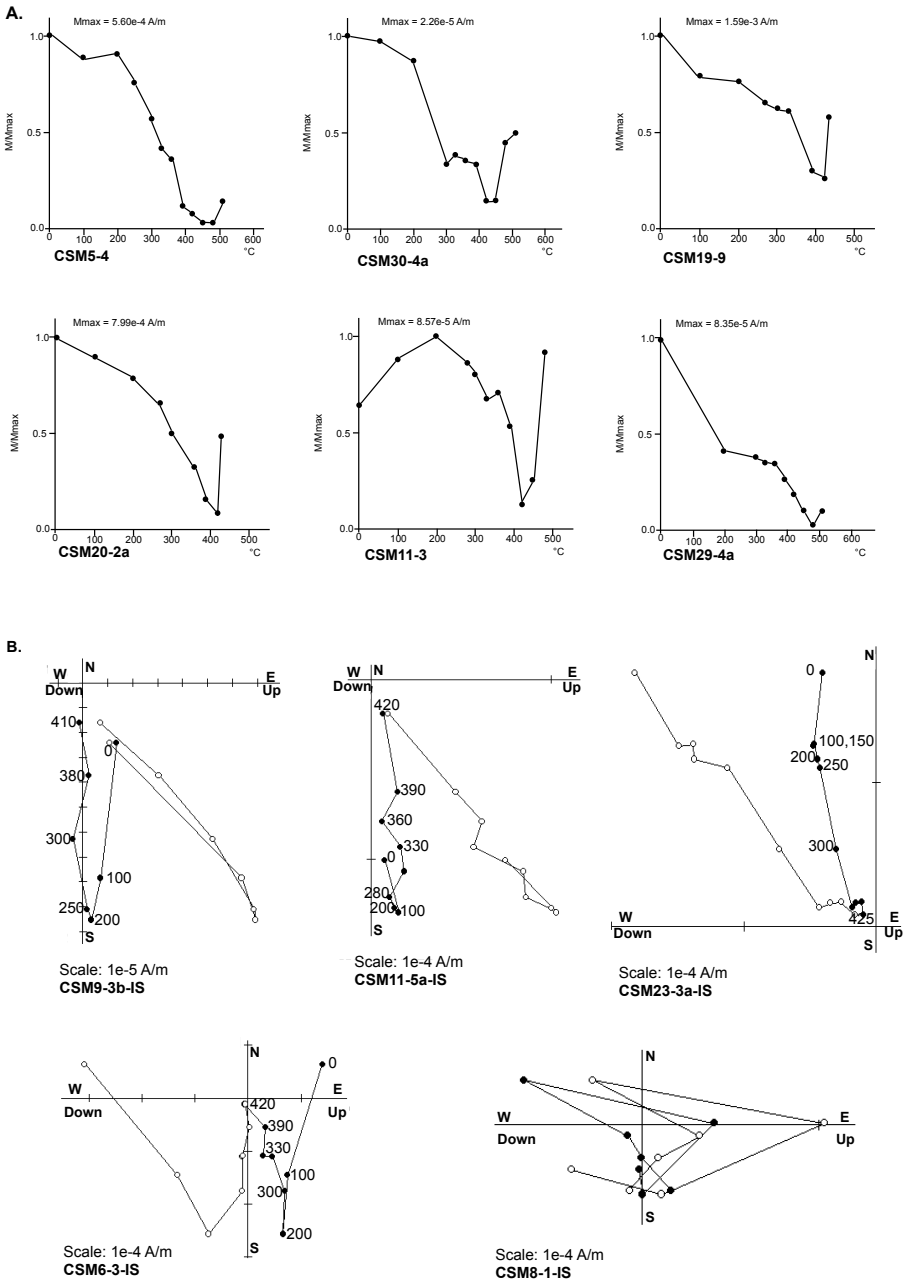

Figure 4.3: (A) Intensity plots showing normalized magnetic intensity versus temperature (°C). Most samples show a characteristic spike in magnetization after ~420 °C. Mmax—maximum magnetization; M/Mmax—measured magnetization divided by the maximum magnetization. (B) Representative thermal demagnetization plots of the Tamaulipas Formation limestones in geographic coordinates (IS, in situ). Temperature steps in °C. Black symbols represent vector endpoints plotted in the horizontal plane; white symbols represent vector endpoints plotted in the vertical plane. CSM8-1 is an example showing chaotic decay; samples showing this behavior are not used in the analysis.

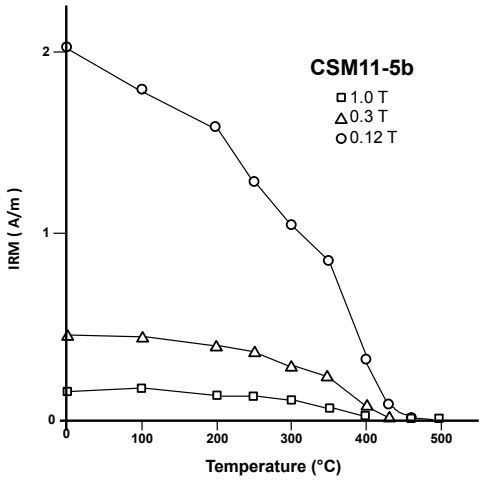

Figure 4.4: (A) Thermal demagnetization of a three-dimensional isothermal remanent magnetization (IRM) acquired in an orthogonal system with the applied fields of 1.0 T, 0.3 T, and 0.12 T (Lowrie, 1990). (B) Alternating field demagnetization intensity plot for CSM11-1 showing near-complete elimination of the remanence at 80 mT. Mmax— maximum magnetization; M/Max—measured magnetization divided by the max magnetization.

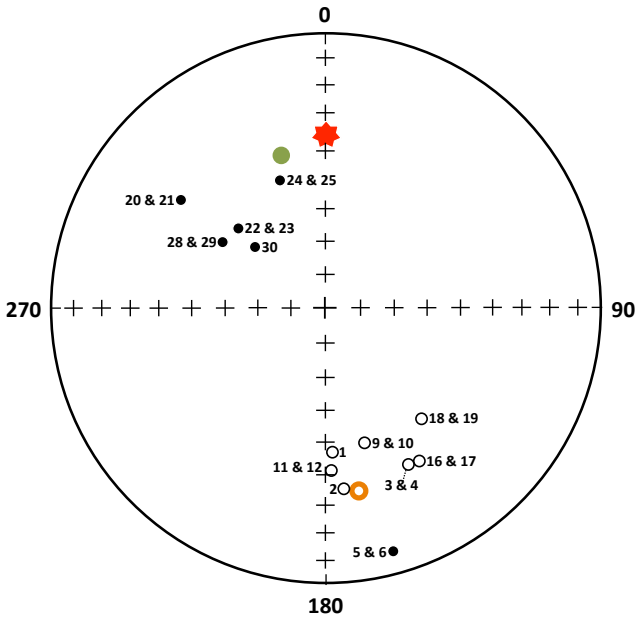

	Optimal Clustering			
Sites	% Unfolding	k max	Dec.	Inc.
3/4	0	138.4	150.4	-35.8
5/6	0	149.3	164.3	9.3
9/10	35	378.6	163.7	-47.7
11/12	70	584.5	177.3	-40.9
16/17	70	166.1	149.0	-35.4
18/19	5	114.0	138.8	-45.5
20/21	5	152.9	306.7	35.4
22/23	10	151.0	312.1	55.3
24/25	30	99.2	340.5	49.6
28/29	45	69.9	302.6	53.7

Figure 4.5: Stereoplot showing present-day location of the direction of the axial magnetic dipole (red star) in the study area. The green circle represents the expected Late Cretaceous direction for Mexico (determined from Besse and Courtillot, 2002); the orange circle represents the expected Eocene direction. The site means represent the optimal clustering for each fold (values in table on right) with the exception of sites 1, 2, and 30 in which the in situ magnetization is plotted. Dec.—declination; Inc.—inclination; k max—precision parameter that describes maximum clustering

4.5 DISCUSSION

In this study, remagnetizations from synfolding remanence in carbonates were examined and dated in conjunction with folded clay-bearing units. Of the possible magnetic carriers in the studied samples, goethite and sulfides can be excluded as possible carriers since there is no decay at 120 °C or 320 °C. Titano-hematite or titanomagnetite are unlikely as an authigenic chemical remanent magnetization or depositional remanent magnetization carrier in these rocks. The remaining possibilities are titanium-free magnetite and hematite. The Lowrie 3D IRM test (Fig. 4.4A) supports the identification of magnetite in site 11, and is typical of the carbonates sampled. The high coercivity component shown in the Lowrie test is probably a result of anisotropy in the sample and does not reflect hematite as the magnetic carrier. Alternating field demagnetization of another sample within the same site reveals a median destructive field of 30 mT and a nearly complete elimination of the remanence at 80 mT, which does not support the presence of hematite (Fig. 4.4B). The lower blocking temperature (~420 °C) as well as a combination of superparamagnetic and stable single-domain magnetite is a common occurrence in remagnetized carbonates (Jackson and Swanson-Hysell, 2012). The presence of superparamagnetic grains is supported by a spike in bulk susceptibility values at liquid nitrogen temperatures as com- pared to room temperature measurements before and after (Tauxe, 2010).

According to blocking curves for magnetite (as shown in Pullaiah et al., 1975), with a laboratory blocking temperature of ~420 °C and a relaxation time of 10–100 m.y., the required temperature for acquisition of a thermoviscous remanent magnetization (TVRM) is ~250 °C. Based on microthermometry of fluid inclusions in syntectonic veins and vitrinite reflectance, temperatures within the Tampico-Misantla Basin ranged from 80 to 180 °C, and in the Zimapán Basin ranged from 220 to 250 °C during deformation (Gray et al., 2001; Fitz-Díaz et al., 2014).

Since the basins did not reach temperatures necessary for a TVRM, we conclude that the remanent magnetization in the Tampico-Misantla Basin is a chemical remagnetization. Synfolding results in the Zimapán Basin indicate a relatively quick acquisition of a remanent magnetization instead of the required longer acquisition for thermoviscous remagnetization at these temperatures. We infer that during chemical remagnetization there is growth of magnetite from a superparamagnetic state to a stable single-domain structure. For samples in which magnetite grains have grown to the stable single-domain range, a magnetic remanence is preserved during remagnetization (Butler, 1992). The origin of this chemical remagnetization connects with folding and illitization, likely reflecting tectonically related fluid pulses.

The peak in magnetization after ~420 °C, illustrated in the magnetic moment plot of Figure 4.3A, suggests the presence of a nonmagnetic Fe sulfide component that oxidizes at higher temperatures. This sulfide is most likely present in low concentrations, but concentrated enough to cause a spike in magnetization upon heating and alteration. Sites with chaotic decay of the magnetization were not used in the analysis of this area. Among many explanations of this behavior (e.g., sample CSM8-1 in Fig. 4.3B), sparse or swamped magnetic mineral growth during remagnetization events may be a cause.

The Zimapán Basin and Tolimán Sequences, farthest to the west in the study area, have deformation ages ranging from 83.5 ± 1.5 to 76.5 ± 1.0 Ma (determined by Fitz-Díaz et al., 2014). The coeval remagnetization is of normal polarity and its directions are concentrated to the northwest and down. Folding progressed temporally from west to east with a late synfolding remagnetization in sites 20-21 in the Zimapán Basin. Sites 22-23, 24-25 and 28-29 show synfolding remagnetizations in folds that are Late Cretaceous (76.5 ± 1.0 Ma; Fitz-Díaz et al., 2014). Therefore, combining the synfolding nature of the magnetizations with the absolute ages

of the folding, it is concluded that synfolding remagnetization in the Zimapán Basin is Late Cretaceous (ca. 77 Ma).

The Tampico-Misantla Basin is farthest to the east with the youngest deformation ages for this study area. The sites in this area are dominated by southeast and upward magnetization directions, which are likely to have been acquired during one of the latest Cretaceous to Eocene reversed polarity intervals. Sites 9-10, 11-12, and 16-17 produce synfolding results with a corresponding age for these folds of 43.5 ± 0.5 Ma (from Fitz-Díaz et al., 2014). Very late synfolding magnetization is seen in sites 18-19 and postfolding remagnetizations are observed in sites 3-4 and 5-6 of this area. Site 5 is near the other sites and is of reversed polarity, but the fold test result of sites 5-6 is not as reliable due to anomalous results from site 6. Thus, this area under- went deformation and/or folding in the west and, as folding proceeded to the eastern portion of the area, a younger remagnetization event occurred ca. 44 Ma (mid-Eocene).

Folds in the study area have different ages, despite their geographic proximity, which indicates that regional metasomatism was not the cause of illitization. Illitization occurred primarily within bentonitic shale layers, while remagnetization was studied in neighboring limestone layers. These units within the same fold structures are connected through a pore fluid that was active during deformation, as demonstrated through comparative d2H data measured in illite and in water of primary fluid inclusions trapped in syntectonic veins within the carbonate layers (Fitz-Díaz et al., 2014). Comparison of d18O and d13C in calcite from veins and host carbonates supports dissolution-precipitation within lime- stone layers during deformation, allowing for the formation of stylolites and veins (Fitz-Díaz et al., 2011b). Illitization occurred during folding and magnetite remagnetization is synfolding; therefore, the chemical remagnetization and illitization are of the same geologic age.

Using ages obtained from sampled folds and paleomagnetic results from this study, a progressive deformation-magnetization history from west to east is recognized in the central Sierra Madre Oriental. The fold test results and radiometric dates support a sequence of sediment deposition, deformation (faulting and folding; D1, D2, D2′, and D3), synfolding and postfolding remagnetization events (with reversals; R1 and R2), ending with the acquisition of a present-day field magnetization (Fig. 4.6). In the Tampico-Misantla Basin, the westernmost side shows postfolding magnetizations, suggesting a scenario of early folding in the west followed by regional remagnetization as the eastern portion of each basin is deforming.

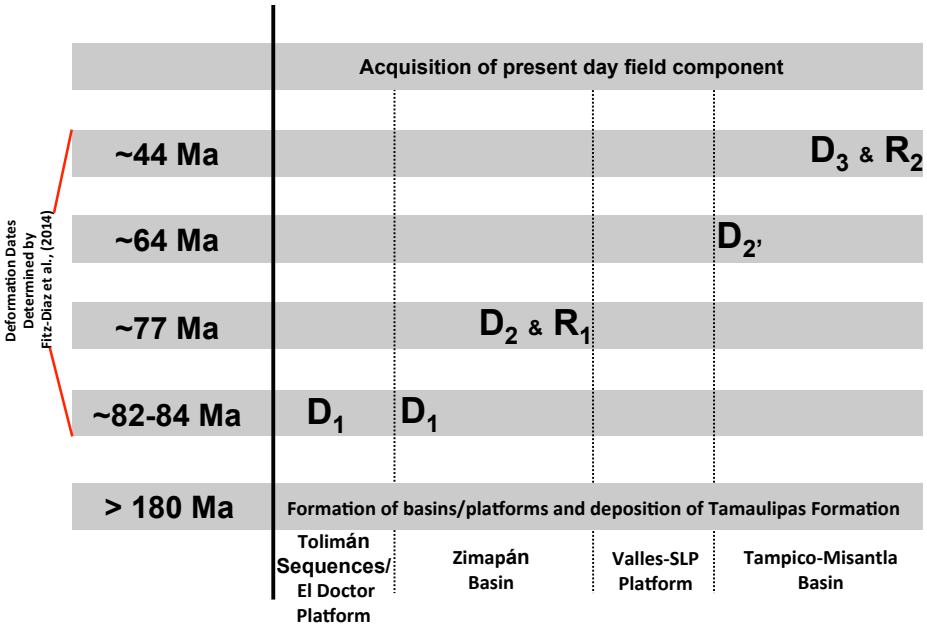

Figure 4.6: Remagnetization history of central Sierra Madre Oriental utilizing dates in Fitz-Díaz et al. (2014) and results from this study. SLP—San Luis Potosi; D—deformation event; R—remagnetization event.

A regional history of deformation and remagnetization emerges. The basins and platforms were formed in the Jurassic during opening of the Gulf of Mexico, followed by deposition of the Tamaulipas Formation in the Barremian– Cenomanian (mid-Cretaceous). From

the Late Cretaceous to Paleogene, deformation developed a fold-thrust belt in the area that progressed from west to east, both regionally and within each basin. Sites in the Tolimán Sequences and Zimapán Basin record Late Cretaceous deformation, and as folding progressed eastward, the area underwent a remagnetization event ca. 77 Ma. This remagnetization event occurred near the end of the long Cretaceous Normal Superchron. Folding continued into the Tampico-Misantla Basin in the Paleogene and during a reversed geomagnetic field, the Tampico-Misantla Basin was remagnetized ca. 44 Ma. Remagnetization patterns are rarely of mixed polarity, but this study is an exception.

4.6 CONCLUSIONS

Absolute dating of synfolding remagnetizations can be obtained by integration with 40Ar/39Ar dating of deformation-induced illitization. Combining the ages from Fitz-Díaz et al. (2014) and paleomagnetic results from this study, the remagnetization history of the central Sierra Madre Oriental (Mexican Fold-thrust belt) involved two events ca. 77 Ma and ca. 44 Ma. Deformation occurred synchronously with remagnetization in several places (synfolding re-magnetizations), but also occurred without simultaneous remagnetization in the Tampico-Misantla Basin (postfolding remagnetizations); the latter indicates that crystallization of illite does not a priori result in magnetite growth and remagnetization. If the illitization process was the single cause of remagnetization in this scenario, then all of the studied folds should show synfolding re- magnetization. Therefore, a parallel process is involved to produce synfolding remagnetization in some deforming rocks, but not others, that we speculate is the regional infiltration of (Fe bearing) fluids. Thus, a spatiotemporal link between regional deformation and remagnetization exists, but not one in which deformation and illitization alone result in remagnetization.

By providing a new approach and demonstrating a robust correlation between the age of regional-scale deformation and remagnetization, we show that fold dating can also be used to determine the timing of synfolding remagnetizations, using rock types that are common in many foreland deformation belts. Our approach, therefore, has potential application to many orogenic systems around the world

TABLE

Table 4.1: Data collected for samples collected from the Tamaulipas Formation in the central Sierra Madre Oriental

					Bedding		IS Mean Magnetization		TC Mean Magnetization		Statistics	
	Site	Latitude (°N)	Longitude (°W)	n/N	Strike	Dip	Dec.	Inc.	Dec.	Inc.	$a95_{IS\&TC}$	$k_{IS\&TC}$
VSLPP	1	21°02'31.0"	99°16'56.0"	6/7	231.3	20.8	177.1	-46.2	168.7	-28.4	6.8	98.2
Tampico-Misantla Basin	2	21°05'0.5"	99°05'38.0"	6/6	154.5	39.0	174.2	-34.4	144.4	-37.9	10.1	44.6
	3*	21°00'13.4"	98°59'15.9"	5/5	332.0	121.0	150.9	-31.8	180.4	14.9	3.9	375.9
	4	21°00'13.4"	98°59'15.9"	3/4	157.0	41.3	149.6	-42.8	121.5	-26.6	6.1	405.2
	5	21°01'19.0"	98°59'45.8"	6/7	113.5	35.5	168.0	10.0	166.3	-18.9	4.8	198.3
	6	21°01'19.0"	98°59'45.8"	5/6	342.0	67.0	159.9	8.5	153.3	1.4	4.6	276.1
	7	21°07'4.9"	98°59'37.8"	Chaotic decay did not allow for analysis of samples								
	8*	21°07'4.9"	98°59'37.8"	Chaotic decay did not allow for analysis of samples								
	9	21°12'34.5"	98°49'47.4"	6/7	178.3	17.7	171.2	-51.1	151.8	-45.9	2.1	993.5
	10*	21°12'34.5"	98°49'47.4"	6/8	354.5	135.5	132.8	-22.8	220.4	-8.9	3.7	332.0
	11	21°14'50.1"	98°54'34.1"	5/6	13.5	6.5	174.8	-38.5	179.9	-40.4	3.0	662.7
	12	21°14'50.1"	98°54'34.1"	9/9	173.7	71.0	209.2	-23.5	158.5	-39.3	2.2	565.0
	13	21°10'19.5"	98°50'19.2"	Volcanic unit that is not being utilized in this study								
	14	21°20'1.0"	98°54'12.6"	Chaotic decay did not allow for analysis of samples								
	15	21°20'1.0"	98°54'12.6"	Chaotic decay did not allow for analysis of samples								
	16	21°20'56.5"	98°51'44.5"	3/7	128.7	35.7	165.1	-26.1	142.4	-41.9	9.0	187
	17	21°20'56.5"	98°51'44.5"	7/8	301.3	36.3	128.9	-41.9	154.0	-28.7	4.6	173.1
	18	21°11'8.5"	99°07'15.4"	7/7	99.7	44.0	142.9	-48.0	78.8	-58.5	4.6	171.7
	19*	21°11'8.5"	99°07'15.4"	6/8	295.0	134.0	131.0	-43.1	141.7	38.3	5.3	162.5
Zimapán Basin	20*	20°54'5.4"	99°33'32.8"	6/9	331.3	156.3	303.9	30.3	7.7	-17.6	3.2	452.9
	21	20°54'5.4"	99°33'32.8"	4/8	100.0	9.5	304.4	37.8	297.0	41.2	10.2	82.2
	22*	20°53'44.7"	99°30'14.4"	3/7	340.3	125	301.6	47.9	38.6	-4.8	10.5	138.7
	23	20°53'44.7"	99°30'14.4"	5/8	170.5	38.5	315.0	58.1	289.7	28.3	6.6	135.2
	24	20°53'42.3"	99°30'25.8"	8/10	335.5	60	315.6	51.4	19.8	35.1	5.5	104.0
	25	20°53'42.3"	99°30'25.8"	6/7	162	69.7	0.8	40.4	306.0	27.0	2.7	604.5
	26	20°53'36.4"	99°28'32.0"	Volcanic unit that is not being utilized in this study								
	27	20°53'36.4"	99°28'32.0"	Cobble in volcanic unit that is not being utilized in this study								
	28	20°57'37.6"	99°26'49.4"	5/9	138	72.3	346.2	50.2	269.4	31.5	10.7	52.3
	29	20°57'37.6"	99°26'49.4"	7/8	312	74	270.4	38.3	349.6	42.2	7.0	74.5
TS	30	20°53'15.5"	99°53'58.7"	8/9	243.3	23	310.9	62.9	320.0	40.9	4.9	131.1
EDP	31	20°54'27.2"	99°40'37.2"	Chaotic decay did not allow for analysis of samples								

Note: VSLPP—Valles–San Luis Potosi Platform; TS—Tolimán Sequences; EDP—El Doctor Platform. n/N—number of samples accepted/measured; IS Dec.—in situ declination; IS Inc.—in situ inclination; TC Dec.—tilt-corrected declination; TC Inc.—tilt-corrected inclination; α95—radius of confidence circle in degrees; k—precision parameter (Fisher,1953). Tilt correction is 100% untilting. Strike and dip measured using the left hand rule. *Indicates overturned bed; strikes are rotated 180° to comply with Paleomac conventions (Cogne, 2003).

CHAPTER 5

CONCLUSIONS

This chapter summarizes the outcomes of studies that aim to assign quantitative ages to synfolding carbonate remagnetizations in the North American Cordillera. The main outcomes are:

5.1: Carbonates are remagnetized concurrently with regional tectonic activity for a given region.

5.2: Remagnetization ages and spatial division of synfolding and pre- or postfolding directions help decipher local-scale deformation.

5.3: Remagnetization intensities and distributions yield insights into the mechanism(s) of remagnetizations.

5.1: Carbonates are remagnetized concurrently with regional tectonic activity for a given region.

The remagnetization ages determined for the North American Cordillera are 53.6 Ma in Montana (Chpt. 2), 48-52 Ma in the Monterrey Salient of Northern Mexico (Chpt. 3), and two remagnetization events at 77 and 44 Ma in the Mexican fold-thrust belt in central Mexico (Chpt. 4). Synfolding directions were not observed for the Idaho/Wyoming study in between these study areas, but results from Idaho show a postfolding Eocene remagnetization based on paleomagnetic directions (Appendix A). All the remagnetizations fall within the expected Late Cretaceous – Eocene regional tectonic regime. Consequently, future studies can hypothesize that

the age of an observed remagnetization will occur within the tectonic window for that region and further fold dating with synfolding directions can be used to provide a more quantitative date.

5.2: Remagnetization ages and spatial division of synfolding and pre- or postfolding directions can help decipher local scale deformation.

From work reported in this thesis it is observed that remagnetizations do not necessarily take place as one large regional event. Multiple remagnetizations can be preserved in carbonates as deformation progresses through a study area. In the Mexican fold-thrust belt of central Mexico (Chpt. 4), two distinct remagnetization events were recorded within a West-to-East sampling area. The first magnetization event was recorded at 77 Ma when folding had commenced in the Zimapán basin and as folding progressed towards the east, a later event was preserved at 44 Ma in the Tampico-Misantla Basin. In Montana (Chpt. 2) the development of folding is also revealed by syn- and prefolding directions, all experiencing a similar remagnetization that produced the same preserved directions. In this case, the most frontal folds (prefolding) of the Montana Rockies were still flat lying during the 53.6 Ma remagnetization event.

Synfolding ages can also be used to constrain the timing of oroclinal events, reflecting vertical-axis rotations of mountain belts, where paleomagnetic directions and ages were previously unavailable. In such curved mountain belts, synfolding directions can be used in strike versus declination tests to ascertain the timing of vertical axis rotation. In chapter 3, a strike versus declination test with the synfolding directions from the Monterrey Salient in northern Mexico illustrates that the region experienced a late secondary rotation. The age of this rotation occurs after 48 Ma based on the timing of folding.

5.3: Remagnetization intensities and distributions yield insights into the mechanism(s) of remagnetizations.

Two prevalent mechanisms for the growth of magnetite in chemically remagnetized carbonates are typically offered: (1) the release of iron during illitization reactions (e.g. Katz et al., 1998 & Woods et al., 2000), or (2) the interaction of the carbonate with an iron bearing fluid (e.g., Zechmeister et al., 2012; Zwing et al., 2009). Chapters 2, 3, 4, and Appendix A do not support illitization as the remagnetization mechanism and instead it is proposed that magnetite grows to a stable single domain range as a result of the interaction of an iron-bearing fluid with the carbonates. An origin from illitization reactions is rejected as the mechanism in these carbonates because there are folds that have experienced illite growth, but do not show coincident synfolding magnetization (i.e., they were not remagnetized during folding). Specifically, in chapters 2 (Montana) and 4 (central Mexico) authigenic illite is found in folds that do not show a synfolding remagnetization. Thus, whether or not an illitization phase is releasing iron, it is not resulting in the growth of magnetite to a remanence acquiring state in these studies. Instead it is hypothesized that the growth of magnetite results from interaction of a fluid within the remagnetized rock unit.

It is also revealed from studies in this dissertation that not all carbonates within a study region exhibit a remagnetization. This may reflect a decrease in the fluid, the absence of pre-existing weaknesses in the studied units, insufficient magnetic mineralization, or facies change in a study region. In chapter 2, in the frontal portion of the Montana Rockies, the more inboard folds exhibit synfolding remagnetizations and as one advances eastward into the foreland, the remanence weakens and a remagnetization is not detected. From a weakening intensity it can be postulated that fluid activity started to diminish in the very eastern portion of the study area,

where there was minimal iron remaining in the fluid to allow sufficient magnetite growth for a stable direction. The movement and diminishing fluid role in magnetite growth may also have effected carbonates from Appendix A, where samples from Idaho are remagnetized and samples from central Wyoming, further to the east of the orogenic front, did not produce detectable paleomagnetic directions.

Remagnetizations may also be influenced by the characteristics of carbonate units in that certain lithologies will not facilitate the movement of fluid and/or growth of magnetite. The deformed muddy carbonates from central Mexico show overall stronger ferromagnetic signals as compared to the clean, coarsely crystalline Madison limestone sampled in Montana and Wyoming. Additionally, pre-existing weaknesses would permit fluid flow and allow magnetite to grow, while the lack of such pathways diminishes the ability for fluid to interact with the carbonate host rock. An example of this is chapter 3, where we show a division of pre- and synfolding sites, with the prefolding sites recording weaker paleomagnetic intensities. Illite was found in folds throughout the Monterrey Salient, so we deduce that fluids were present throughout the study area with pre- and synfolding remagnetization sites. Therefore, with the presence of fluids in all folds, we surmise that a facies transition from deeper deposition carbonates (synfolding sites) to shallower carbonates (prefolding sites; Goldhammer, 1999) did not produce favorable conditions for the growth of magnetite in the latter, resulting in prefolding directions and weak intensities.

Application of synfolding remagnetization and fold dating provides a powerful application to unraveling and understanding the intricate structural and paleomagnetic histories of many regions, given the widespread occurrence of (remagnetized) carbonates worldwide.

In an additional study, andesites were analyzed in Morocco to detect a possible remagnetization and to expand the technique to a different lithology; however, primary magnetizations were preserved (Chpt. 5). These primary directions address the Pangea A vs. Pangea B controversy in the Early Permian.

APPENDICES

APPENDIX A: PALEOMAGNETIC RESULTS FROM MISSISSIPPIAN CARBONATES IN IDAHO AND WYOMING

A.1 INTRODUCTION

Remagnetizations in carbonates are globally widespread, with seemingly many of the remagnetizations acquired during folding (McCabe and Elmore, 1989; Jackson and Swanson-Hysell, 2012; Van der Voo and Torsvik, 2012; Nemkin et al, 2015). It is generally inferred that carbonate remagnetizations are chemical in nature as magnetite grows to a stable single-domain (SD) state (Elmore et al., 2012; McCabe and Elmore, 1989; Font et al., 2012 and Zegers et al., 2003). The growth of magnetite to a SD state in carbonates can produce a directionally stable secondary remanence (called a remagnetization). If this remagnetization happens during folding, which is determined by a stepwise fold test, then along with fold dating, a quantitative age can be assigned to the remagnetization. This would significantly improve the application of the fold test, as remagnetizations were previously only qualitatively assigned an age by comparison to the relevant apparent polar wander path (APWP) of the region.

This technique has been successfully applied to folded carbonates throughout the North American Cordillera in central Mexico, northern Mexico (Monterrey Salient) and Montana (Nemkin et al., 2015, Nemkin et al., 2016, and Nemkin et al., 2017 in review). Following the application of fold dating and carbonate remagnetizations in these areas, folded carbonates in the Idaho/Wyoming fold-thrust belt and central Wyoming were targeted.

The North American Cordillera extends from Canada to southern Mexico and was formed by Sevier and Laramide style deformation from the mid-Mesozoic to Eocene (Burchfiel et al., 1992; DeCelles, 2004; Dickinson, 2004). Sevier style thrusts and folds characterize the easternmost Cordillera, which are the target of this study in the Idaho-Wyoming fold-thrust belt (Armstrong and Oriel, 1965; Armstrong, 1968; DeCelles, 2004; Wiltschko and Dorr, 1983).

A.2 METHODS

Sampling

Samples were collected from folded Mississippian Madison limestone in the Idaho-Wyoming thrust belt and north central Wyoming in the Bighorn Mountains (Fig. A.1). Local scale folds were targeted; four in Idaho and five in Wyoming. Five to ten cores were collected per site using a portable Pomeroy EZ Core Drill. A Brunton compass and inclinometer were used to determine the orientation of the beds, and the azimuth and plunge of the cores.

Figure A.1: Local scale folds were sampled from Mississippian carbonates in Idaho and Wyoming. Four folds were sampled form the Sawtooth Range in Idaho, one fold in the Wyoming fold thrust belt, and the remaining sites were collected from the Bighorn Mountains.

Laboratory Work

Samples were cut to 2.5 cm length with a dual bladed saw at the University of Michigan paleomagnetic laboratory. Velvet Underglaze non-magnetic temperature resistant paint was used to label all of the samples and alumina cement was used when necessary to glue samples back together.

Remanent magnetizations were measured using a three-axis 2G superconducting magnetometer. Alternating field (AF) and thermal treatments were used to demagnetize the samples and to reduce the acquisition of a viscous magnetization, specimens were measured directly after each demagnetization step. All specimens were measured, demagnetized, and stored in a magnetically shielded room, with a rest field of 200 nT, to minimize accumulation of any viscous magnetization. Magnetic hysteresis loops were acquired using a Princeton Measurements vibrating sample magnetometer at the Institute for Rock Magnetism (IRM) in order to determine the characteristic magnetic coercivities.

Paleomac software by Cogné (2003) was used to analyze final demagnetization results with principal component analysis (PCA) (Kirschvink, 1980). Site means are calculated by averaging the sample set directions (Fisher, 1953). In order to determine the relative timing of the magnetization acquisition (pre-, syn- or postfolding), principal component analysis (PCA) was used to examine the data (Kirschvink, 1980). The fold test proportionally untilts the fold limbs from their current orientation to horizontal (0-100% unfolding), using the field measured bedding dips (Tauxe and Watson, 1994; Watson and Enkin, 1993).

A.3 RESULTS

Data is obtained for samples from the Mississippian Madison limestone. Samples are not considered for further examination if the maximum angular deviation (MAD) angle is greater

than 10° and sites are deemed invalid when a95 is greater than 20. Remanence directions are recorded by magnetite. Results are listed in Table A.1, with gray indicating sites that were not used for further analysis in this study.

A.4 DISCUSSION

All of the sites from Idaho are remagnetized and yield steep inclinations (~60-70°) as compared to the shallow (near 0°) directions expected for North American Mississippian rocks (Besse and Courtillot, 2002; Torsvik et al., 2012). The direction for ID1 is reversed, while the directions for ID3, ID5, ID7, and ID8 are of normal polarity, likely indicating that this remagnetization spanned a reversal. Based on the selection criteria of sites with an a95 less than 20, many sites are eliminated and only one local scale fold test could be performed with ID7 & ID8. The ID7/ID8 fold test is clearly postfolding (Fig. A.2).

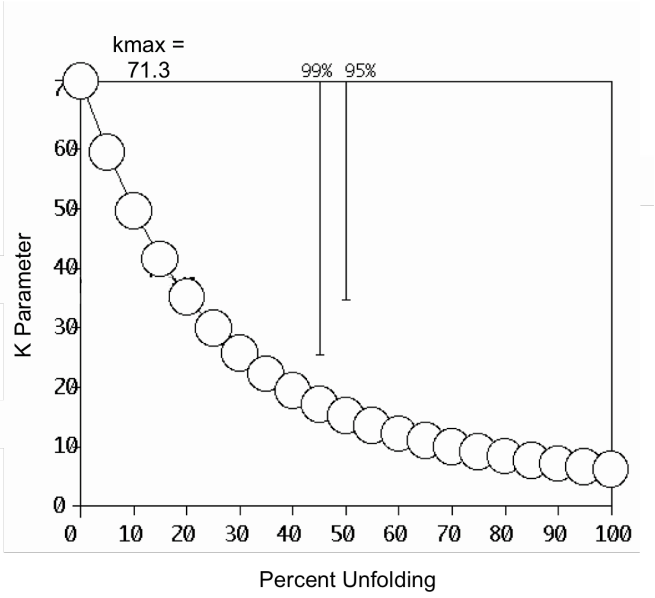

Figure A.2: Postfolding fold test for ID7 & ID8 from the Sawtooth Range. The 99% and 95% bars indicate the level of significance of the k ratio with respect to the kmax (precision parameter that is a proxy for kappa, a measure of the dispersion of a population that describes maximum clustering) (Fisher, 1953).

Two sites (1 fold) were collected from the Wyoming fold-thrust belt. Samples from these sites display a clean decay of the characteristic magnetization; however, the direction from each site matches the present-day field and no record of an ancient direction is apparently preserved

(Fig. A.3). McWhinnie et al. (1990) sampled the Jurassic Twin Creek limestone in the Idaho-Wyoming fold-thrust belt. Samples for that study from the more easterly Prospect thrust recorded a Tertiary direction. Re-analysis of data from more westerly thrusts (Absaroka & Darby Thrusts) in the belt show a late Mesozoic remagnetization by comparison to the North America apparent polar wander path (McWhinnie et al., 1990). Fold tests suggest that the directions are synfolding but the authors cannot statistically distinguish 80% synfolding results from a prefolding direction (McWhinnie et al., 1990). An older remagnetization to the west with a transition to a younger remagnetization to the east is similar to observations in other studies along the belt. In Nemkin et al. (2015) an older remagnetization was found in the western portion of the study area and as deformation progressed east, a younger remagnetization was recorded.

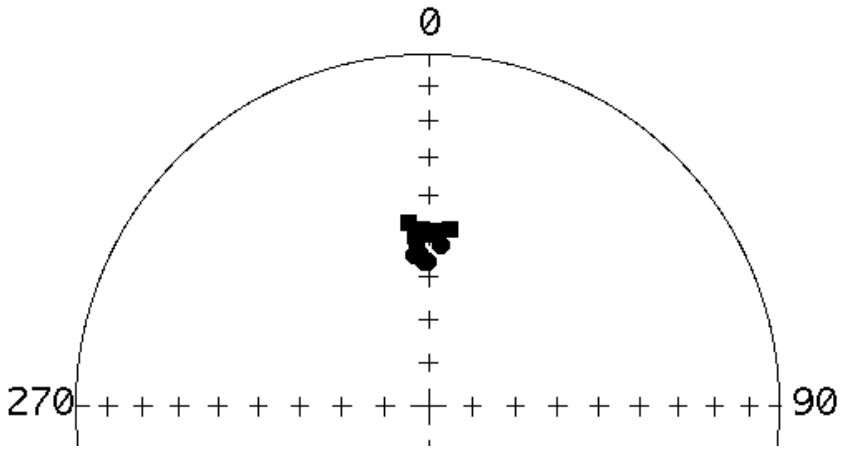

Figure A.3: Stereonet with in situ (IS) directions from WY1 (circles) and WY2 (squares).

Only two sites (WY5 & WY9) from Bighorn Mountain in the east pass the selection criteria. All other sites consist of samples with very erratic demagnetization behavior, likely because the remanence is too weak for instrumentation to detect or the remagnetization is non-existent. Figure A.4 displays the bulk magnetic susceptibility of samples from each of the sites,

with those from the Bighorn Mountains showing values around zero. The sites that exhibit bulk magnetic susceptibility greater than zero are the remagnetized postfolding results from Idaho and the present-day field remanence from WY1 (Fig. A.4). The near zero magnetic susceptibilities suggest that the magnetic carrier is limited in quantity or too small to retain a measureable remanence.

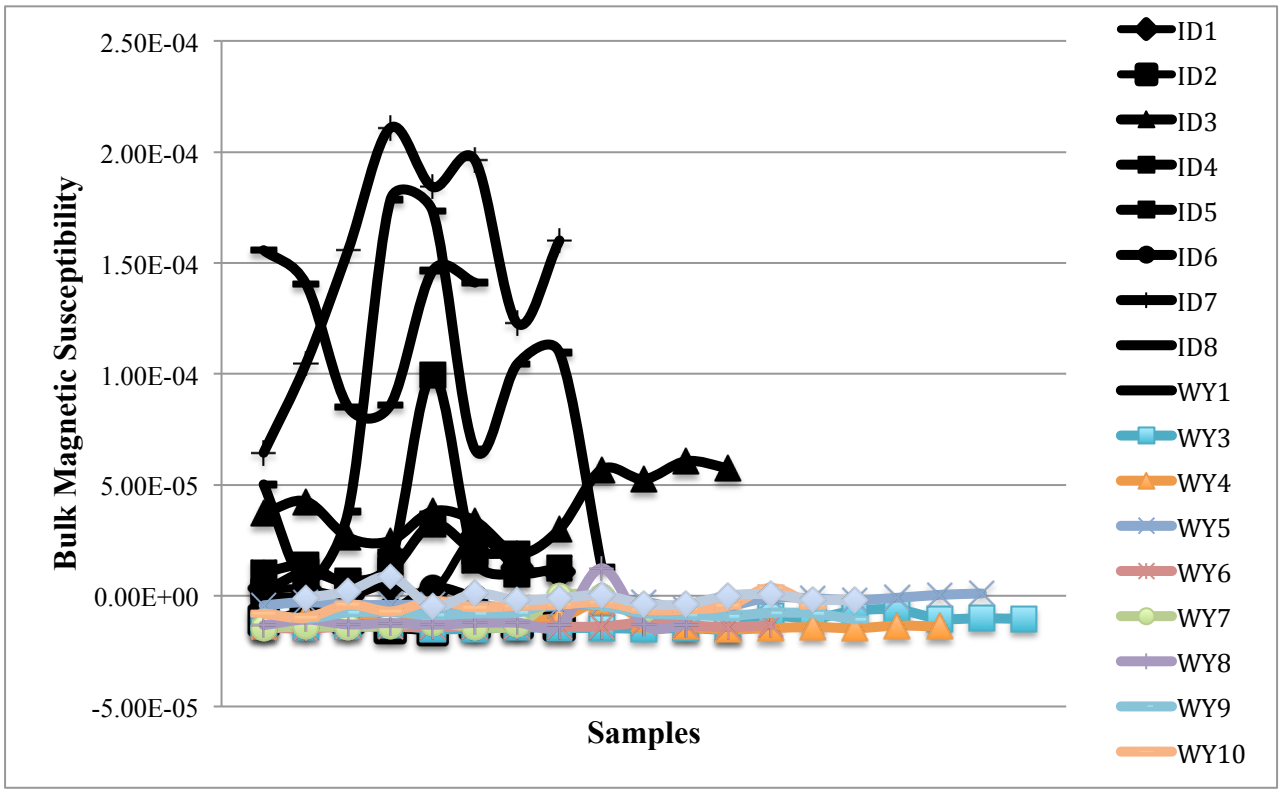

Figure A.4: Chart of bulk magnetic susceptibility for different samples from each site. Black indicates sites with susceptibilities above 0.

In hysteresis experiments, a stronger ferrimagnetic signal is seen in the Idaho samples (ID1-ID8) and present-day field in two WY samples (WY1-WY2) as compared to the Bighorn Mountain sampled carbonates (WY3-WY10; Fig. A.5). However, a weak magnetic remanence is also depicted in hysteresis loops that measure the variation in a recorded magnetization in response to a changing applied magnetic field (Butler, 1992; Tauxe et al., 1996). If there is a limited quantity of a remanence carrying mineral (ex. magnetite) in the samples, during a

hysteresis experiment, then the ferromagnetic signal is too weak to be separated from other sources. In this case the paramagnetic (ex. clay) or diamagnetic (ex. calcite) nature of a sample will dominate the measured signal. For example, after removal of the diamagnetic component, sample WY3-9a displays a very large error, overwhelming a very weak ferrimagnetic signal (Fig. A.5). Beske-Diehl and Shive (1978) found similar erratic directions in limestone samples in the Bighorn Mountains. They detected a late Paleozoic direction in samples that are more dolomitic (Beske-Diehl and Shive, 1978).

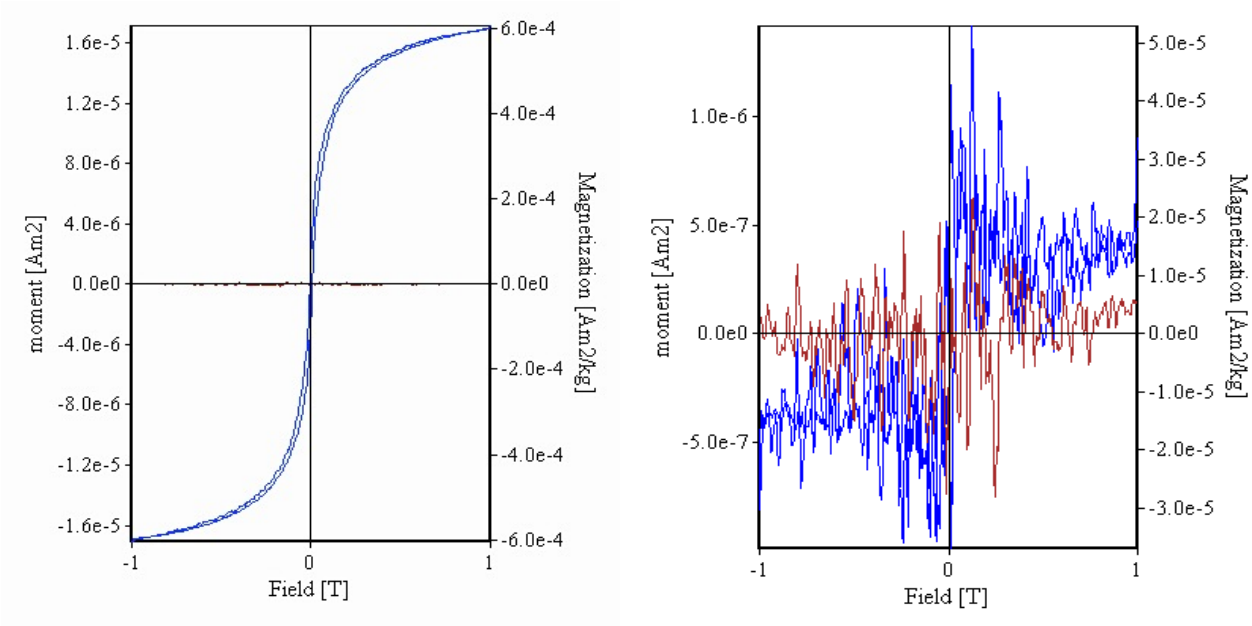

Figure A.5: Hysteresis loops of ID8-6 (left) and WY3-9a(right) corrected for diamagnetic and paramagnetic background with blue/red representing the ferrimagnetic component/error respectively.

A remagnetization is clearly recorded in the Mississippian carbonates sampled from Idaho and two sites in Wyoming based on the steep recorded inclinations. The remagnetization is recorded after folding has completed in Idaho as clearly indicated with postfolding directions. These recorded directions are very steep (60-70°), so it is difficult to decipher with the declinations if the remagnetizations are separate events. However, based on previous studies where a progression towards the foreland shows a transition from older to younger

remagnetization events, we can postulate that the magnetization preserved in the Idaho samples is slightly older than the central Wyoming samples (Nemkin et al., 2015; Nemkin et al., 2016).

Additional sampling and more fold tests could mediate this problem and help decipher between remagnetization events. However, these carbonates may instead not be suitable for the growth of magnetite as suggested by the absence of a present day field and no viscous component of the magnetization. In a viscous experiment, representative samples from Wyoming and Idaho were kept outside of the shielded room in the presence of a geomagnetic field over a span of a few weeks and measured once a week. After that, the samples were placed back in the shielded room and measured once a week. During these measurements there was no marked change in intensity inside or outside of the shielded room. This lack of change in the magnetic intensity suggests the non-existent to very limited presence of magnetite as compared to a study by Nemkin et al. (2017 *in review*). Samples from Nemkin et al. (2017 *in review*) possessed enough magnetite to record a present day field and show an increase in the magnetic intensity after a viscous acquisition outside of the shielded room. Therefore, samples from Wyoming do not show a viscous acquisition likely because not enough magnetite grew in the samples to record the field, which is also reflected in why the samples did not retain a measurable secondary remanence.

A key improvement to this study would be to try and sample more folds from the Wyoming fold-thrust belt as a transition between Idaho and central Wyoming. Even if folds cannot be sampled, the large Madison cliffs can also be sampled in order to better understand the paleomagnetic nature in the coarsely crystalline samples.

TABLE

Table A.1: Paleomagnetic data for folded Mississippian carbonates from Idaho and Wyoming

					Bedding		IS Mean Magnetization		TC Mean Magnetization		Statistics	
	Site	**Latitude** (°N)	**Longitude** (°W)	**n/N**	**Strike**	**Dip**	**Dec.**	**Inc.**	**Dec.**	**Inc.**	**a95** IS&TC	**k** IS&TC
Idaho	1	43°53'49"	113°40'26"	6/6	187.3	46.3	131.0	-69.6	109.7	-25.9	2.5	736.0
	2	43°53'47"	113°40'31"	3/6	340.3	44.7	140.8	-77.0	231.8	-48.2	26.9	22.0
	3	43°57'37"	113°26'45"	9/10	178.8	58.0	55.4	76.3	279.0	43.0	5.4	93.2
	4*	43°57'37"	113°26'45"	2/6	299.7	55.0	4.4	21.7	2.8	-28.4		
	5	43°51'34"	113°28'21"	5/5	346.3	54.7	349.3	60.9	42.6	29.0	12.9	36.1
	6	43°51'34"	113°28'21"	4/5	127.8	64.0	25.9	51.3	234.4	63.2	32.9	8.8
	7	43°45'19"	113°28'43"	6/6	188.0	35.0	1.5	69.4	309.5	48.1	2.7	619.2
	8	43°45'23"	113°28'35"	6/7	330.0	24.2	31.4	66.0	44.4	43.4	8.8	59.5
Wyoming	1	42°54'19"	110°52'31"	5/5	64.0	68.2	358.9	55.0	130.9	51.9	2.6	841.6
	2	42°54'16"	110°52'35"	8/9	162.4	48.2	359.1	49.1	307.5	40.1	2.2	623.9
	3	44°36'42"	108°8'21"	4/11	96.3	27.5	307.9	-26.6	315.6	-10.4	85.7	2.1
	4	44°36'46"	108°8'56"	7/9	314.0	28.0	109.9	68.3	74.6	48.5	24.3	7.1
	5	44°47'39"	107°58'7"	7/9	107.0	45.5	83.1	68.1	165.4	49.3	14.4	18.5
	6	44°47'43"	107°58'3"	1/7	328.4	75.1	8.8	48.4	27.2	-12.9	only 1 sample	
	7	44°48'19"	107°19'11"	2/7	315.4	32.4	340.0	48.9	2.1	29.3	71.7	14.4
	8	44°48'20"	107°19'11"	3/8	355.2	24.8	170.7	-34.7	187.6	-32.9	27.9	20.6
	9	44°4'18"	107°20'43"	4/10	123.7	14.5	11.4	75.5	293.0	84.5	9.7	90.1
	10*	44°4'18"	107°20'43"	2/7	312.2	9.2	154.8	-31.5	159.5	-27.6		

Note: n/N, number of samples accepted/measured; IS Dec., In situ declination; IS Inc., In situ inclination; TC Dec., Tilt-corrected declination; TC Inc., Tilt-corrected inclination; a95, radius of 95% cone of confidence in degrees; k, precision parameter (Fisher, 1953). Tilt-correction is 100% un-tilting. Strike and dip are measured in degrees using the left hand rule (LHR). Gray shading indicates sites that were not considered for fold test analysis since the site a95 value is over the set criteria of 20. An * denotes a site where there are only two samples and a site a95 and k cannot be determined.

APPENDIX B: PALEOMAGNETIC RESULTS OF MOROCCAN ~284 MA EXTRUSIVES; TESTING THEIR AGREEMENT WITH THE PANGEA-A RECONSTRUCTION

ABSTRACT

The Carboniferous-Early Permian configuration of Pangea has been debated ever since paleomagnetists postulated an overlap of the continents when trying to fit together the APWP's of Gondwana and Laurussia. Late Permian rocks have been examined to better develop the position of Pangea during this pre-Triassic time; however, analysis for the earlier Permian remains incomplete. The results of this study agree with previously published directions and add more precise age determinations (average U/Pb 284.7±6 Ma). This age puts the rocks in the Early Permian (at the base of the Artinskian Stage). Seven sites contain hematite as the remanence carrier and two sites resulted in magnetite carrying the recorded direction. Six sites have SE declinations and near-zero inclinations. From this study, two conclusions can be drawn involving the inclination and age of the directions. The near-zero inclinations (as well as the average declination of about 135 degrees from Morocco) are what is to be expected of a conventional Pangea-A fit and agree with previously measured paleomagnetic data, leaving ages as the important aspect to be further studied. Previous analyses of Early Permian paleopoles have compared results from Baltica, the southern Alps in Italy, and Morocco. The Italian and Moroccan rocks have ages about 270-280 Ma, whereas the early Permian rocks from Baltica are mostly confined to the 290-300 Ma interval. Comparing the ~295 Ma results from Baltica and the ~275 Ma results from Italy and Morocco, causes a ~20 myr mismatch. This may result in an

error of up to 8 degrees, because of Pangea's drift of 0.4 degrees per myr during the Early Permian. Therefore, the paleomagnetic data and crucial ~284 Ma age add to the African APWP and support the "Pangea A" configuration for the Early Permian.

B.1 INTRODUCTION

Pangea existed as a supercontinent from the late Paleozoic to early Mesozoic when it began to rift apart, initiating the formation of the Atlantic Ocean (du Toit, 1937; Funnel and Smith, 1968; Van der Voo, 1993; Stampfli et al., 2013; Wegener, 1915,1922). Geological and paleomagnetic evidence supports the location of the landmasses of the supercontinent in the Jurassic prior to rifting, similar to the reconstruction made by Alfred Wegener and this is known as the "Pangea A" configuration (Bullard et al., 1965; Muttoni et al., 2003; Van der Voo et al., 1976; Wegener, 1915,1922). The positioning of the continents in Pangea constructed by Wegener were a little muddled and Carey (1958) improved upon some ambiguity in the reconstruction by using spherical trajectories. Many other researchers have further improved upon the Pangea configuration, especially in the Permian, with paleomagnetic data (e.g. Derder et al., 2001; Domeier et al., 2011; Domeier et al., 2012; Dominguez et al., 2011; Irving, 1977).

Multiple studies support the widely held configuration of Pangea in the Late Triassic-Early Jurassic (Irving, 1977; Klitgord and Schouten, 1986; Muttoni et al., 1996; Muttoni et al., 2003). However, from the Carboniferous to Permian there is a gap in data that has brought about two competing theories on the positioning of Pangea. This problem arose when poles from the Carboniferous through Permian no longer fit with the expected apparent polar wander paths (APWP's) for the region (Carey, 1958; De Boer, 1963, 1965; Jeager & Irving 1957). If the landmasses of Laurussia and Gondwana are left in the configuration of "Pangea A" in the Paleozoic with current paleomagnetic data and dates then there is a latitudinal overlap of the

continents that is reflected in ~1000km of continental overlap (Fig. B.1)(Muttoni et al., 2003). In order to correct for this overlap, Irving (1977) shifted Gondwana east relative to Laurussia and called this arrangement "Pangea B". Others supported the idea of a "Pangea B" configuration in the Carboniferous through Triassic (Torcq et al., 1997; Morel and Irving, 1981; Irving, 1977; Westphal, 1977). This range for "Pangea B" was later narrowed to the Carboniferous- mid-Permian with more samples and better defined age dates for the measured paleomagnetic poles (Muttoni et al., 1996; Muttoni et al., 2003).

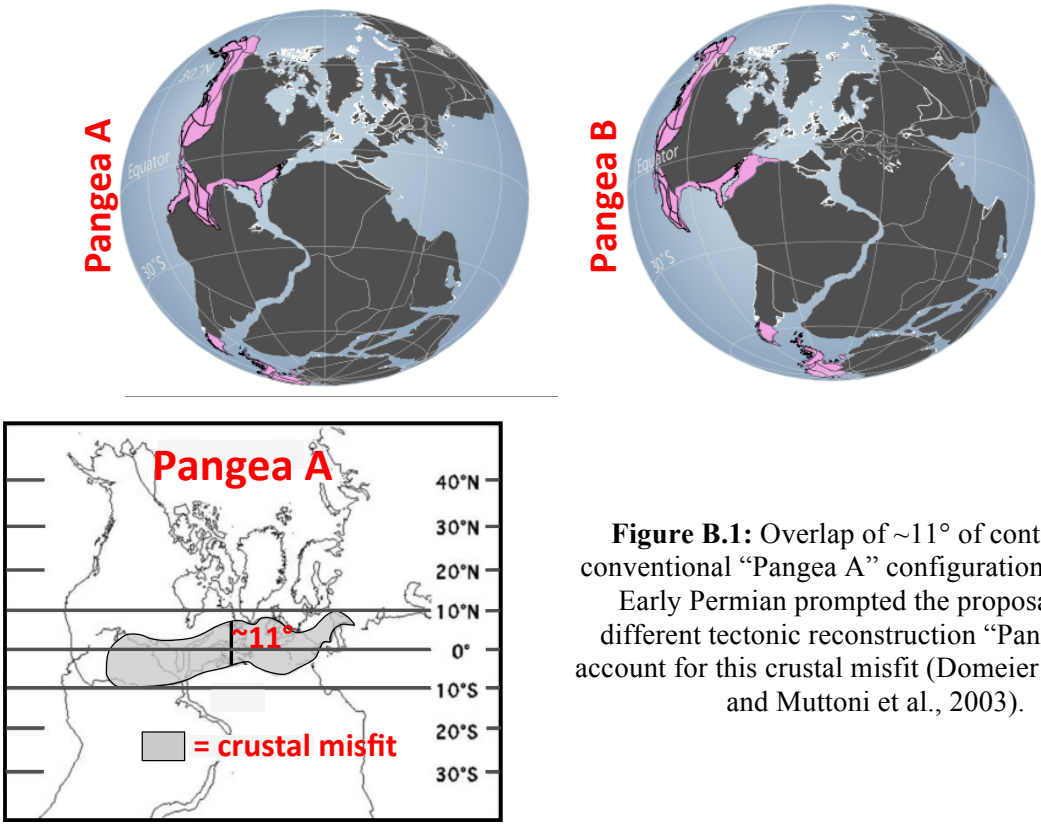

Figure B.1: Overlap of ~11° of continents in conventional "Pangea A" configuration during the Early Permian prompted the proposal of the different tectonic reconstruction "Pangea B" to account for this crustal misfit (Domeier et al., 2012 and Muttoni et al., 2003).

Even with discrepancies in the Paleozoic for the arrangement of the components of Pangea, data still supported a "Pangea A" configuration in the Jurassic prior to the opening of the Atlantic (Klitgord and Schouten, 1986). This meant there needed to be a large shift of

Gondwana from the Paleozoic "Pangea B" to Mesozoic "Pangea A". A large ~3500 km megashear was proposed as the mechanism to address this necessary shift (Irving, 1977; Irving, 2004; Muttoni et al., 2003). This large movement would need to occur prior to the Late Permian, for which there is little evidence to support such a large tectonic motion.

Muttoni et al. (1996 & 2003) supported this large megashear and the resulting motion of "Pangea B" to "Pangea A". In their study they stated that this large displacement needed to occur prior to the Late Permian because the Late Permian position of Africa fit the "Pangea A" model (Muttoni et al., 1996; Van der Voo and French, 1974). In Muttoni et al. (2003) the issue of inclination shallowing with sedimentary samples (Muttoni et al., 1996) was addressed by only sampling igneous rocks. These samples included well-dated rocks (284-276 Ma) from the Southern Alps (Adria) that were used as a proxy for Gondwana in order to figure out the positions of Gondwana in the Early Permian. With these samples, the authors found a large overlap of continental elements by averaging the Adria and Morocco paleopole dataset and comparing that averaged pole with the European pole for the Early Permian. This overlap is the support for a large megashear and "Pangea B" configuration in the Carboniferous- mid Permian (Bachtadse et al., 2002; Muttoni et al. 2003;Rapalini et al., 2006).

Advocates of "Pangea B" recognize that the Atlantic opens from the conventional "Pangea A" alignment in the Jurassic, so any additional proposed configurations would need to involve the movement of the continents to the "Pangea A" position by the Late Permian. This movement requires the proposed 3500 km megashear (Irving, 1977 and Muttoni et al., 2003), for which there is no evidence (Ross, 1979 and Hallam, 1983). Therefore, supporters of "Pangea A" have been looking for ways to correct the overlap without having to invoke this large-scale displacement, one being different tectonic reconstructions. Three other mechanisms being

corrected/double checked are flawed paleomagnetic data, a possible octupole contribution, and finding better age dates to go along with the paleomagnetic data.

While three out of the four proposals have been verified and shown not to be in conflict with the Early Permian Pangea configuration, examination of Early Permian rocks and better dates may remediate this problem (Domeier et al, 2012). With a 4 cm/year change in the pole position during the Early Permian, age incongruities may produce large errors in pole positions (Marcano et al., 1999). For example a 20 million year difference in ages can produce 8° of error in paleolatitude. In addition to better controlled age dates, rocks from the continent of Africa need to be sampled instead of using rocks from other continents that may deceptively act as a proxy for Africa (Veevers, 2013). Therefore, roughly defined Early Permian igneous rocks from NW Morocco were the target of this study in order to check the paleomagnetic data and date the samples.

B.2 GEOLOGIC SETTING

Morocco is located at a major tectonic junction between Africa, the Atlantic, and the Alpine system, producing a complex geologic history for the region (Hoepffner et al., 2006; Michard et al., 2008; Pique and Carpenter, 2001). Most of the area is underlain by Precambrian basement rock and much of the deformation/tectonic history in the area is in the Paleozoic and Cenozoic (Wartiti et al., 1990). The Paleozoic in Morocco is dominated by collision events that resulted in the amalgamation of the supercontinent Pangea (Matte, 2001). Initial major activity in Paleozoic formed the Anti-Atlas, from the collision of North America, Europe, and Africa (related to the Alleghenian Orogeny) (Burkhard et al., 2006; Hoepffner et al., 2005; Hoepffner et al., 2006). The Permian (late Paleozoic) represents a transition period for Morocco from the Paleozoic compressional setting to extension and stretching in the Mesozoic that led up the

opening of the Atlantic Ocean (Michard et al., 2008; Pique and Carpenter, 2001). Extension in the Mesozoic resulted in many intercontinental sedimentary basins (Wartiti et al., 1990). Later deformation in Cenozoic from collision between Europe and Africa resulted in the formation of the Middle and High Atlas Mountains (Sébrier et al., 2006).

Samples have been collected from the Moroccan Meseta to the west of the Atlas Mountains. The Meseta is a region of high plateaus and plains between the Atlantic Coast to the west and Atlas mountains to the east (Fig. B.2) (Stearns, 1978). Folded Paleozoic rocks and igneous intrusions dominate the Meseta (Michard, 1976). Within the Meseta, different basins were chosen because of the Early Permian volcanic outcrops. The Permian volcanics intrude into continental sediments (Wartiti et al., 1990). Volcanism began slightly before sedimentation in the Permian and continued in the Permian; resulting in rhyolite, andesite, dacite, and tuff deposits (Boushaba and Gagny, 1986) Volcanic ages are poorly constrained based on dates by early K-Ar dating and fossil evidence with age ranges from the Sakmarian to Wordian (Early Permian) (Wartiti et al., 1990).

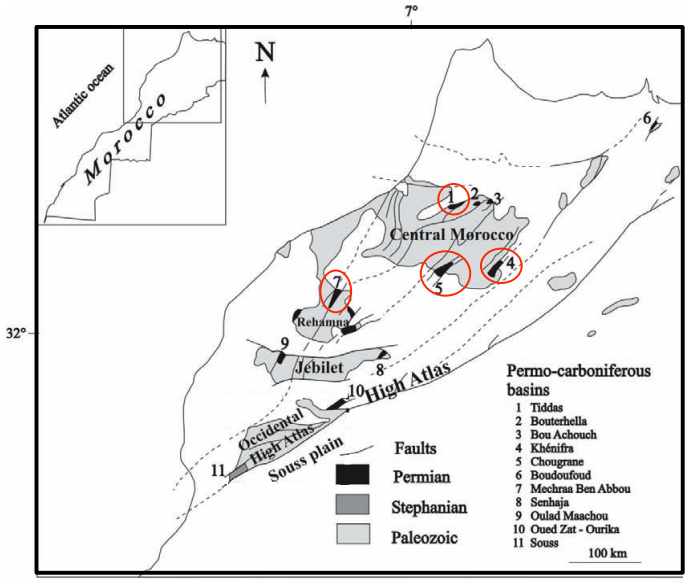

Sampling Areas

Figure B.2: Map of northwest Morocco with Carboniferous-Permian basins labeled 1-11. Samples were collected from the Tiddas, Khenifra, Chougrane, and Mechraa Ben Abbou basins (circled red). Image from Nasrrddine Youbi

B.3 METHODS

Sampling

The goal of this study is to improve upon the Early Permian position of Africa in the context of the Pangean configuration; therefore, samples were collected from various Carboniferous-Permian basins in NW Morocco. These basins include the Tiddas, Khenifra, Chougrane, and Mechraa Ben Abbou and are located to the northwest of the High Atlas Mountains. From these four basins nine volcanic sites were sampled. About 5-10 cores were collected per site using a portable Pomeroy EZ Core Drill and a Brunton compass/inclinometer was used to determine the azimuth and plunge of the core samples and the orientation of the beds.

Tiddas Basin: 2 sites (TL1, SA2)

Khenifra Basin: 4 sites (GB1, GB2, GB3, GB4)

Chougrane: 2 sites (TC1, TC2)

Mechraa Ben Abbou: 1 site (MB1)

Laboratory Work

Cylindrical samples were collected and then sent to the University of Michigan where they were cut with a dual bladed saw to a 2.2 cm length. Broken samples were glued back together with alumina cement and all specimens were labeled with Velvet Underglaze non-magnetic temperature resistant paint.

All specimens were measured and demagnetized in a magnetically shielded room, with a rest field of less than 200 nT, to minimize accumulation of any viscous magnetization. Remanent

magnetizations were measured using a three-axis 2G superconducting magnetometer. Specimens were thermally demagnetized using an ASC TD-48 demagnetizer after trials revealed the presence of hematite in some samples that could not be demagnetized with an alternating field. The specimens were heated until ~580° for some and then ~680° for samples that were not demagnetized by 580°. Results from the demagnetization process were analyzed with the Paleomac software by Cogné (2003) and graphed in orthogonal or stereographic projections (Zijderveld, 1967). Principal component analysis (PCA) was used to examine the demagnetization data (Kirschvink, 1980).

B.4 RESULTS

Magnetic directions of 9 sites collected from NW Morocco are presented in Table 1. Thermal demagnetization was employed to reveal the characteristic magnetic direction (ChRM) in the andesitic samples, which resulted in primarily univectorial decay of hematite and some magnetite bearing samples. Samples from MB1, GB1, GB2, GB3, GB4, TL1, and SA2 show a decay of the magnetization by 680°C and samples from TC1 and TC2 decay by ~580° (Fig. B.3). All but one site (GB2) resulted in interpretable results, with all of the sites having low alpha95 values (<15) and high k values (>25). GB2 is not included in further analysis because the k value (4.9) is less than the set criteria of 10 (Fisher, 1953).

Six of the nine sites (MB1, TC1, TC2, GB3, Tl1, and SA2) have tectonic corrected declinations in the southeast quadrant with very shallow inclinations and the remaining two sites (GB1 and GB4) have tectonically corrected directions to the north (Table B.1; Fig. B.4). Directions from the sites that are to the SE and very shallow are near the expected Early Permian direction for Morocco. For GB3, the current directions do not place it near the expected position in the Permian and may instead represent an anomalous result.

The global APWP of Torsvik et al. (2012) is utilized to estimate the expected Permian directions for Morocco by rotating the path to a NW African reference frame. Calculated poles will be compared to the expected Early Permian (280.5 and 273 Ma) poles of -36°, 58° and -33.4°, 66° (Plat, Plong) from volcanic and red bed samples, respectively in the Chougrane and Mechra ben Abbou basins (Fig. B.5)(Torsvik et al., 2012). Three sites (TL1, TC1 & TC2) have paleomagnetic poles that are close to the expected early Permian direction on the APWP (Table 2).

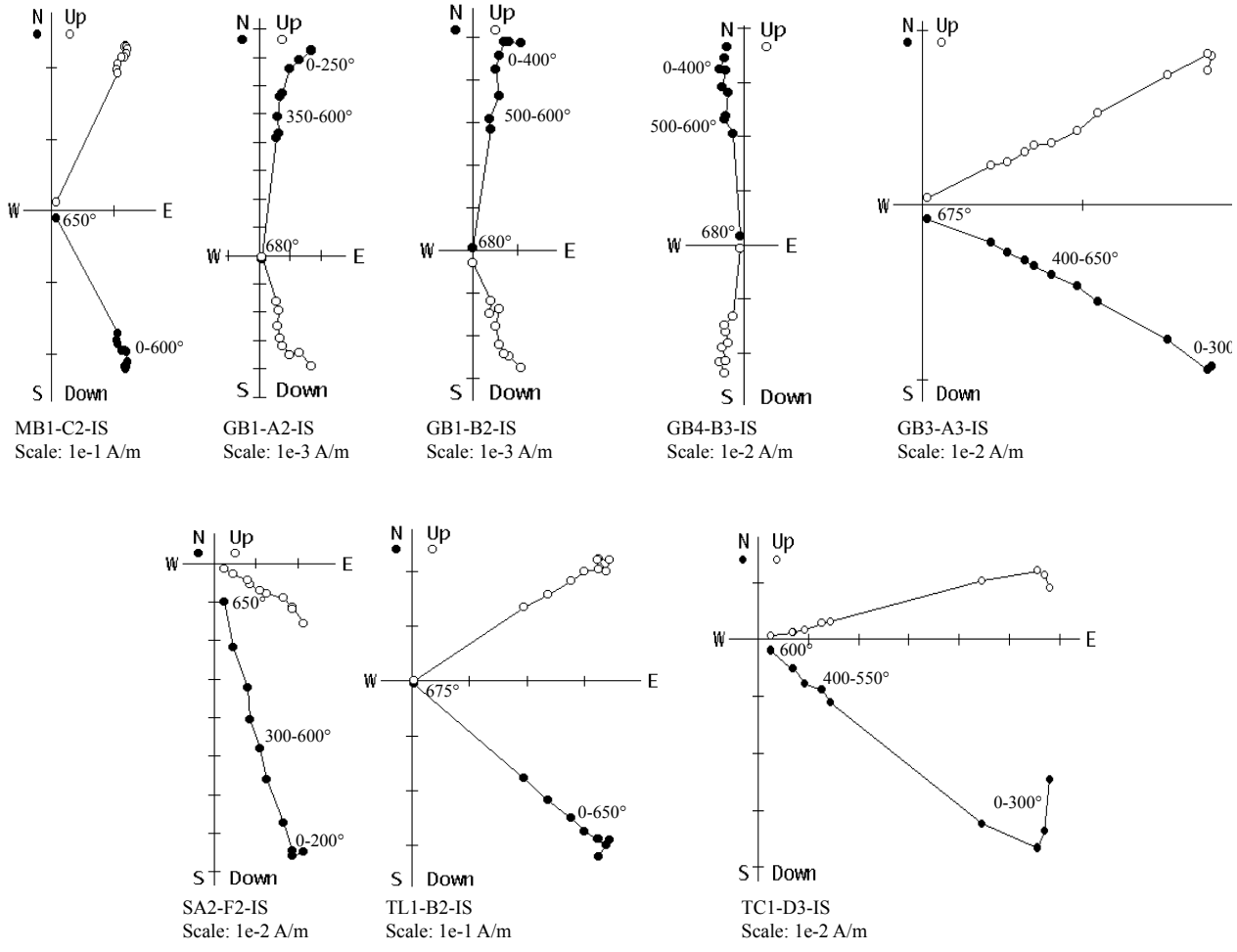

Figure B.3: Representative thermal demagnetization plots of igneous samples from NW Morocco in geographic coordinates (IS, in situ) (Zijderveld, 1967). Closed (open) symbols represent vector endpoints plotted in the horizontal (vertical) plane. Numbers on the demagnetization plots indicate degrees Celsius.

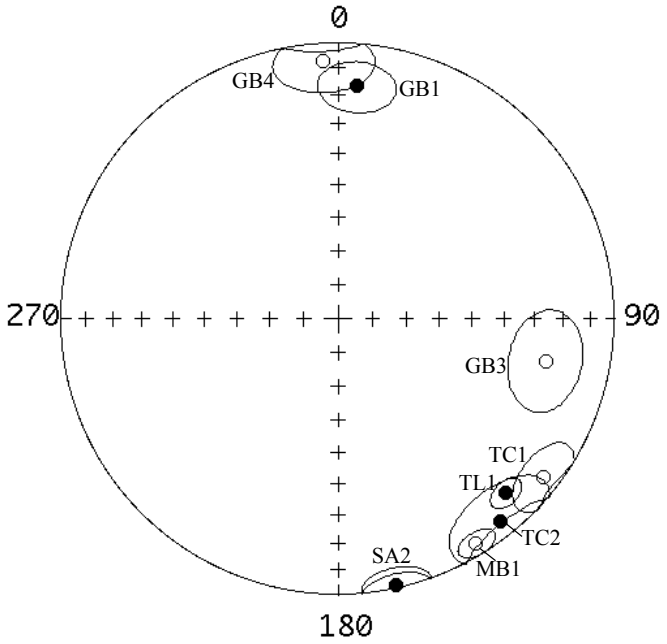

Figure B.4: Stereonet with tilt-corrected (TC) directions from Morocco.

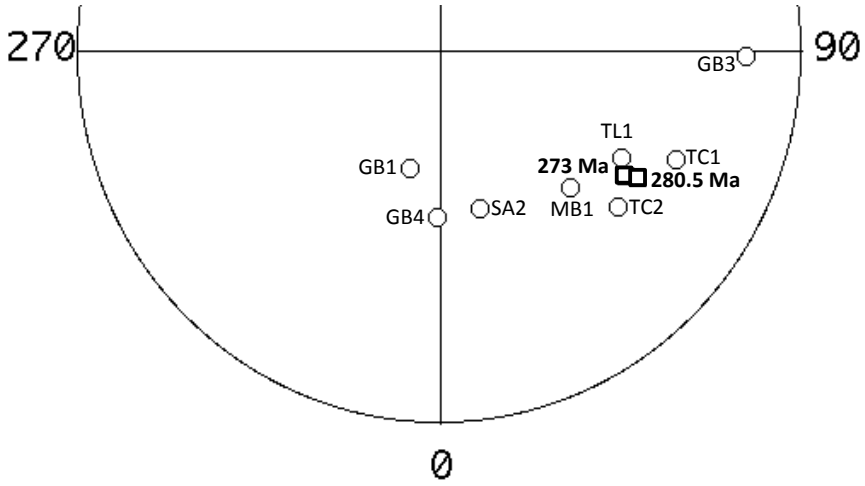

Figure B.5: Representative poles plotted for Morocco for 280.5 Ma, and 273 Ma (squares) in the southern hemisphere (Torsvik et al., 2012). Calculated poles from this study are also plotted in order to compare to the expected Permian directions.

B.5 INTERPRETATION

Directional Analysis

Sites from the Chougrane Basin, TC1 and TC2, show a fairly clean decay of the characteristic magnetization. Daly and Pozzi. (1979) also report on data from the Chougrane

Basin with a tilt-corrected declination and inclination of 127°, -6°, essentially identical to the TC1 tilt-corrected declination and inclination of 127.8°, -6.6° and very close to the tilt corrected TC2 directions (141.3°, 6.6°). The calculated tilt corrected poles of TC1 and TC2 (-29.4°, 65.9° and -35.4°, 49.7°, respectively) and TL1 (-41.5°, 60.3°) from the Tiddas Basin are very close to the Early Permian poles (Fig. B.5). With the close proximity of the poles to the expected corresponding direction for Morocco, these samples provide the possibility to be dated in order to confirm the Early Permian age.

The tilt-corrected direction for MB1 (148.4°, -5.1°) does fall within a 10° declination range to the grouping of TC1, TC2, and TL1, but the tilt-corrected MB1 pole (-47.2°, 44.3°) does not cluster and falls near the Late Permian-Early Triassic segment of the APWP. The Khenifra basin posed many problems for samples directions from GB1, GB2, GB3, and GB4 in terms of significantly more erratic demagnetization behavior as compared to samples from other sites. Directions from GB2 are very scattered and did not produce a coherent site average. The shallow inclinations for GB3 are expected for Morocco but the declinations are very far off (Fig. B.4). Directions from GB1 and GB4 are likely remagnetizations, falling closest to the ~50 Ma section of the APWP. The calculated tilt corrected direction (167.7°, 1.2°) and pole for SA2 (-53.9°, 14.9°), both do not correspond with expected Early Permian results. While the inclinations for SA2 are still very shallow (~0°) as expected for Morocco during the Early Permian, the declination is much more southward, reflecting a possible local rotation (Fig. B.4). The more southward declination for SA2 results in a pole that is far from the expected segment of the APWP. One possibility is that the samples are not andesites and instead very altered sandstones. In this case the sandstones might be a different age while deformation of the sediment may be influencing the measured direction.

Correcting for Pangea A vs. B

Better Tectonic Reconstructions?

Different crustal reconstructions have been attempted to address an overlap of Gondwana and Laurussia in the Carboniferous- Early Permian (e.g. Irving, 1988; Muttoni et al., 2003). This reconstruction as discussed before is "Pangea A" vs. "Pangea B". Pangea B is invoked as a lateral displacement of Gondwana during the Carboniferous to mid-Permian (Domeier et al., 2012). Supporters of "Pangea B" recognize that the continents must shift to "Pangea A" before the opening of the Central Atlantic Ocean in the Early Jurassic, so a large megashear is needed to shift from B to A (Irving, 1977). There is no geological evidence for this large megashear, which has caused Ross (1979) and many others to reject different tectonic reconstructions as the answer to this overlap (e.g. Hallam, 1983; Smith and Livermore, 1991).

Octupole Contribution?

Paleomagnetic studies typically assume a geocentric axial dipole (GAD) when analyzing data. The GAD assumes that the magnetic field averaged over sufficient time will be that of an axial dipole (Opdyke and Henry, 1969). Therefore, one of the proposals to correct for the overlap is to argue for a non-dipole field. Van der Voo and Torsvik (2001) conducted a study that looked at the influence of the octupole field on paleolatitudes. The addition of an octupole field will correct for the overlap but the influence of an octupole field is found to be a minimum (~0°) at the equator in the Carboniferous-early Permian when the paleomagnetic data/overlap of continents is found to be the most problematic (Van der Voo and Torsvik, 2001).

Better Paleomagnetic Data?

One possibility for the unwanted overlap of Gondwana and Laurussia in the Early Permian is that older paleomagnetic data was lacking in accuracy. Comparison of some older

studies and this study have shown that previous paleomagnetic data although lacking in quantity is there in quality. One example is Daly and Pozzi, (1975) where directions from that paper show similar declinations and inclinations to this study (~144°, 2°). Calculated directions are also close those reported by Westphal et al. (1975) who reported site-mean directions of 141°, -5° and 137°, -5°. Seeing that previous and current paleomagnetic data concur, the next step is to better constrain the pole positions with more accurate age dates.

Better Age Dates?

The apparent polar wander path for Pangea in the Early Permian changes by ~4 cm/year (Marcano et al., 1999). Therefore, age differences in rocks that are being compared can produce large errors in the paleomagnetic pole position. For example if one compares results from Baltica that are ~295 Ma with results from Morocco that are ~275 Ma, the 20 million year mismatch of rock ages can produce an error in the pole positions of ~8°.

As an example, we examine the results of Morel et al. (1981), who sampled what they believe to be Early Permian rocks based on stratigraphically correlating ages. From that paper, declinations of roughly 129° and inclinations of +11° were obtained. The authors calculate a pole for NW Africa (from the Saharan Craton & Moroccan Meseta) that differs from the APWP of North America. Consequently, they invoke Pangea B and shift Africa into a more suitable position based on matching paleomagnetic poles. Morel et al. (1981) do not have well defined ages for their samples, possibly causing mismatched paleomagnetic poles. Without well-defined ages the authors are comparing directions from samples that may have a very large age difference, producing large errors in the pole position.

Consequently, comparing pole positions that result from rocks with different ages can result in the overlap that is observed as a problem in the Early Permian (Veevers, 2013). Given

this need to correct the Early Permian position of Africa, volcanic samples were chosen to check the paleomagnetic position and perform new and improved age dating. The ages of these samples is ~284 Ma. This age combined with the paleomagnetic data, improves the APWP for Africa and confirms the "Pangea A" configuration in the Early Permian.

B.6 CONCLUSIONS

Better age dates are needed to refine the Carboniferous to Early Permian direction of Africa in the Pangea model. The very shallow (near 0°) inclinations and SE declinations are the expected directions for Africa in a "Pangea A" fit for the Early Permian (Domeier et al, 2012; Torsvik et al., 2012). This is further supported by age dates that constrain the age of the samples to ~284 Ma and add to the APWP for Africa.

TABLES

Table B.1: Paleomagnetic data for samples collected from andesites in the Moroccan Meseta.

		Bedding		IS Mean Magnetization		TC Mean Magnetization		Statistics	
Site	**n/N**	**Strike**	**Dip**	**Dec.**	**Inc.**	**Dec.**	**Inc.**	**a95** IS & TC	**k** IS & TC
MB1	5/5	223.5	34.5	152.5	-38.2	148.4	-5.1	4.5	286.8
TC1	4/6	170.0	5.0	128.3	-10.0	127.8	-6.6	8.9	75.1
TC2	6/6	94.6	6.4	140.6	11.2	141.3	6.6	12.9	28.1
GB1	5/5	252.8	15.6	7.3	31.1	4.6	16.8	9.3	68.5
GB2	5/5	265.0	16.5	336.6	24.3	338.1	8.6	38.6	4.9
GB3	4/4	102.0	49.8	120.8	-15.7	101.6	-24.3	12.8	52.1
GB4	6/6	295.8	35.6	354.3	23.2	356.8	-7.8	11.3	36.0
TL1	11/13	264.4	10.3	133.5	-20.7	136.2	-13.5	4.3	112.8
SA2	6/8	130.4	12.8	166.8	8.9	167.7	1.2	7.4	83.0

Note: n/N, number of samples accepted/measured; IS Dec., In situ declination; IS Inc., In site inclination; TC Dec., Tilt-corrected declination; TC Inc., Tilt-corrected inclination; a95, radius of confidence circle in degrees; k, precision parameter (Fisher,1953). Tilt- correction is 100% un-tilting. Strike and dip are measured in degrees using the left hand rule (LHR). Gray shading indicates a site that was not used in further analysis because the site k value is less than 10.

Table B.2: Calculated poles of measured directions from andesitic sites collected from Morocco.

Site	Plat (IS)	Plon (IS)	Plat (TC)	Plon (TC)
MB1	-62.9°	64.4°	-47.2°	44.3°
TC1	-30.8	67.5°	-29.4°	65.9°
TC2	-33.4°	48.8°	-35.4°	49.7°
GB1	-70.6°	336.5°	-63.2°	345.9°
GB3	-30.0°	73.8°	-16.4°	89.1°
GB4	-68.4°	9.6°	-52.9°	359.6°
TL1	-41.8°	66.6°	-41.5°	60.3°
SA2	-49.9°	14.4°	-53.9°	14.9°

Note: Pole latitude (Plat) and pole longitude (Plon) are listed for the in situ (IS) and tilt-corrected (TC) directions for each site collected.

REFERENCES

Altaner, S.P., and Ylagan, R.F., 1997, Comparison of structural models of mixed-layer illite/smectite and reaction mechanisms of smectite illitization: Clays and Clay Minerals, v. 45, p. 517–533, doi:10.1346/CCMN.1997.0450404.

Aranda-Gómez, J.J., Torres-Hernández, R., Carrasco-Nuñez, G., and Aguillón-Roblez, A., 2000, Contrasting styles of Laramide folding across the west-central margin of the Cretaceous Valles–San Luis Potosi carbonate platform, Mexico: Revista Mexicana de Ciencias Geológicas, v. 17, p. 97–111.

Armstrong, R.L., 1968, Sevier orogenic belt in Nevada and Utah: Geological Society of America Bulletin, v. 79, v. 429-458.

Armstrong, R.L., 1974, Magmatism, orogenic timing, and orogenic diachronism in the Cordillera from Mexico to Canada: Nature, v. 247, p. 348–351, doi:10.1038/247348a0.

Armstrong, F.C., and Oriel, S.S., 1965, Tectonic development of Idaho-Wyoming thrust belt: AAPG Bulletin, v. 49, p. 1847-1866.

Bachtadse, V., Zaenglein, R., Tait, J., and Soffel, H.C., 2002, Paleomagnetism of the Permo/Carboniferous (280 Ma) Jebel Nehound ring complex, Kordofan, Central Sudan: Journal of African Earth Sciences, v. 35, p. 89-97.

Ballard, M.M., Van der Voo, R., and Hälbich, I.W., 1986, Remagnetizations in late Permian and early Triassic rocks from southern Africa and their implications for Pangea reconstructions: Earth and Planetary Science Letters, v. 79, p. 412-418.

Beske-Diehl, S., and Shive, P.N., 1978, The rock magnetism of the Mississippian Madison Limestone north-central Wyoming: Geophysical Journal International, v. 55, p. 351-362.

Besse, J., and Courtillot, V., 2002, Apparent and true polar wander and the geometry of the geo- magnetic field over the last 200 Myr: Journal of Geophysical Research, v. 107, no. B11, p. 2300, doi:10.1029/2000JB000050.

Bullard, E., Everett, J.E., and Smith, A.G., 1965, The fit of the continents around the Atlantic: Philosophical Transactions of the Royal Society of London, v. 258, p. 41-51.

Burchfiel, B.C., Cowan, D.S., and Davis, G.A., 1992,Tectonic overview of the Cordilleran orogen in the western U.S., in Burchfiel, B.C., Lipman, P.W., and Zoback, M.L., eds.,The Cordilleran Orogen: Conterminous U.S.: Boulder, Colorado, Geological Society of America, The Geology of North America, v. G-3, p. 407–480, doi:10.1130/dnag-gna-g3.407.

Burkhard, M., Caritg, S., Helg, U., Robert-Charrue, C., and Soulaimani, A., 2006, Tectonics of the Anti-Atlas of Morocco: Geoscience, v. 338, p. 11-24.

Butler, R.F., 1992, Paleomagnetism: Magnetic domains to geologic terranes: Oxford, Blackwell Science, 319 p.

Camerlo, R.H., 1998, Geometric and kinematic evolution of detachment folds, Monterrey salient, Sierra Madre Oriental, Mexico, M.S> Thesis, University of Texas at Austin, 399p.

Campa-Uranga, M.F., 1983, The tectonostratigraphic terranes and the thrust belt in Mexican territory: Stanford University Publications in Geological Sciences 18, p. 44–46.

Cardozo, N., and Allmendinger, R.W., 2013, Spherical projections with OSXStereonet: Computers & Geosciences, v. 51, p. 193 – 205, doi:10.1016/j.cageo.2012.07.021.

Carey, S.W., 1958, The Tectonic Approach to Continental Drift, in Continental Drift, a symposium, 1956, University of Tasmania, p. 177-358.

Carrillo-Martinez, M., Valencia, J.J., and Vázquez, M.E., 2001, Geology of the southwestern Sierra Madre Oriental fold-and-thrust belt, east-central Mexico, a review: American Association of Petroleum Geologists Memoir 75, p. 145–158.

Cederquist, D.P., Van der Voo, R., and van der Pluijm, B.A., 2006, Syn-folding remagnetization of Cambro-Ordovician carbonates from the Pennsylvania Salient post-dates oroclinal rotation: Tectonophysics, v. 422, p. 41–54, doi:10.1016/j.tecto.2006.05.005.

Chavez-Cabello, G., Aranda-Gomez, J.J., Garza-Molina, R.S., Cossio-Torres, T., Arvizu-Gutierrez, I.R., and Gonzalez-Naranjo, G.A., 2007, The San Marcos Fault; a Jurassic multireactivated basement structure in northeastern Mexico. Geological Society f America, Special Paper, v. 422, p. 261-286.

Chávez-Cabello, G., Cossío-Torres, T., and Peterson-Rodríguez, R.H., 2004, Change of the maximum principal stress during the Laramide Orogeny in the Monterrey salient, northeast México: Geological Society of America Special Papers, v. 383, p. 145–159, doi: 10.1130/0-8137-2383-3(2004)383[145:COTMPS]2.0.CO;2.

Chávez-Cabello, G., Torres-Ramos, J.A., Porras-Vazquez, N.D., Torres, T.C., and Aranda-Gomez, J..J., 2011, Evolución estructural del frente tectónico de la Sierra Madre Oriental en el Cañón Santa Rosa, Linares, Nuevo León: Boletín de la Sociedad GeolóGica Mexicana, v. 63, p. 253-270.

Cioppa, M.T., Al-Asam, I.S., Symons, D.T.A., and Gillen, K.P., 2004, Causes of multiple magnetizations in the Devonia Upper Member, Wabamun Group, Alberta, Canada: Fluid Flow and Diagenesis?: in Swennen,R., Roure, F., and Granath, J.W., eds., Deformation, fluid flow and reservoid appraisal in foreland fold and thurst belts: AAPG Hedberg Series, v. 1, p. 331-346

Çinku, M.C., Hisarli, M., Orbay, N., Ustaomer, T., Hirt, A.M., Kravchenko, S., Rusakov, O., and Sayin, N., 2013, Evidence of Early Cretaceous remagnetization in the Crimean Peninsula: a palaeomagnetic study from Mesozoic rocks in the Crimean and Western Pontides, conjugate margins of the Western Black Sea: Geophysical Journal International, v. 195, p. 821-843, doi: 10.1093/gji/ggt260.

Clement, B.M., Poetisi, E., Bralower, T.J., CoBabe, E., and Longoria, J., 2000, Magnetostratigraphy of mid-Cretaceous limestones from the Sierra Madre of northeastern Mexico: Geophysical Journal international, v. 143, p. 219-229.

Cogné, J.P., 2003, PaleoMac: A MacintoshTM application for treating paleomagnetic data and making plate reconstructions: Geochemistry, Geophysics, Geosystems, v. 4, 1007, doi:10.1029 /2001GC000227.

Cox, A., and Doell, R.R., 1960, Review of paleomagnetism: Geological Society, London, Special Publications, v. 71, p. 645-768.

Creer, K.M., 1962, The dispersion of the geomagnetic field due to secular variation and its determination for remote times from paleomagnetic data: Journal of Geophysical Research, v. 67, p. 3461-3476, doi: 10.1029/JZ067i009p03461.

Creer, K.M., 1968, Paleozoic Paleomagnetism, Nature, v. 219, p. 246-250.

Day, R., Fuller, M., and Schmidt, V.A., 1977, Hysteresis properties of titanomagnetites: Grain- size and compositional dependence: Physics of the Earth and Planetary Interiors, v. 13, p. 260–267, doi:10.1016/0031-9201(77)90108-X.

de Boer, J., 1963, The geology of the Vicentinian Alps (NE Italy), with special reference to their paleomagnetic history [Ph.D. Thesis]: Utrecht, Utrecht University, 178 p.

de Boer, J., *1965,* Paleomagnetic indications of megatectonic movements in the Tethys: Journal of Geophysical Research, v. 70, p. 931-944.

DeCelles, P.G., 2004, Late Jurassic to Eocene evolution of the Cordilleran thrust belt and foreland basin system, western U.S.A.: American Journal of Science, v. 304, no. 2, p. 105–168, doi:10.2475/ajs.304.2.105.

Deiss, C.R., 1943, Structure of the central part of the Sawtooth Range, Montana: Geological Society of America Bulletin, v. 54, p. 1123–1168, doi:10.1130/GSAB-54-1123.

Derder, M.E.M., Henry, B., Merabet, N., Amenna, M., and Bourouis, S., 2001, Upper Carboniferous Paleomagnetic pole from the stable Saharan Craton and Gondwana reconstructions: Journal of African Earth Sciences, v. 32, p. 491-502.

Dickinson, W.R., 2004, Evolution of the North American Cordillera: Annual Review of Earth and Planetary Sciences, v. 32, p. 13–45, doi:10.1146/annurev.earth.32.101802.120257.

Domeier, M., Van der Voo, R., and Torsvik, T.H., 2012, Paleomagnetism and Pangea: The road to reconciliation: Tectonophysics, v. 514-517, p. 14-43, doi:10.1016/j.tecto.2011.10.021.

Domeier, M., Van der Voo, R., Tohver, E., Tomezzoli, R.N., Vizan, H., Torsvik, T.H., Kirshner, J.A., 2011a. New Late Permian constraint on the apparent polar wander path of Gondwana: Geochemistry Geophysics Geosystems, v. 12. doi:10.1029/2011GC003616.

Domeier, M., Van der Voo, R., Tomezzoli, R.N., Tohver, E., Hendriks, B.W.H., Torsvik, T.H., Vizán, H., Dominguez, A., 2011b. Support for an "A-type" Pangea reconstruction from high-fidelity Late Permian and Early to Middle Triassic paleomagnetic data from Argentina: Journal of Geophysical Research, v. 116, p. 1-26, doi:10.1029/2011JB008495.

Dominguez, A.R., Van der Voo, R., Torsvik, T.H., Hendriks, B.W.H., Abrajevitch, A., Domeier, M., Larsen, B.T., Rousse, S., 2011. The 270 Ma paleolatitude of Baltica and its significance for Pangea models. Geophysical Journal International 186, 529–550.

du Toit, 1937, Our Wandering Continents: A hypothesis of Continental Drifting: Oliver and Boyd, London.

Dunlop, D.J., 2002a,Theory and application of the Day plot (Mrs/Ms versus Hcr/Hc): 1.Theoretical curves and tests using titanomagnetite data: Journal of Geophysical Research, v. 107, p. 5-1−5-15, doi:10.1029/2001JB000486.

Dunlop, D.J., 2002b, Theory and application of the Day plot (Mrs/Ms versus Hcr/Hc) 2. Application to data for rocks, sediments, and soils: Journal of Geophysical Research, v. 107, p. 5-1 – 5-15, doi: 10.1029/2001JB000487.

Eguiluz de Antuñano, S.E., Marrett, R., and García-Aranda, M., 2000, Tectónica de la Sierra Madre Oriental, México. Boletin de la Sociedad Geológica Mexicana, v. 53, p. 1-26.

Eldredge, S., and Van der Voo, R., 1988, Paleomagnetic study of thrust sheet rotations in the Helena and Wyoming Salients of the northern Rocky Mountains, in Schmidt, C., and Perry, W.J., eds., Interaction of the Rocky Mountain Foreland and the Cordilleran Thrust Belt: Geological Society of America Memoir 171, p. 319–332.

Eldredge, S., Bachtadse, R., and Van der Voo, R., 1985, Paleomagnetism and the orocline hypothesis: Tectonosphysics, v. 119, p. 153-179, doi: 10.1016/0040-1951(85)90037-X.

Elliott, W.C., Osborn, S.G., O'Brien, V.J., Elmore, R.D., Engel, M.H., and Wampler, J.M., 2006, On the timing and causes of illite formation and remagnetization in the Cretaceous Marias River Shale, Disturbed Belt, Montana: Journal of Geochemical Exploration, v. 89, p. 92–95, doi:10.1016/j.gexplo.2005.11.033.

Elmore, R.D., Kelley, J., Evans, M., and Lewchuk, M.T., 2001, Remagnetization and orogenic fluids: Testing the hypothesis in the central Appalachians: Geophysical Journal International, v. 144, p. 568–576, doi:10.1111/j.1365-246X.2001.00349.x.

Elmore, R.D., Muxworthy, A.R., and Aldana, M., 2012, Remagnetization and chemical alteration of sedimentary rocks, in Elmore, R.D., et al., eds., Remagnetization and chemical alteration of sedimentary rocks: Geological Society of London Special Publication 371, p. 1–21, doi:10 .1144/SP371.15.

Elston, D.P., and Bressler, S.L., 1977, Paleomagnetic poles and polarity zonation from Cambrian and Devonian strata of Arizona: Earth and Planetary Science Letters, v. 36, no. 3, p. 423–433, doi: 10.1016/0012-821X(77)90067-X.

Enkin, R.J., Osadetz, K.G., Baker, J., and Kisilevsky, D., 2000, Orogenic remagnetizations in the Front Ranges and Inner Foothills of the southern Canadian Cordillera: Chemical harbinger and thermal handmaiden of Cordilleran deformation: Geological Society of America Bulletin, v. 112, p. 929–942, doi:10.1130/0016-7606(2000)112<929:ORITFR>2.0.CO;2.

Evans, M.A., Elmore, R.D., and Lewchuk, M.T., 2000, Examining the relationship between remagnetization and orogenic fluids: Central Appalachians: Journal of Geochemical Exploration, v. 69–70, p. 139–142, doi:10.1016/S0375-6742(00)00120-5.

Evans, S.C., Elmore, R.D., Dennie, D., and Dulin, S.A., 2012, Remagnetization of the Alamo Breccia, Nevada: in Elmore, R.D., et al., eds., Remagnetization and chemical alteration of sedimentary rocks: Geological Society of London Special Publication 371, p. 1–21, doi:10 .1144/SP371.15.

Facer, R.A., 1983, Folding, strain and Graham's fold test in paleomagnetic investigations: Royal Astronomical Society Geophysical Journal, v. 72, p. 165–171, doi:10.1111/j.1365-246X.1983 .tb02810.x.

Feng, J., Buffler, R.T., and Kominz, M.A., 1994, Laramide orogenic influence on late Mesozoic-Cenozoic subsidence history, western deep Gulf of Mexico basin, Geology, v. 22, p. 359-362.

Fisher, R.A., 1953, Dispersion on a sphere: Royal Society of London Proceedings, ser. A, v. 217, p. 295–305, doi:10.1098/rspa.1953.0064.

Fitz-Díaz, E., Camprubí, A., Cienfuegos-Alvarado, E., Morales-Puente, P., Schleicher, A.M., and van der Pluijm, B., 2014, Newly-formed illite preserves fluid sources during folding of shale and limestone rocks; an example from the Mexican Fold-Thrust Belt: Earth and Planetary Science Letters, v. 391, p. 263–273, doi: 10.1016/j.epsl.2013.12.025.

Fitz-Díaz, E., Hall, C.M., and van der Pluijm, B.A., 2016, XRD-based 40Ar/39Ar age correction for fine-grained illite, with application to folded carbonates in the Monterrey Salient (northern Mexico): Geochimica et Cosmochimica Acta, v. 181, p. 201–216, doi: 10.1016/j.gca.2016.02.004.

Fitz-Díaz, E., Hudleston, P., and Tolson, G., 2011a, Comparison of tectonic styles in the Mexican and Canadian Rocky Mountain Fold-Thrust Belt, in Poblet, J., and Lisle, R.J., eds., Kinematic evolution and structural styles of fold-and-thrust belts: Geological Society of London Special Publication 349, p. 149–167, doi:10.1144/SP349.8.

Fitz-Díaz, E., Hudleston, P., Kirschner, D., Siebenaller, L., Camprubí, A., Tolson, G., and Pi-Puig, T., 2011b, Insights into fluid flow and water-rock interaction during deformation of carbonate sequences in the Mexican fold-thrust belt: Journal of Structural Geology, v. 33, p. 1237–1253, doi:10.1016/j.jsg.2011.05.009.

Fitz-Díaz, E., Hudleston, P., Tolson, G., and van der Pluijm, B., 2014, Progressive, episodic deformation in the Mexican fold-thrust belt (central Mexico): Evidence from isotopic dating of folds and faults: International Geology Review, v. 56, p. 734–755, doi:10.1080 /00206814.2014.896228.

Fitz-Díaz, E., Tolson, G., Hudleston, P., Bolanos-Rodriguez, D., Ortega-Flores, B., and Serrano, V., 2012, The role of folding in the development of the Mexican fold-and-thrust belt: Geosphere, v. 8, p. 931–949, doi:10.1130/GES00759.1.

Fitz-Díaz, E., and van der Pluijm, B., 2013, Fold dating: A new Ar/Ar illite datingapplication to constrain the age of deformation in shallow crustal rocks: Journal of Structural Geology, v. 54, p. 174–179, doi: 10.1016/j.jsg.2013.05.011.

Font, E., Rapalini, A.E.,Tomezzoli, R.N.,Trindade, R.I.F., and Tohver, E., 2012, Episodic remagnetizations related to tectonic events and their consequences for the South America polar wander path, in Elmore, R.D., et al., eds., Remagnetization and Chemical Alteration of Sedimentary Rocks: Geological Society, London, Special Publication 371, p. 1–21, doi:10.1144/SP371.15.

Fuentes, F., DeCelles, P.G., Constenius, K.N., and Gehrels, G.E., 2011, Evolution of the Cordilleran foreland basin system in northwestern Montana, U.S.A.: Geological Society of America Bulletin, v. 123, p. 507–533, doi:10.1130/B30204.1.

Funnell, B.M., and Smith, A.G., 1968, Opening of the Atlantic Ocean: Nature, v. 219, p. 1328-1333.

Gill, J.D., Elmore, R.D., and Engel, M.H., 2002, Chemical remagnetization and clay diagenesis: Testing the hypothesis in the Cretaceous sedimentary rocks of northwestern Montana: Physics and Chemistry of the Earth, v. 27, p. 1131–1139, doi:10.1016/S1474-7065(02)00108-0.

Gillen, K.P., Van der Voo, R., and Thiessen, J.H., 1999, Late Cretaceous–Early Tertiary remagnetization of the Devonian Swan Hills Formation recorded in carbonate cores from the Caroline Gas Field, Alberta, Canada: American Association of Petroleum Geology Bulletin, v. 83, p. 1223–1235.

Gillett, S.L., and Karlin, R.E., 2004, Pervasive late Paleozoic-Triassic remagnetization of miogeoclinal carbonate rocks in the basin and range and vicinity, SW USA: regional results and possible tectonic implications: Physics of the Earth and Planetary Interiors, v. 141, no. 2, p. 95–120, doi: 10.1016/j.pepi.2003.11.001.

Goldhammer, R.K., 1999, Mesozoic sequence stratigraphy and paleogeographic evolution of northeast Mexico IN: Mesozoic Sedimentary and tectonic History of North-Central Mexico (ed. C. Bartolini, J.L. Wilson, T.F., Lawton) Geological Society America Special Paper 340. P.1-58.

Gong, Z., Dekkers, M.J., Dinarès-Turell, J., Mullender, T.A.T., 2008a. Remagnetization mechanism of Lower Cretaceous rocks from the Organyà Basin (Pyrenees, Spain). Stud. Geophis. Geod. 52, 187–210.

Gose, WA., Belcher, R.C. and Scott, G.R., 1982. Paleomagnetic results from northeastern Mexico: evidence for large Mesozoic rotations. Geology, v. 10, p. 50—54.

Graham, J.W., 1965, Paleomagnetism and magnetostriction: Journal of Geophysical Research, v. 61, p. 735-739.

Gray, G. G. and Lawton, T. F., 2011, New constraints on timing of Hidalgoan (Laramide) deformation in the Parras and La Popa basins, NE Mexico. Boletin de la Sociedad Geológica Mexicana, v. 63, p. 333-343.

Gray, G.G., Pottorf, R.J., Yurewicz, D.A., Mahon, K.I., Pevear, D.R., and Chuchla, R.J., 2001, Thermal and chronological record of syn- to post-Laramide burial and exhumation, Sierra Madre Oriental, Mexico, in Bartolini, C., et al., eds., The Western Gulf of Mexico Basin: Tectonics, sedimentary basins, and petroleum systems: American Association of Petroleum Geologists Memoir 75, p. 159–181.

Guyodo,Y., Mostrom, A., Penn, R.L., and Banerjee, S.K., 2003, From nanodots to nanorods: Oriented aggregation and magnetic evolution of nanocrystalline goethite: Geophysical Research Letters, v. 30, p. 19-1–19-4, doi:10.1029/2003GL017021.

Guzmán, E.J., and de Cserna, Z., 1963, Tectonic history of Mexico, in Childs, O.E., and Beebe. B.W., eds.. Backbone of the Americas: Tectonic history from pole to pole: American Association of Petroleum Geologists Memoir 2, p. 113–129.

Guzzy-Arredondo, G.S., Murillo-Muñetón, G., Morán-Zenteno, D.J., Grajales-Nishimura, J.M., Martínez-Ibarra, R., and Schaaf, P., 2007, High-temperature dolomite in the Lower Cretaceous Cupido Formation, Bustamante Canyon, northeast Mexico: petrologic, geochemical and microthermometric constraints: Revista Mexicana de Ciencias Geológicas, v. 24, p. 131-149.

Haines, S.H., and van der Pluijm, B., 2008, Clay quantification and Ar-Ar dating of synthetic and natural gouge: Application to the Miocene Sierra Mazatán detachment fault, Sonora, Mexico: Journal of Structural Geology, v. 30, p. 525–538, doi:10.1016/j.jsg.2007.11.012.

Hallam, A., 1983. Supposed Permo-Triassic megashear between Laurasia and Gondwana: Nature, v. 301, p. 499–502.

Higuera‐Díaz, I. C., Fischer, M. P., & Wilkerson, M. S. (2005). Geometry and kinematics of the Nuncios detachment fold complex: Implications for lithotectonics in northeastern Mexico. Tectonics, 24(4).

Hirt, A.M., Banin, A., and Gehring, A.U., 1993,Thermal generation of ferromagnetic minerals from iron-enriched smectites: Geophysical Journal International, v. 115, p. 1161–1168, doi: 10.1111/j .1365–246X.1993.tb01518.x.

Hnat, J. S., van der Pluijm, B. A., Van der Voo, R., and Thomas, W. A., 2008, Differential displacement and rotation in thrust fronts: A magnetic, calcite twinning and palinspastic study of the Jones Valley thrust, Alabama, US Appalachians: Journal of Structural Geology, v. 30, p. 725-738.

Hnat, J.S., van der Pluijm, B.A., and Van der Voo, R., 2009, Remagnetization in the Tennessee Salient, Southern Appalachians, USA: Constraints on the timing of deformation: Tectonophysics, v. 474, p. 709–722, doi:10.1016/j.tecto.2009.05.017.

Hoepffner, C., Abderahmane, S., and Piqué, A., 2005, The Moroccan Hercynides: Journal of African Earth Sciences, v. 43, p. 144-165.

Hoepffner, C., Houari, M.R., and Bouabdelli, M., 2006, Tectonics of the North African Variscides (Morocco, western Algeria): an outline: Geosciences, v. 338, p. 25-40.

Hoffman, J., and Hower, J., 1979, Clay mineral assemblages as low-grade metamorphic geothermometers: Application to the thrust faulted Disturbed Belt of Montana, U.S.A., in Scholle, P.A., and Schluger, F.R., eds., Aspects of Diagenesis: Society of Economic Paleontologists and Mineralogists Special Publication 26, p. 55–79.

Hoffman, J., Hower, J., and Aronson, J.L., 1976, Radiometric dating of time of thrusting in the disturbed belt of Montana: Geology, v. 4, p. 16–20, doi:10.1130/0091-7613(19756)4 <16:rdotot>2.0.co;2

Imlay, R.W., 1944, Cretaceous formations of Central America: American Association of Petroleum Geologists Bulletin, v. 28, p. 1107–1195.

Irving, E., 1977, Drift of the major continental blocks since the Devonian: Nature, v. 270, p. 304-309.

Irving, E., 2004, The case for Pangea B, and the Intra-Pangean Megashear: Timescales of the paleomagnetic field, Geophysical Monograph, v. 145, p. 59-76.

Jackson, M. J., Rochette, P., Fillion, G., Banerjee, S. K. and Marvin, J. A., 1993, Rock magnetism of remagnetized Paleozoic carbonates: low-temperature behavior and susceptibility characteristics: Journal of Geophysical Research B: Solid Earth, v. 98, p. 6217 – 6225.

Jackson, M., and Solheid, P., 2000, On the quantitative analysis and evaluation of magnetic hysteresis data: Geochemistry, Geophysics, Geosystems, v. 11, p. 1-25, doi: 1 0.1029/2009GC002932.

Jackson, M., and Swanson-Hysell, N.L., 2012, Rock magnetism of remagnetized carbonate rocks: Another look, in Elmore, R.D., et al., eds., Remagnetization and chemical alteration of sedimentary rocks: Geological Society of London Special Publication 371, p. 229–251, doi:10.1144 /SP371.3.

Jackson, M., Gruber, W., Marvin, J., and Banerjee, S.K., 1988, Partial anhysteretic remanence and its anisotropy: Applications and grain size dependence: Geophysical Research Letters, v. 15, p. 440–443, doi:10.1029/GL015i005p00440.

Katz, B., Elmore, R.D., Cogoini, M., and Ferry, S., 1998, Widespread chemical remagnetization: Orogenic fluids or burial diagenesis of clays?: Geology, v. 26, p. 603–606, doi:10.1130/0091-7613 (1998)026<0603:WCROFO>2.3.CO;2.

Katz, B., Elmore, R.D., Cogoini, M., Engel, M.H., and Ferry, S., 2000, Associations between burial diagenesis of smectite, chemical remagnetization, and magnetite authigenesis in the Vocontian trough, SE France: v. 105, p. 851–868.

Kent, D. V., and Opdyke, N. D., 1979, The early Carboniferous paleomagnetic field of North America and its bearing on tectonics of the northern Appalachians: Earth and Planetary Science Letters, v. 44, v. 365-372.

Kent, D.V., 1985, Thermoviscous remagnetization in some Appalachian limestones: Geohysics Research Letters, v. 12, p. 805-808.

Kirschvink, J.L., 1980, The least squares line and plane and the analysis of paleomagnetic data: Royal Astronomical Society Geophysical Journal, v. 62, p. 699–718, doi:10.1111/j.1365-246X .1980.tb02601.x.

Kleist, R., Hall, S.A., and Evans, I., 1984, A paleomagnetic study of the Lower Cretaceous Cupido Limestone , northeast Mexico: Evidence for local rotation within the Sierra Madre Oriental: Geological Society of America Bulletin, v. 95, p. 55-60.

Klitgord, K.D., and Schouten, H., 1986. Plate kinematics of the Central Atlantic. In: Vogt, P.R., Tucholke, B.E. (Eds.), The Geology of North America: The Western North Atlantic Region. Geol. Soc. Am, Boulder, CO (USA).

Kollmeier, J.M., van der Pluijm, B.A., and Van der Voo, R., 2000, Analysis of Variscan dynamics; early bending of the Cantabria–Asturias Arc, northern Spain: Earth and Planetary Science Letters, v. 181, p. 203-216.

Kodama, K.P., 1988, Remanence rotation due to rock strain during folding and the stepwise application of the fold test. Journal of Geophysical Research, v. 93, p. 3357-3371.

Lageson, D.R., 1987, Structural geology of the Sawtooth Range at Sun River Canyon, Montana Disturbed Belt, Montana, in Beus, S.S., ed., Rocky Mountain Section of the Geological Society of America: Geological Society of America Centennial Field Guide 2, p. 37–39, doi:10.1130/0-8137-5402-x.37.

Lawton, T. F., Bradford, I. A., Vega-Vera, F. J., Gehrels, G. E. and Amato, J. M. 2009. Provenance of Upper Cretaceous-Paleogene sandstone in the foreland basin system of the Sierra Madre Oriental, Northeastern Mexico, and its bearing on the fluvial dispersal systems of the Mexican Laramide Province. Geological Society of America Bulletin, v. 121, p. 820-836.

Lehmann, C., Osleger, D.A., and Montanez, I.P., 1998, Controls on cyclstratigraphy of Lower Cretaceous carbonates and evaporates, Cupido and Coahuila platforms, northeastern Mexico: Journal of Sedimentary Research, v. 68, p. 1109-1130.

Lehmann, C., Osleger, D.A., Montanez, I.P., Sliter, W., Arnaud-Vanneau, A., and Banner, J., 1999, Evolution of Cupido and Coahuila carbonate platforms, Early Cretaceous, northeastern Mexico, Geological Society of America Bulletin, v. 111. P. 1010-1029.

Lerman, R., 1994, High Temperature Fluids and Calcite Vein Formation in the Montana Disturbed Belt, West-Central Montana [Ph.D. thesis]: Missoula, Montana, University of Montana, 77 p.

Lewchuk, M.T., Evans, M., and Elmore, R.D., 2003, Synfolding remagnetization and deformation: Results from Paleozoic sedimentary rocks in West Virginia: Geophysical Journal International, v. 152, p. 266–279, doi:10.1046/j.1365-246X.2003.01820.x.

Lowrie, W., 1990, Identification of ferromagnetic minerals in a rock by coercivity and unblock- ing temperature properties: Geophysical Research Letters, v. 17, p. 159–162, doi:10.1029 /GL017i002p00159.

Marcano, M.C., Van der Voo, R., and Mac Niocaill, C., 1999, true polar wander during the Permo-Triassic: Geodynamics, v. 28, p. 75-95.

Martin, D.L., 1975, A paleomagnetic polarity transitions in the Devonia Columbus Limestone of Ohio: A possible stratigraphic tool: Tectonophysics, v. 28, p125-134.

Matte, P., 2001, The Variscan collage and orogeny (480-290 Ma) and the tectonic definition of the Armorica microplate: a review: Terra Nova, v. 13, p. 122-128.

McCabe, C., and Elmore, R.D., 1989,The occurrence and origin of late Paleozoic remagnetization in the sedimentary rocks of North America: Reviews of Geophysics, v. 27, p. 471–494, doi:10. 1029/RG027i004p00471.

McCabe, C., Jackson, M., and Ellwood, B.B., 1985, Magnetic anisotropy in theTrenton Lime- stone: Results of a new technique, anisotropy of anhysteretic susceptibility: Geophysical Research Letters, v. 12, p. 333–336, doi:10.1029/GL012i006p00333.

McCabe, C., Jackson, M., and Saffer, B., 1989, Regional patterns of magnetite authigenesis in the Appalachian Basin: Implications for the mechanism of late Paleozoic remagnetization: Journal of Geophysical Research, v. 94, p. 10,429–10,443, doi:10.1029/JB094iB08p10429.

McCabe, C., Van der Voo, R., and Ballard, M.M., 1984, Late Paleozoic remagnetization of the Trenton Limestone: Geophyscial Research Letters, v. 11, p. 979-982.

McCabe, C., Van der Voo, R., Peacor, D.R., Scotese, C.R., and Freeman, R., 1983, Diagenetic magnetite carries ancient yet secondary remanence in some Paleozoic sedimentary carbonates: Geology, v. 11, p. 221-223.

McElhinny, M.W., and Opdyke, N.D., 1973, Remagnetization hypothesis discounted: A paleomagnetic study of the Trenton Limestone, New York State: Bulletin of the Geological Society of America, v. 84, no. 11, p. 3697–3708, doi: 10.1130/0016-7606(1973)84<3697:RHDAPS>2.0.CO;2.

McMannis, W.J., 1965, Resumé of depositional and structural history of western Montana: American Association of Petroleum Geologists Bulletin, v. 49, p. 1801–1823, doi:10.1306 /a6633868-16c0-11d7-8645000102c1865d.

McWhinnie, S.T., van der Pluijm, B.A., and Van der Voo, R., 1990, Remagnetizations and thrusting in the Idaho-Wyoming overthrust belt: Journal of Geophysical Research, v. 95, p. 4551–4559, doi:10.1029/JB095iB04p04551.

Michard, A., 1976, Éléments de géologie marocaine: Notes et Mémoires du Service géologique, v. 252, p. 1-408.

Michard, A., Frizon de Lamotte, D., Saddiqi, O., and Chalouan, A., 2008, Continental Evolution: The Geology of Morocco: Lecture Notes in Earth Sciences, v. 116, p. 1-31.

Miller, J.D., and Kent, D.V., 1988, Regional trends in the timing of Alleghanian remagnetization in the Appalachians: Geology, v. 16, p. 588-591.

Morel, P., and Irving, E., 1981, Paleomagnetism and the evolution of Pangea: Journal of Geophysical Research, v. 86, p. 1858-1872.

Mudge, M.R., 1970, Origin of the Disturbed Belt in northwestern Montana: Geological Society of America Bulletin, v. 81, p. 377–392, doi:10.1130/0016-7606(1970)81[377:OOTDBI]2.0.CO;2.

Mudge, M.R., 1982, A resume of the structural geology of the Northern Disturbed Belt, Northwestern Montana: in Powers, R.B., ed., Geological studies of the Cordilleran thrust belt: Rocky Mountain Association of Geologists, v. 1, p. 91-122.

Mudge, M.R., Sando, W.J., and Dutro Jr., J.T., 1962, Mississippian rocks of Sun River Canyon area, Sawtooth Range, Montana: Bulletin of the American Association of Petroleum Geologists, v. 46, p. 2003-2018, doi:10.1306/bc743945-16be-11d7-8645000102c1865d

Muttoni, G., Kent, D., Garzanti,E., Brack, P., Abrahamsen, N., and Gaetani, M., 2003, Early Permian Pangea 'B' to Late Permian Pangea 'A': Earth and Planetary Science Letters, v. 215, p. 379-394.

Muttoni, G., Kent, D.V., and Channell, J.E.T., 1996, Evolution of Pangea: paleomagnetic constraints from the Southern Alps, Italy: Earth and Planetary Science Letters, v. 140, p. 97-112.

Nairn, A.E.M., 1976, A paleomagnetic study of certain Mesozoic formations in Northern Mexico: Physics of the Earth and Planetary Interiors, v. 13, p. 47-56.

Nemkin, S.R., Fitz-Díaz, E., van der Pluijm, B., and Van der Voo, R., 2015, Dating synfolding remagnetization: Approach and field application (central Sierra Madre Oriental, Mexico): Geosphere, v. 11, p. 1-12, doi:10.1130/GES01187.1

Nemkin, S.R., Lageson, D., van der Pluijm, B., and Van der Voo, R., 2016, Remagnetization and folding in the frontal Montana Rocky Mountains: Lithosphere, v. 8, p. 716-728, doi: 10.1130/L579.1.

Nowicki, M.J., Hall, S. A., and Evans, I., 1993, Paleomagnetic evidence for local and regional post-Eocene rotations in northern Mexico: Geophysical Journal International, v. 117, p. 63-75.

Nowicki, M.J., Hall, S. A., and Evans, I., 1993, Paleomagnetic evidence for local and regional post-Eocene rotations in northern Mexico: Geophysical Journal International, v. 117, p. 63-75.

O'Brien, V.J., Elmore, R.D., Engel, M.H., and Evans, M.A., 2006,Timing and origin of orogenic

Opdyke, N. D., and K. W. Henry., 1969, A test of the dipole hypothesis: Earth and Planetary Science Letters, v. 6, p. 139-151.

Padilla y Sanchez, R.J., 1982, Geologic evolution of the Sierra Madre Oriental between Linares, Concepcion del Oro, Saltillo, and Monterrey, Mexico, Ph.D. Thesis, University of Texas at Austin, 217p.

Pana, D.I., and van der Pluijm, B.A., 2015, Orogenic pulses in the Alberta Rocky Mountains: Radiometric dating of major faults and comparison with the regional tectono-stratigraphic record: GSA Bulletin, v. 127, p. 480-502, doi: 0.1130/B31069.1.

Piqué, A., and Carpenter, M.S., 2001, Geology of northwest Africa: v. 29, Gebrüder Borntraeger.

Pique, A., and Michard, A., 1989, Moroccan Hercynides: a synopsis. The Paleozoic sedimentary and tectonic evolution at the Northern Margin of West Africa: American Journal of Science, v. 289, p. 286-330.

Prost, G.L., 1996, The role of remote sensing in understanding the structural development of the Sierra Madre Oriental, Mexico. Eleventh Thematic Conference and Workshops on Applied Geologic Remote Snesing

Pullaiah, G., Irving, E., Buchan, K.L., and Dunlop, D.J., 1975, Magnetization changes caused by burial and uplift: Earth and Planetary Science Letters, v. 28, p. 133–143, doi:10.1016/0012-821X (75)90221-6.

Rapalini, A.E., Fazzito, S., Orue, D., 2006, A new Late Permian paleomagnetic pole for stable South America: the Independencia Group, eastern Paraguay: Earth, Planets, and Space, v. 58, p. 1247-1253.

Ross, C.A., 1979. Late Paleozoic collision of North and South America: Geology, v. 7, p. 41–44.

Schottenfels, E.R., 2015, A Paleomagnetic Exploration of the Sierra Madre Oriental: University of Michigan Undergraduate Honors Thesis

Scotese, C.R., Voo, R. Van Der, and McCabe, C., 1982, Paleomagnetism of the Upper Silurian and Lower Devonian carbonates of New York State: evidence for secondary magnetizations residing in magnetite: Physics of the Earth and Planetary Interiors, v. 30, no. 4, p. 385–395, doi: 10.1016/0031-9201(82)90048-6.

Scott, G.R., 1979, Paleomagnetic studies of the Early Carboniferous St. Joe limestone, Arkansas: Journal of Geophysical Research, v. 84, p.6277-6285.

Sears, J.W., 2001, Emplacement and denudation history of the Lewis-Eldorado-Hoadley thrust slab in the northern Montana Cordillera, USA: Implications for steady-state orogenic processes: American Journal of Science, v. 301, p. 359-373.

Sears, J.W., Braden, J., Edwards, J., Geragthy, E., Janiszewski, F., McInenly, M., McLean, J., Riley, K., and Salmon, E., 2005, Rocky mountain foothills traingle zone, Sun River, Northwest Montana: Northwest Geology, v. 34, p. 45-70.

Sébrier, M., Siame, L., Zouine, E.M., Winter, T., Missenard, Y., and Leturmy, P., 2006, Active tectonics in the Moroccan High Atlas: Geoscience, v. 338, p. 65-79.

Smith, A.G., and Livermore, R.A., 1991, Pangea in the Permian to Jurassic time: Tectonophysics, v. 187, p. 135-179.

Smith Jr., L.B., Eberli, G.P., and Sonnenfeld, M., 2004, Sequence-stratigraphic and paleographic distribution of reservoir-quality Dolomite, Madison Formation, Wyoming and Montana: in Integration of outcrop and modern analogs in reservoir modeling: AAPG Memoir 80, p. 67-92

Solum, J.G., and van der Pluijm, B.A., 2007, Reconstructing the Snake River/Hoback River Canyon section of the Wyoming thrust belt through direct dating of fault rocks, in Sears, J.W., Harms, T.A., and Evenchick, C.A., eds. Whence the Mountains? Enquiries into the Evolution of Orogenic Belts (Ray Price Volume): Geological Society of America Special Paper 433, p. 183–196.

Stamatakos, J., and Hirt, A.M., 1994, Paleomagnetic considerations of the development of the Pennsylvania Salient in the Central Appalachians: Tectonophysics, v. 231, p. 237–255, doi:10.1016/0040-1951(94)90037-X.

Stamatakos, J., Hirt, A.M., and Lowrie, W., 1996, The age and timing of folding in the Central Appalachians from paleomagnetic results: Geological Society of America Bulletin, v. 108, p. 815–829, doi:10.1130/00167606(1996)108<0815:TAATOF>2.3.CO;2.

Stampfli, G.M., Hochard, C., Verard, C., Wilhem, C., and vonRaumer, J., 2013, The formation of Pangea: Tectonophysics, v. 593, p.1-19.

Stearns, C.E., 1978, Pliocene-Pleistocene emergence of the Moroccan Meseta: Geological Society of American Bulletin, v. 89, p. 1630-1644.

Stearns, C., and Van der Voo, R., 1987, A paleomagnetic reinvestigation of the Upper Devonian Perry Formation: evidence for Late Paleozoic remagnetization: Earth and Planetary Science Letters, v. 86, p. 27-38.

Strangway, D.W., Honea, R.M., McMahon, B.E., and Larson, E.E., 1968,The magnetic proper- ties of naturally occurring goethite: Geophysical Journal International, v. 15, p. 345–359, doi:10.1111/j.1365-246X.1968.tb00191.x.

Suk, D.W. and Halgedahl, S. L. 1996, Hysteresis properties of magnetic spherules and whole-rock specimens from some Paleozoic platform carbonate rocks: Journal of Geophysical Research, v. 101, p. 25053–25076.

Suter, M., 1987, Structural traverse across the Sierra Madre Oriental fold-and-thrust belt in east-central Mexico: Geological Society of America Bulletin, v. 98, p. 249–264, doi:10.1130/0016 -7606(1987)98<249:STATSM>2.0.CO;2.

Tardy, M., Longoria, J.F., Martinez-Reyes, J., Mitre, L.M., Patino, M., Podilla Y Sanchez, R., and Ramirez, R., 1975, Observaciones Generales Sobre La Estructura De La Sierra Madre Oriental: La Aloctonia Del Conjunto Cadena Alta-Altiplano Central, Entre Torreon, Coah. Y San Luis Potosi, S.L.P. Mexico: Revista Geology, v. 75, p. 1-11.

Tauxe, L., 2010, Essentials of paleomagnetism: Berkeley: University of California Press, 489 p.

Tauxe, L., and Watson, G.S., 1994, The fold test: An Eigen analysis approach: Earth and Planetary Science Letters, v. 122, p. 331–341, doi:10.1016/0012-821X(94)90006-X.

Tauxe, L., Mullender, T.A.T., and Pick, T., 1996, Potbellies, wasp-waists, and superparamagnetism in magnetic hysteresis: Journal of Geophysical Research, v. 101, p. 571–583, doi: 10.1029/95JB03041.

Tohver, E., Weil, A.B., Solum, J.G., and Hall, C.M., 2008, Direct dating of carbonate remagnetization by 40Ar/39Ar analysis of the smectite–illite transformation: Earth and Planetary Science Letters, v. 274, p. 524–530.

Torcq, F., Besse, J., Vaslet, D., Marcoux, J., Ricou, L.E., Halawani, M., and Basahel, M., 1997, Paleomagnetic results from Saudia Arabia and the Permo-Triassic Pangea configuration: Earth and Planetary Science Letters, v. 148, p. 553-567.

Torsvik, T.H., Van der Voo, R., Predeen, U., Mac Niocaill, C., Steinberger, B., Doubrovine, P.V., van Hinsbergen, D.J.J., Domeier, M., Gaina, C., Tohver, E., Meert, J.G., McCausland, P.J.A., and Cocks, R.M., 2012, Phanerozoic polar wander, paleogeography and dynamics: Earth-Science Reviews, v. 114, p. 325-368, doi:10.1016/j.earscirev.2012.06.007.

Urrutia-Fucugauchi, J., 1981, Paleomagnetic evidence for tectonic rotation of northern Mexico and the continuity of the Cordilleran orogenic belt between Nevada and Chihuahua: Geology, v. 9, p. 178-183.

van der Pluijm, B.A., 1987, Grain-scale deformation and the fold test- evaluation of synfolding remagnetization. Geophysics Research Letters, v. 14, p. 155-157.

van der Pluijm, B.A., Hall, C.M., Vrolijk, P.J, Pevear, D.R., and Covey, M.C., 2001, The dating of shallow faults in the Earth's crust: Nature (London), v. 412, p. 172–175.

Van der Voo, R., 1993, Paleomagnetism of the Atlantic, Tethys and Iapetus Oceans, Cambridge University Press, 411 p.

Van der Voo, R., and Torsvik, T.H., 2012, The history of remagnetization of sedimentary rocks: De- ceptions, developments and discoveries, in Elmore, R.D., et al., eds., Remagnetization and chemical alteration of sedimentary rocks: Geological Society of London Special Publication 371, p. 23–53, doi:10.1144/SP371.2.

Van der Voo, R., Mauk, F.J., and French, R.B., 1976, Permian–Triassic continental configurations and the origin of the Gulf of Mexico: Geology, v. 4, p. 177–180.

Van der Voo, R., and Torsvik, T.H., 2001, Evidence for Late Paleozoic and Mesozoic non- dipole fields provides an explanation for the Pangea reconstruction problems: Earth and Planetary Science Letters, v. 187, p. 71–81.

Veevers, J.J., 2013, Pangea: Geochronological correlation of successive environmental and strati-tectonic phases in Europe and Australia: Earth-Science Reviews, v. 127, p. 48-95.

Vrolijk, P., and van der Pluijm, B.A., 1999, Clay gouge: Journal of Structural Geology, v. 21, p. 1039– 1048, doi:10.1016/S0191-8141(99)00103-0.

Wartiti, M.E., Broutin, J., Freytet, P., Larhrib, M., and Toutin-Morin, N., 1990, Continetnal deposits in Permian basins of the Mesetian Morocco, geodynamic history: Journal of African Earth Sciences, v. 10, p. 361-368.

Watson, G.S., and Enkin, R.J., 1993, The fold test in paleomagnetism as a parameter estimation problem: Geophysical Research Letters, v. 20, p. 2135–2137, doi:10.1029/93GL01901.

Wegener, A., 1915 & 1922, Die Entstehung der Kontinente und Ozeane: The origin of continents and species, English translation of 4th edition by J. Biram (1966), New York, Dover Publications. 262 p.

Weil, A.B., and Van der Voo, R., 2002, Insights into the mechanism for orogen-related carbonate remagnetization from growth of authigenic Fe-oxide: A scanning electron microscopy and rock magnetic study of Devonian carbonates from northern Spain: Journal of Geophysical Research, v. 107, p. 1-1 – 1-4, doi: 10.1029/2001JB000200.

Weil, A.B., Gutiérrez-Alonso, G., and Wicks, D., 2012, Investigating the kinematics of local thrust sheet rotation in the limb of an orocline: a paleomagnetic and structural analysis of the Esla tectonic unit, Cantabrian–Asturian Arc, NW Iberia: International Journal of Earth Sciences, v. 102, no. 1, p. 43–60, doi: 10.1007/s00531-012-0790-3.

Weil, A.B., Van der Voo, R., van der Pluijm, B.A., and Pares, J.M., 2000, The formation of an orocline by multiphase deformation: A paleomagnetic investigation of the Cantabria- Asturias Arc (northern Spain): Journal of Structural Geology, v. 22, p. 735–756, doi:10.1016/S0191-8141 (99)00188-1.

Westphal, M., 1977, Configuration of the magnetic field and reconstruction of Pangaea in the Permian period: Nature, v. 267, p. 136-137.

Willis, B., 1902, Stratigraphy and structure, Lewis and Livingston Ranges, Montana: Geological Society of America Bulletin, v. 13, p. 305–352, doi:10.1130/GSAB-13-305.

Wiltschko, D.V., and Dorr Jr, J.A., 1983, Timing of deformation in Overthrust Belt and foreland of Idaho, Wyoming, and Utah: AAPG bulletin, v. 67, p. 1304-1322.

Woods, S.D., Elmore, R.D., and Engel, M.H., 2000, The occurrence of pervasive chemical remanent magnetizations in sedimentary basins: implications for dating burial diagenetic events: Journal of Geochemical Research, v. 69-70, p. 381-385.

Woods, S.D., Elmore, R.D., and Engel, M.H., 2002, Paleomagnetic dating of the smectite-to-illite conversion: Testing the hypothesis in Jurassic sedimentary rocks, Skye, Scotland: Journal of Geophysical Research, v. 107, p. 2-1–2-10, doi:10.1029/2000JB000053.

Worm, H.U., 1998, On the superparamagnetic-stable single domain transition for magnetite, and frequency dependence of susceptibility: Geophysical Journal International, v. 133, p. 201–206.

Xu, W., Van der Voo, R., and Peacor, D.R., 1998, Electron microscopic and rock magnetic study of remagnetized Leadville carbonates , central Colorado: v. 296, p. 333–362.

Zechmeister, M.S., Pannalal, S., and Elmore, R.D., 2012, in Elmore, R.D., et al., eds., Remagnetization and chemical alteration of sedimentary rocks: Geological Society of London Special Publication 371, p. 229–251, doi:10.1144 /SP371.3.

Zegers, T.E., Dekkers, M.J., and Bailly, S., 2003, Late Carboniferous to Permian remagnetization of Devonian limestones in the Ardennes: Role of temperature, fluids, and deformation: Journal of Geophysical Research, v. 108, p. 5-1–5-19, doi:10.1029/2002JB002213.

Zijderveld, J.D.A., 1967, A.C. demagnetization of rocks: Methods in Palaeomagnetism, Collinson, D.W., Creer, K.M., Runcorn, S.K. editors, p. 256-286, Elsevier, New York.

Zwing, A., Clauer, N., Liewig, N., and Bachtadse, V., 2009, Identification of remagnetization processes in Paleozoic sedimentary rocks of the northeast Rhenish Massif in Germany by K-Ar dating and REE tracing of authigenic illite and Fe oxides: v. 114, p. 1–19, doi: 10.1029/2008JB006137.